JOINT TRANSPORTATION
RESEARCH PROGRAM
INDIANA DEPARTMENT OF TRANSPORTATION
AND PURDUE UNIVERSITY

Friction Surface Treatment Selection: Aggregate Properties, Surface Characteristics, Alternative Treatments, and Safety Effects

Shuo Li, Rui Xiong, Demei Yu, Guangyuan Zhao,
Peiliang Cong, Yi Jiang

SPR-3832 • Report Number: FHWA/IN/JTRP-2017/09 • DOI: 10.5703/1288284316509

RECOMMENDED CITATION

Li, S., Xiong, R., Yu, D., Zhao, G., Cong, P., & Jiang, Y. *Friction surface treatment selection: Aggregate properties, surface characteristics, alternative treatments, and safety effects* (Joint Transportation Research Program Publication No. FHWA/IN/JTRP-2017/09). West Lafayette, IN: Purdue University. https://doi.org/10.5703/1288284316509

AUTHORS

Shuo Li, PhD, PE
Research Engineer
Division of Research and Development
Indiana Department of Transportation
(765) 463-1521 x247
sli@indot.in.gov
Corresponding Author

Rui Xiong, PhD
Research Associate

Demei Yu, PhD
Research Associate

Guangyuan Zhao
Graduate Research Assistant

Peiliang Cong, PhD
Research Associate
School of Construction
Management Technology

Yi Jiang, PhD
Professor
School of Construction
Management Technology
Purdue University
(765) 494-5602
jiang2@purdue.edu
Corresponding Author

ACKNOWLEDGMENTS

This research project was sponsored by the Indiana Department of Transportation (INDOT) in cooperation with the Federal Highway Administration (FHWA) through the Joint Transportation Research Program (JTRP). The authors would like to thank the study advisory committee members, Bill Tompkins, Tim Wells, Matthew Beeson, Mike Holowaty, Michael Prather, Scott Chandler, Chris Moore, Ed Spahr, and Enass Zayed of INDOT, and Rick Drumm of FHWA Indiana Division for their guidance and expertise. Sincere thanks are extended to Bob Rees and Bart Williamson of INDOT, and Ayesha Shah of North Central SuperPave Center for their help and support in laboratory testing. The authors recognize the assistance provided by Randy Large, Tony Johnson, Aaron Ping, and Kamron Yates of INDOT in field testing.

This report would not have been possible without the help of many people, in particular, Georgia Eusner of Great Lake Minerals LLC, Michael Blackwell of Beemsterboer Slag Corporation, Don Edwards and Scott Bain of Dayton Superior Corporation, Doug Fromm of Nevada DOT, Patrick Malfitano of EWS Steel Aggregate LLC, Julian Yan of Cornerstone Construction Material LLC, Frank Julian of FHWA, David Merritt of The Transtec Group, George Wang of East Carolina University, Jan Olek of Purdue University, Junmin Shen of Shanxi Transportation Research Institute, and Huaxin Chen of Changan University.

JOINT TRANSPORTATION RESEARCH PROGRAM

The Joint Transportation Research Program serves as a vehicle for INDOT collaboration with higher education institutions and industry in Indiana to facilitate innovation that results in continuous improvement in the planning, design, construction, operation, management and economic efficiency of the Indiana transportation infrastructure. https://engineering.purdue.edu/JTRP/index_html

Published reports of the Joint Transportation Research Program are available at http://docs.lib.purdue.edu/jtrp/.

NOTICE

COPYRIGHT

Print ISBN: 978-1-62260-478-4

TECHNICAL REPORT STANDARD TITLE PAGE

1. Report No.	2. Government Accession No.	3. Recipient's Catalog No.
FHWA/IN/JTRP-2017/09		

4. Title and Subtitle	5. Report Date
Friction Surface Treatment Selection: Aggregate Properties, Surface Characteristics, Alternative Treatments, and Safety Effects	July 2017
	6. Performing Organization Code

7. Author(s)	8. Performing Organization Report No.
Shuo Li, Rui Xiong, Demei Yu, Guangyuan Zhao, Peiliang Cong, Yi Jiang	FHWA/IN/JTRP-2017/09

9. Performing Organization Name and Address	10. Work Unit No.
Joint Transportation Research Program Purdue University 550 Stadium Mall Drive West Lafayette, IN 47907-2051	11. Contract or Grant No. SPR-3832

12. Sponsoring Agency Name and Address	13. Type of Report and Period Covered
Indiana Department of Transportation State Office Building 100 North Senate Avenue Indianapolis, IN 46204	Final Report
	14. Sponsoring Agency Code

15. Supplementary Notes
Prepared in cooperation with the Indiana Department of Transportation and Federal Highway Administration.

16. Abstract
This study aimed to evaluate the long term performance of the selected surface friction treatments, including high friction surface treatment (HFST) using calcined bauxite and steel slag, and conventional friction surfacing, in particular pavement preservation treatments such as chip seal, microsurfacing, ultrathin bonded wearing course (UBWC), and diamond grinding. This study also attempted to determine the correlation between vehicle crash and pavement surface friction, which makes it possible to quantitatively establish the so-called crash modification factors (CMFs) that are extremely useful in selecting a cost-effective solution to reduce wet pavement vehicle crashes.

In-depth reviews were conducted to identify the aspects of the properties for aggregates used in HFST, including aggregate abrasion value (AAV), Los Angeles abrasion (LAA), Micro-Deval abrasion, and polished stone value (PSV). Extensive laboratory testing was conducted to examine the LAA, Micro-Deval abrasion, and PSV, and to provide first-hand data on the calcined bauxite and steel slag that may be used for HFST and friction surfacing in Indiana. Laboratory accelerating polishing was carried out to evaluate the effect of aggregate gradation and identify the HFST systems with satisfactory friction performance with respect to surface macro-texture and friction. Test strips were installed in the pavement on a real-world road to further evaluate the friction performances of the promising HFST systems under the true traffic polishing and assess the potential effect of winter and snow plow. Pull-off testing was also conducted to examine the bonding between the proposed HFST systems and the substrate surface. Field friction test data was utilized to evaluate the long-term friction performances of pavement preservation treatments, including chip seal, microsurfacing, UBWC, and diamond grinding. Statewide vehicle crash data between 2010 and 2014 was examined to determine the crash statistics associated with pavement friction. The crash data was also matched to the annual pavement inventory friction data to quantify the probabilistic association between vehicle crash and pavement friction with respect to interstate, US, and state highways, respectively.

Specification requirements were established for the properties of calcined bauxite and steel slag for HFST and friction surfacing with respect to LAA, Micro-Deval abrasion, PSV, Al_2O_3 content, and fine aggregate angularity (FAA). Specification requirements were also developed for HFST aggregate gradation and surface friction performance. Regression models were developed for predicting the friction numbers of chip seal, microsurfacing, UBWC, and diamond grinding over their service lives. Regression models were also provided to quantify the effectiveness of friction surfacing for interstate, US, and state highways, respectively.

17. Key Words	18. Distribution Statement
friction surfacing, high friction surface treatment, calcined bauxite, steel slag, aggregate abrasion value, Los Angeles abrasion, Micro-Deval abrasion, polished stone value, Al_2O_3 content, fine aggregate angularity, chip seal, microsurfacing, ultrathin bonded wearing course, diamond grinding, macro-texture, mean profile depth, friction number, friction crash modification factor	No restrictions. This document is available to the public through the National Technical Information Service, Springfield, VA 22161.

19. Security Classif. (of this report)	20. Security Classif. (of this page)	21. No. of Pages	22. Price
Unclassified	Unclassified	54	

Form DOT F 1700.7 (8-69)

EXECUTIVE SUMMARY

FRICTION SURFACE TREATMENT SELECTION: AGGREGATE PROPERTIES, SURFACE CHARACTERISTICS, ALTERNATIVE TREATMENTS, AND SAFETY EFFECTS

Introduction

For this project, in-depth reviews were conducted to identify the property aspects of aggregates used for high friction surface treatment (HFST), including aggregate abrasion value (AAV), Los Angeles abrasion (LAA), Micro-Deval abrasion, and polished stone value (PSV). Extensive laboratory testing was conducted to examine the selected property aspects for the calcined bauxite and steel slag that may be used in Indiana. Both laboratory accelerated polishing and true traffic polishing were carried out to evaluate the effects of aggregate properties and the long-term friction performance of the HFST candidates.

Field friction test data was utilized to evaluate the long-term friction performances of chip seal, microsurfacing, ultrathin bonded wearing course (UBWC), and diamond grinding. Statewide vehicle crash data over a 5-year period was examined to determine the crash statistics associated with pavement friction. Statistic models were developed to predict the crash rate in terms of pavement friction for interstate, US, and state highways, respectively.

Findings

Aggregate Mechanical, Physical, Chemical, and Geometric Properties

- The PSV of BS EN 1097-8 test differs from the polish value, i.e., PV-10 of ASTM D3319-11, in many aspects, such as load, polishing time, abrasion condition, and reading scale. The Micro-Deval abrasion test was reported to be a better indicator for the durability of aggregate. The exposed aggregate particles of HFST protrude above the binder and undergo greater shear force and impact from vehicle tires, which may be measured in terms of LAA.
- The LAA loss increased as aggregate size decreased, regardless of aggregate type. Steel slag experienced greater LAA losses than calcined bauxite. However, the difference between the LAA losses of calcined bauxite and steel slag became much smaller as aggregate size decreased. Steel slag experienced a greater Micro-Deval abrasion loss than calcined bauxite. The 1/3-mm aggregates yielded greater polish value than the 6.3/9.5-mm aggregates for both calcined bauxite and steel slag. The polish values for 1/3-mm aggregates also demonstrated greater variations than those for 6.3/9.5-mm aggregates.
- Specification requirements for the mechanical properties of aggregates in terms of LAA, Micro-Deval abrasion, and PV-10 can be easily implemented by the state departments of transportation (DOTs). Synthetic aggregates such as calcined bauxite tend to contain an excessive amount of rounded particles. It is necessary to minimize the content of rounded particles with reference to a minimum fine aggregate angularity (FAA).

Evaluation of Friction under Laboratory Accelerated and True Traffic Polishing

- Under laboratory accelerated polishing, the HFST candidates with No. 8 steel slag (1–5 mm) and No. 4 calcined bauxite (1–5 mm) yielded similar mean profile depth (MPD) values before polishing. After polish conditioning, the three candidates—No. 8 steel slag, No. 4 calcined bauxite, and No. 6 calcined bauxite—demonstrated a reduction of 20%, 18%, and 22%, respectively, in MPD and a reduction of 8%, 4%, and 4%, respectively, in terms of DFT friction at 20 km/h. Smaller aggregates tended to experience greater reduction in MPD. Nevertheless, the candidates with larger surface MPD did not produce greater surface friction.
- Under true traffic polishing, the MPD values were 2.27 mm, 1.98 mm, and 1.98 mm before traffic polishing; 1.46 mm, 1.60 mm, and 1.58 mm after 3 months of service; and 1.49 mm, 1.46 mm, and 1.60 mm after 9 months of service for one-course No. 8 steel slag, one-course No. 6 calcined bauxite, and two-course No. 6 calcined bauxite, respectively. The average DFT friction coefficients at 20 km/h were 0.682, 0.932, and 0.905 after 3 months of service and 0.540, 0.812, and 0.798 after 9 months of service for these three candidates, respectively.

Long-Term Friction Performance of Preservation Treatments

- Applying a fog seal onto a new chip seal tended to reduce the surface friction by 25%. Chip seals using crushed stone demonstrated friction 25% greater than that using crushed gravel. No clear trend existed to indicate the differences in surface friction between No. 11, No. 12, and No. 16 aggregates. A successful chip seal is capable of providing satisfactory friction performance for a period of 5 years or more.
- Microsurfacing surface friction increased in the first 12 months and afterwards decreased very slowly, remaining very stable over time. Overall, microsurfacing is capable of providing better surface friction than chip seals for a wide range of traffic volumes and providing durable friction over a period longer than 6 years.
- UBWC surface friction tended to increase in the first 6 to 10 months, then decreased between 6 and 30 months in service. Afterwards, the friction fluctuated around a certain value greater than 30. UBWC with limestone aggregate demonstrated greater variation in friction properties. UBWC is capable of maintaining durable, sound surface friction for a period of at least 8 years under high traffic conditions.
- On hot-mix asphalt (HMA) pavement, diamond grinding surface friction fluctuated over time, and no trend existed to indicate a significant reduction in surface friction. On concrete pavement, such a surface friction decreased over time. Diamond grinding on new concrete pavement produced greater friction than on old concrete pavement. It can provide durable, sound surface friction for both concrete and asphalt pavements.

Quantifying Effectiveness of Friction Surfacing

The proposed crash-friction prediction models were developed from well-documented crash and friction data, and, therefore, are capable of providing reliable results.

Implementation

The laboratory aggregate test and analysis results have been utilized to determine the aggregate specification requirements for the HFST program recently implemented by the Indiana Department of Transportation (INDOT). The results of both laboratory accelerated and field true traffic polishing have also been used to establish the surface MPD and friction requirements

for HFST. The regression models for predicting the long-term friction performance of pavement preservation treatment can be used to estimate the surface friction of chip seal, microsurfacing, UBWC, and diamond grinding over the periods of anticipated service lives for the particular treatment. The models for quantitatively predicting the association between pavement surface friction and crash probability can be utilized to determine the dynamic crash modification factors (CMFs) for friction surfacing, including HFST and conventional friction treatments, with respect to interstate, US, and state highways.

CONTENTS

LIST OF TABLES

LIST OF FIGURES

1. INTRODUCTION

1.1 Problem Statement

Each year, vehicle crashes cause approximately 750 fatalities on Indiana roads (NHTSA, 2011). It is also estimated that horizontal curves make up 5 percent of the Nation's highway miles (FHWA, n.d.a). Based on the vehicle crash statistics provided by FHWA (n.d.c); however, approximately 28% of roadway fatalities occur at or near horizontal curves and three times as many crashes occur on horizontal curves as on tangential sections. In addition, more than 70% of the fatal crashes on horizontal curves occur on two-lane highways (McGee & Hanscom, 2006; Torbic et al., 2004). As a result, run-off-road (ROR) and head-on crashes with high fatalities are the two most prevalent crashes that have occurred on horizontal curves, and the safety strategies or countermeasures applied on horizontal curves should aim at reducing both the frequency and severity of these types of crashes. While the majority of crashes on horizontal curves can be attributed to human related factors such as inattention, in a hurry, and familiarity with the roadway, the roadway condition, particularly the pavement surface friction, also plays a more important role in safe driving on horizontal curves.

It is well known that the appropriate design for a horizontal curve is an optimal balance of curve radius, cross-section super-elevation, and surface friction. A vehicle can only negotiate a horizontal curve if a centripetal force is applied. In the meantime, a centrifugal force is caused as a reaction corresponding to the centripetal force. The centrifugal force is the opposite of centripetal force and is directed away from the center of circular motion. On a two-lane highway, the centrifugal force tends to pull the vehicle inside the curve into the opposite lane for the oncoming traffic and the vehicle outside the curve off the road. Consequently, a head-on crash or a ROR crash tends to occur on a horizontal curve if the pavement surface friction is low. Therefore, maintaining sufficient pavement surface friction is critical for safe driving on horizontal curves, particularly in inclement weather.

When a vehicle travel travels on a horizontal curve, the shear forces acting on the pavement surface by the side thrust of the tires increase. These forces cause the pavement surface to polish more quickly on a curve than on a tangent segment. Negotiating a horizontal curve requires a greater pavement surface friction. It becomes more demanding to safely negotiate horizontal curves when the pavement surface is wet. Therefore, enhancing surface friction on horizontal curves is one of several proven safety countermeasures included in the Every Day Counts initiative by FHWA. An effective safety solution qualifies for 100% FHWA safety funding under highway safety improvement programs.

A greater surface friction can be achieved by either using a special high friction surface treatment (HFST) or a conventional treatment. HFST is the application of very high quality, polish resistant aggregate with epoxy binder. FHWA has recognized the HFST as a surface treatment for critical safety spot locations that helps vehicles stay in their lane. It has been reported that HFST can reduce crashes by more than 30% (FHWA, n.d.b). In addition, HFST can help reduce crash fatalities and serious injuries on horizontal curves. Due to the use of proprietary materials, the initial cost of HFST can be expensive. Pavement preservation treatments, such as microsurfacing, chip seal, ultrathin bonded wearing course (UBWC), and diamond grinding, have also demonstrated high and durable friction performance (Li, Noureldin, Jiang, & Sun, 2012). Their initial costs are historically less expensive than HFST. Based on the projects completed by INDOT to date, the typical unit prices are $1.10, $3.63, and $6.44 per square yard for chip seal, microsurfacing, and UBWC, respectively.

While many state departments of transportation (DOTs) have formally applied HFST as a low cost safety countermeasure. Since 2007, INDOT has only placed one high friction surface treatment with no apparent information. In addition, INDOT dedicates at least $18 million to the pavement preservation initiative (PPI) program each year. Utilization of pavement preservation treatments may also be a sustainable solution to pavement friction on horizontal curves. To fully utilize both the HFST and pavement preservation treatments to enhance horizontal curve safety, INDOT proposed this study to address the potential concerns associated with HFST and alternative friction surface treatments.

1.2 Research Objective

The objectives of this study were threefold. First, this study aimed to evaluate the long-term performance of the selected surface friction treatments. This will help INDOT incorporate the surface friction treatments into safety improvement programs, pavement preservation programs and statewide resurfacing programs. Second, this study aimed to evaluate the mechanical properties of polish resistant aggregates including imported calcined bauxite and local steel slag in addition to the frictional properties of HFSTs using these two types of aggregates. The findings can be utilized by INDOT to develop technical specifications for HFST. Third, this study attempted to determine the correlation between vehicle crashes and pavement surface friction. This information can be utilized to develop crash modification factors (CMFs) that are extremely useful in selecting a cost-effective solution to reduce wet pavement vehicle crashes.

1.3 Business Case

The benefits identified for this study would include but are not limited to the following:

- **Enhance travel safety for the public**. Friction surface treatment at locations such as horizontal curves, ramps and intersections can immediately restore pavement surface friction characteristics. This can reduce vehicle run-off-road (ROR) crashes by decreasing vehicle stopping distance and hydroplaning possibility.

- **Utilize safety funds**. Various funds and grants are available from Federal, State, and local governments to support state highway safety programs. Justification for use of these funds and grants will require data-driven performance measures such as CMFs.
- **Encourage innovations**. Successful friction surface treatments, particularly HFST, require knowledge and technology on tire-pavement friction interaction, polymer formulation and aggregate production. This can only be achieved through continuous innovations by all potential partners.
- **Spawn economic growth**. On the one hand, HFST is made of superior polymer binders and durable aggregates that are typically produced by industries. HFST promotes use of the proprietary and patented materials and products, which is crucial for some companies and firms during the unstable economic conditions. On the other hand, steel slag is readily available in Indiana. Use of friction surfacing with steel slag at locations with less extreme friction demands not only spurs the use of locally sustainable materials, but also substantially reduces transportation-related carbon footprint and cost.
- **Shorten project delivery**. Advancement of innovative practices to routine use helps the agency accelerate construction and can potentially reduce congestion.
- **Assist local public agencies (LPAs).** The tools developed by this study can be utilized by LPAs to address local road safety issues, particularly data collection, case analysis, and involvement and participation in roadway safety improvements.

1.4 Research Scope and Tasks

In order to fulfill the study objectives and provide INDOT and LPAs with updated information and first-hand data on the best friction surface treatment, the scope of work included the following research tasks:

1. Synthesis of friction surface treatment. This task conducted a critical review on current FHWA's policies, procedures and recommendations for use of HFST and qualifications for safety improvement funding. This task also obtained the state-of-practice strategies utilized by other state DOTs to improve travel safety at critical safety spots, particularly horizontal curves and intersections. In particular, intensive review was conducted to examine the properties and requirements for HFST aggregates in the United Kingdom (UK) and identify the differences between the US and UK standard test methods on these aggregate properties.
2. Aggregate laboratory evaluation. This task included selection of the key property aspects of HFST aggregates and laboratory testing. The selection of HFST aggregate property aspects was made with respect to the frictional requirements, published research findings, specifications for high friction surfacing in the UK, and the current INDOT's practice. Laboratory tests were conducted to evaluate the mechanical properties that may affect HFST friction performance.
3. HFST system evaluation. The proposed HFST system candidates were first evaluated through three wheel polishing in the laboratory to determine the effect of aggregate gradation and size. The potential system candidates were further evaluated through real traffic polishing. Test strips were installed on an active highway. Tests were conducted over a period of nine months to evaluate the performance of HFST system candidates in terms of surface friction properties and durability.
4. Alternative friction treatments. This task included intensive consultation with INDOT personnel responsible for materials management, pavement preservation, and traffic safety to identify appropriate alternative friction treatments for restoring friction for large area applications and locations with less extreme friction demands. Alternative friction treatments, such as microsurfacing, UBWC, chip seal and diamond grinding, were selected from the pavement preservation projects. Friction measurements were made over time to determine the long-term performance for the alternative friction treatments.
5. Technical Specifications. Specifications form a part of a contract document and are important for the performance control of HFST involving proprietary products. This task reviewed the current HFST specifications across the country and in the United Kingdom. Based on the results of laboratory and in-situ test and evaluation, specification requirements for aggregate properties and surface friction properties were recommended for consideration in the development of HFST specifications.
6. Development of CMFS for friction treatments. This task first examined Indiana vehicle crash data to determine the current friction-related traffic safety situation and major factors. Global information system (GIS) technologies were used for vehicle crash data filtering. The filtered vehicle crash data was coupled with the pavement friction data using the Pythagoras' theorem to evaluate the correlations between vehicle crash and pavement friction. Crash frequency functions were developed with respect to pavement friction for three categories of roadways, including state, US, and interstate highways.
7. Final report. The final report was prepared to document all test data, analysis procedures, findings, and recommendations.
8. Life cycle cost (LCC) analysis. Life cycle cost analysis will be incorporated into the INDOT HFST Program-FY2017 to determine the actual cost and benefit of HFST over a period of five years. A tool will be developed using MS Excel spreadsheet to allow users to accomplish site-specific LCC analysis, candidate selection, and treatment selection.

1.5 Deliverables

The following deliverables were provided to the potential users, including Office of Traffic Safety, Office of Maintenance Field Support, Office of Materials Management, and LPAs:

1. Mechanical properties of the aggregates including calcined bauxite and steel slag for HFST or friction surfacing.
2. Friction properties of both HFST and friction surfacing systems using calcined bauxite and steel slag.
3. Long-term friction performance for alternative friction surface treatments, including microsurfacing, UBWC, chip seal, and diamond grinding, in terms of friction numbers over the anticipated service life.
4. Proposed specification requirements for aggregate properties and system performance for HFST and friction surfacing.
5. Crash frequency models and CMFs with respect to pavement friction for safety analysis.

6. Research report on the best practice and application of surface friction treatments at horizontal curves and intersections.

2. DETERMINATION OF PROPERTY REQUIREMENTS FOR CALCINED BAUXITE AND STEEL SLAG FOR FRICTION SURFACE TREATMENTS

2.1 Review of Standard Tests for Frictional Properties of Aggregates

2.1.1 Polished Stone Value

Polished Stone Value (PSV) is a measure of the resistance of coarse aggregates to polishing action of vehicle tires under conditions similar to those on road surfaces. The PSV test shall be carried out in accordance with BS EN 1097-8 (2009), *Tests for Mechanical and Physical Properties of Aggregates-Determination of the Polished Stone Value*, in the United Kingdom (UK), and in accordance with ASTM D3319-11 (2011), *Standard Practice for Accelerated Polishing of Aggregates Using the British Wheel*, in the US. In general, the PSV test is carried out in two stages. In the first stage, the specimen is subjected to a polishing action in an accelerated polishing machine. In the second stage, the state of polishing reached by the specimen is measured using a friction tester. Summarized in Table 2.1 is the comparison of BS EN 1097-8 with ASTM D3319-11 in terms of apparatus, aggregate, materials, specimen, and test procedures.

For the apparatus, the possible differences may arise with the rubber-tired wheel. In BS EN 1097-8, the rubber tire is a solid tire of 200 ± 3 mm in diameter and 38 ± 2 mm wide. In ASTM D3319-11, the standard rubber tire is 203.2 mm in diameter and 50.8 mm wide. The solid rubber tire of 203.2 mm in diameter is one of the three alternative tires recommended in ASTM D-3319-11. For the materials and aggregate, there are differences in almost all aspects, particularly aggregate gradation and abrasive. Although the aggregate gradation in BS EN 1097-8, i.e., 7.2~10 mm, is similar to that in ASTM D3319-11, i.e., 6.3~9.5 mm, the 7.2-mm sieve in BS EN 1097-8 is a grid sieve. The BS EN 1097-8 requires two abrasive materials with different gradations, including corn emery passing a 0.60 mm and emery flour passing 0.05-mm sieve. ASTM D3319-11 requires one abrasive material, i.e., silicon carbide grit having a uniform gradation passing a 0.15-mm sieve (No. 100) and retained on a 0.075-mm sieve (No. 200). For the test procedures, noticeable differences appear in the applied load and polishing process. The total load exerted on the specimen surface by the rubber-tired wheel is 725 ± 10 N in BS EN 1097-8 and 391 ± 4.5 N (88 ± 1lbf) in ASTM D3319-11. The polishing process of specimen is carried out in two phases in BS EN 1097-8. In the first phase, the specimen is subjected to a polishing action of three hours by feeding the corn emery and water both at 27 ± 9 g/min. In the second phase, the specimen is subjected to a polishing action of three hours by feeding the emery flour at 3 ± 1 g/min and water at 6 ± 1 g/min. In ASTM D3319-11, the specimen is subjected continuously to a polishing action of 10 hours by feeding the silicon carbide grit at 6 ± 2 g/min and water at 50–75 mL/min.

At the end of polishing process, the friction of the polished specimen is measured using the British pendulum test in both BS EN 1097-8 and ASTM D3319-11. The standard methods for the British pendulum test can be found in BS EN 13036-4 (2011) and ASTM E303-93 (2013). The British pendulum tester in BS EN 13036-4 is the same as that in ASTM E303-93. The only difference is the scale used to measure the British pendulum number (BPN). As shown in Figure 2.1, a typical British pendulum tester commonly provides two scales on the scale plate, including main scale and F-scale. The former is intended for use in the test of road surfaces with a 76.2-mm (3″) wide slider and the latter in the test of aggregates with a 31.75-mm (1.25″) wide slider. Approximately, the BPN in terms of the main scale is 0.6 times the BPN in terms of the F-scale. As specified in BS EN 1097-8, the 31.75-mm wide slider shall be used in conjunction with the F-scale. Although ASTM D3319-11 requires the 31.75-mm wide slider, the main scale is utilized in ASTM E303-93. Another caution should be exercised when calculating the PSV for the test specimens. In addition to the initial and polished aggregate BPN values, ASTM E303-93 requires "adjusted polish values of the test specimens based on the change in the average polish value of control specimens," but does not provide an explicit equation for adjusting the polish values. The equation for calculating the PSV in BS EN 1097-8 is as follows:

$$PSV = S - C + 52.5 \tag{2.1}$$

where, S is the mean value of the four aggregate test specimens; C is the mean value for the four control stone specimens; and 52.2 is the mean value of the specified PSV range for the control stone specimens, i.e., 49.5 to 55.5.

2.1.2 Aggregate Abrasion Value

Aggregate abrasion value (AAV) is a measure of the resistance of aggregate to surface wear by abrasion under traffic and is determined by the AAV test as defined in Annex A of BS EN 1097-8. The apparatus is the Dorry abrasion machine with a steel grinding lap wheel of ϕ600 mm. The aggregate to be tested shall pass a 14-mm sieve and be retained on a 10.2-mm grid sieve. The selected aggregate particles are orientated and embedded in resin in a flat test panel. During test, two test panels are loaded against the surface of the grinding lap wheel rotating at a speed of 28~31 rpm in a horizontal plane. An abrasive aggregate (i.e., sand of 0.30~0.85 mm containing 96% quartz) is fed continuously to the contacting surface of the test panel and lap wheel. After 500 revolutions, the amount of material abraded is measured by calculation of the weight loss of

TABLE 2.1
Comparison of BS EN 1097-8 and ASTM D3319 Standard Test Methods

Content		BS EN 1097-8	ASTM D3319-11
Apparatus	Road Wheel	$\phi 406 \pm 3$ mm 44.5 ± 0.5 mm wide	$\phi 406.4$ mm 44.5 wide
	Rubber-tired Wheel	Solid, $\phi 200 \pm 3$ mm 38 ± 2 mm wide	$\phi 203.2$ mm[a]
	Rubber Hardness	69 ± 3 IRHD[b]	69 ± 3 IRHD
Materials	Control Stone PSV	Quartz dolerite: 49.5-55.5	20-30 Ottawa sand: 850-600μm
	Abrasive	(i) Corn emery Passing 0.60 mm (ii) Emery flour Passing 0.05 mm	Silicon carbide grit: 150-75μm
Specimen	Dimension	$90.6 \pm 0.5 \times 44.5 \pm 0.5 \times 12.5$ mm	$88.9 \times 44.45 \times 16$ mm
	Aggregate Size	10 mm-7.2 mm[c]	9.5 mm-6.4 mm
Procedures	Load on Road Wheel	725 ± 10 N	391.44 ± 4.45N (88 ± 1lbf)
	Temperature	20 ± 5°C	23.9 ± 2.8°C
	Road Wheel Speed	320 ± 5 rpm	320 ± 5 rpm
	Polishing Time	6 hrs: Corn emery, 3 hrs Emery flour, 3 hrs	10 hrs
	Abrasive Feed Rate	(1) Corn emery: 27 ± 9 g/min Water: 27 ± 9 g/min (2) Emery flour: 3 ± 1 g/min Water: 6 ± 2 g/min	(i) Silicon carbide: 6 ± 2 g/min (ii) Water: 50-75 mL/min
Report	BPN	PSV (F-scale)	PV-i/PV-n (Main scale)

[a]Alternative Tire No. 3 in ASTM D3319-11.
[b]International rubber hardness degrees.
[c]The 7.2-mm sieve is the standard grid sieve.

the aggregate. The percentage loss in mass is known as the AAV.

However, the AAV test is rarely used by the state DOTs in the US. Instead, the Los Angeles abrasion (LAA) or Micro-Deval abrasion test has been used to evaluate the aggregate abrasion. The LAA test is a measure of the degradation of mineral aggregates of standard gradings resulting from a combination of actions including abrasion, impact, and grinding according to ASTM C131/C131M-14 (2006). This test is carried out by rotating the sample in a steel drum with a charge of steel balls and determining the difference between the mass of the original sample and the mass of the sample retained on 1.70-mm sieve, expressed as percentage loss by mass of the original sample. The Micro-Deval abrasion test is a measure of the abrasion resistance and durability of aggregates resulting from a combination of abrasions and grinding in the presence of water according to ASTM D6928-10 (2010). This test is carried out by rotating the sample in a steel jar with water and a charge of steel balls and determining the loss of the sample, i.e., the amount of aggregate passing 1.18-mm sieve, as a ratio of the mass of the original sample. Although the LAA and Micro-Deval abrasion tests appear similar, there are three important differences that set these two tests apart:

- The original sample shall be immersed in water for a minimum of one hour in the Micro-Deval abrasion test, but oven-dried in the LAA test.
- The rotating jar contains 2.0 L water during the Micro-Deval abrasion test, but no water is added during the LAA test.
- The charge in the LAA test has a total mass (5000 g) equal to that in the Micro-Deval abrasion test. However, the former consists of 46/48 mm diameter steel balls and the latter consists of 9.5 mm diameter steel balls.

Alexander and Mindess (2005) commented that the LAA test is really a measure of aggregate impact and crushing strength since the mode of action involves impact of particles against steel balls, against each, and against the walls of the cylinder, and the LAA percent loss would seldom reflect actual abrasion in practice. It was also reported that the LAA test for aggregate

abrasion resistance demonstrated poor correlation with field performance (Rogers & Senior, 1994). In the Micro-Deval abrasion, however, the use of saturated aggregate samples can better reflect the effects of the environment and therefore the durability of aggregate properties (Cuelho, Mokwa, Obert, & Miller, 2008; Hunt, 2001; Wu, Parker, & Kandhal, 1998). Rotating the sample in the steel jar with 2.0 L of water can not only maintain aggregate surface in wet condition, but also reduce the action of impact by the steel balls. In addition, the use of smaller steel balls also reduces the impact action. Consequently, the impact action by the steel balls becomes small and surface wear by abrasion and grinding prevail. Senior and Rogers (1991) have reported that there is an association between the AAV and Micro-Deval abrasion tests and the Micro-Deval abrasion test is simpler to complete than the AAV test.

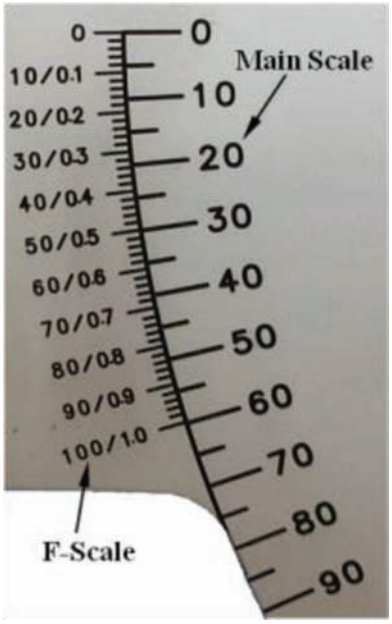

Figure 2.1 F- and main scales on scale plate of British pendulum tester.

2.2 Laboratory Evaluation of Mechanical Properties

2.2.1 LAA Test Results and Analysis

Figure 2.2 shows the LAA test machine and samples before and after grinding. Presented in Table 2.2 are the LAA test results for the calcined bauxite and steel slag aggregates of both Gradings C and D, respectively. There were two reasons to choose both Gradings C and D for conducting the LAA test. First, Grading D better represents the standard size of aggregate widely used for HFST nationwide. Second, it was indicated that no specific trend could be observed on the influence of aggregate grading on the LAA loss (Rangaraju & Edlinski, 2008). Although this was thought to result from the lack of consistency in ball charge and particle surface area (Kandhal & Parker, Jr.), such issue was considered worthy of further investigation because very

(a) LA test machine

(b) Sample before grinding

(c) Sample after grinding

Figure 2.2 LAA test machine and samples.

little LAA information is currently available on both calcined bauxite and steel slag. In addition, Grading C represents the main size of steel slag commonly used in HMA mixes, particularly stone matrix asphalt (SMA) in Indiana.

For the calcined bauxite, the average LAA loss is 9.3% and 12.3% for Grading C and Grading D, respectively. The latter is 3.0% greater than the former. Similar trends can be noted for the test results of steel slag. For the steel slag, however, the average LAA loss associated is 13.1% and 14.0% for Gradings C and D, respectively. The latter is 0.9% greater than the former. Evidently, the LAA loss of calcined bauxite increased as the aggregate size decreased, and however, the LAA loss of steel slag was insensitive to the aggregate size. The steel slag experienced greater LAA losses than the calcined bauxite. The average LAA loss for the steel slag is approximately 41% and 14% greater than that of the calcined bauxite for Gradings C and D, respectively. This implies that the difference between the calcined bauxite and steel slag LAA losses may become much less as the aggregate size decreases.

TABLE 2.2
LAA Test Results, % by Mass

	Calcined Bauxite		Steel Slag	
Sample No.	**Grading C**	**Grading D**	**Grading C**	**Grading D**
1	9.1	12.3	13.2	14.0
2	9.5	12.3	13.0	13.9
Average	9.30	12.30	13.10	13.95
STD[a]	0.28	0.00	0.14	0.07

2.2.2 Micro-Deval Abrasion Test Results and Analysis

Presented in Figure 2.3 are the Micro-Deval test machine and samples before and after grinding. The grading with a maximum nominal size of 9.5 mm was chosen for conducting the Micro-Deval abrasion test due to the aggregate size commonly used for HFST. Table 2.3 presents the Micro-Deval abrasion test results for both the calcined bauxite and steel slag aggregates. The average Micro-Deval loss is 5.2% for the calcined bauxite and 6.1% for the steel slag. The Micro-Deval loss for the steel slag is approximately 17% greater than that for the calcined bauxite. In addition, it is shown that for both the calcined bauxite and steel slag aggregates, all the three samples yielded very consistent test results and the standard deviations are very subtle. This implies that the Micro-Deval abrasion test is a very repeatable test.

2.2.3 Polished Stone Value Test Results and Analysis

As shown in Figure 2.4 are the PSV test polishing machine, test coupons (curved specimens), and placement

(a) Micro-Deval test machine

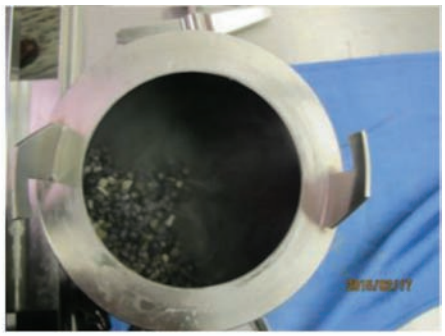

(b) Sample before grinding

(c) Sample after grinding

Figure 2.3 Micro-Deval test machine and samples.

of test coupons. As mentioned earlier, ASTM D3319-11 specifies two aggregate sizes, i.e., the standard aggregate size of 9.5~12.5 mm and the alternative aggregate size of 6.3~9.5 mm. However, neither aggregate size is used for HFST. The accelerated polishing tests were initially conducted on the 6.3~9.5 mm aggregate for both the calcined bauxite and steel slag and the test results are summarized in Table 2.4. The average PV-10 values are 35.4 and 27.8 for the calcined bauxite and steel slag, respectively. The PV-10 values are much less than the published typical PSV, i.e., 70 for the calcined bauxite (Hosking & Tubey, 1972) and 63 for steel slag (Stock, Ibberson, & Taylor, 1996). There are three possible reasons. First, this is probably due in great part to the fact that the typical PSV numbers were measured on 1~3 mm aggregate rather than 6.3~9.5 mm aggregate. Second, the discrepancies between the BS EN 1097-8 and ASTM D3319-11 shown in Table 2.1 could also contribute to the low PV-10 values. Third, larger size aggregates tend to contain more uncrushed particles. The examination of the calcined bauxite test coupons revealed that the round shape particles accounted for at least 7% by weight of the total aggregate.

After weighing all the factors, the authors conducted another set of tests on 1~3 mm aggregate and the results are also presented in Table 2.4. Clearly, the PV-i and PV-10 values for the 1~3 mm aggregate are much greater than those for the 6.3~9.5-mm aggregate. This agrees with the observation by Woodward, Woodside, and Jellie (2005) that PSV generally increases with reducing aggregate size. For the calcined bauxite, the 1~3 mm aggregate yielded friction values approximately 64% and 67% greater than those by the 6.3~9.5 mm aggregate before and after polishing, respectively. For the steel slag, the 1~3 mm aggregate yielded friction values approximately 84% and 86% greater than those by the 6.3~9.5 mm aggregate before and after polishing, respectively. However, both the PV-i and PV-10 values for the 1~3 mm aggregate demonstrate greater variations than those for the 6.3~9.5 mm aggregate. The main reason is that when preparing the specimens, the 1~3 mm aggregate was not only too small to be individually placed in the mold like coarse aggregate, but also too coarse to mix with the resin. Instead, the aggregate was first scattered on the bottom of the mold to achieve a desired single layer, and then epoxy was added over it. Consequently, variability could be increased between the specimens.

TABLE 2.3
Micro-Deval Abrasion Test Results, % by Mass

Sample No.	Calcined Bauxite	Steel Slag
1	5.3	6.1
2	5.2	6.1
3	5.2	6.1
Average	5.23	6.10
STD[a]	0.06	0.0

[a]STD = standard deviation.

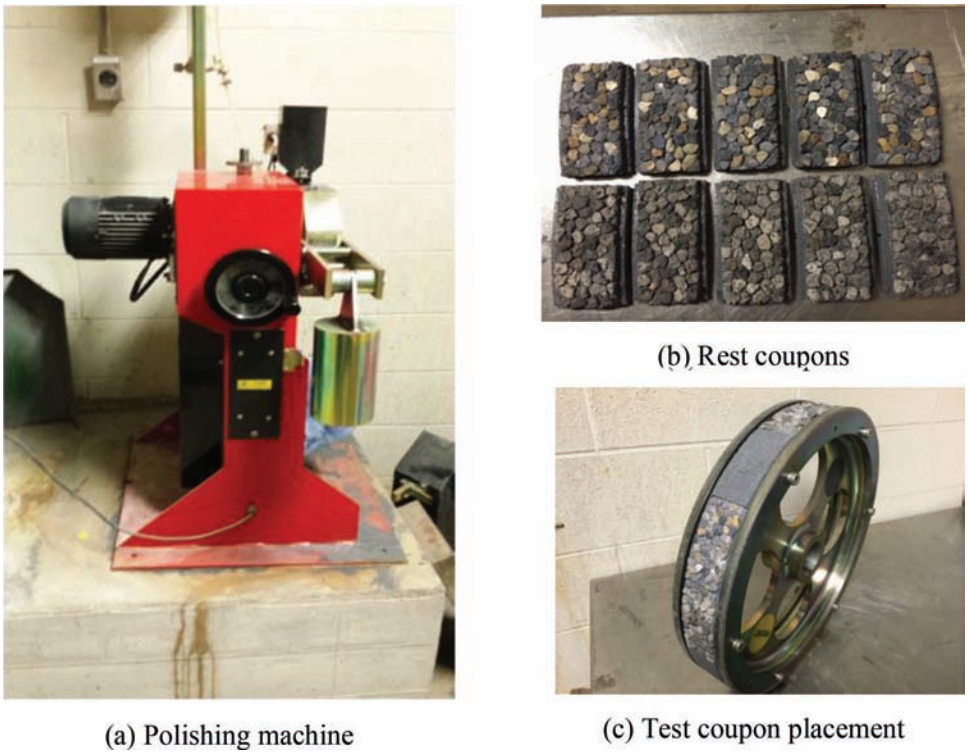

Figure 2.4 PSV test machine and samples.

For the 1~3 mm aggregate after 10 hours of polishing, the friction value decreased approximately by 20 and 23 points for the calcined bauxite and steel slag, respectively. The former represents a reduction of 25% and the latter represents a reduction of 31% in friction value. The PV-10 values are 59.1 and 51.7 with reference to the main scale, and 98.6 and 86.2 with reference to the F-scale for the calcined bauxite and steel slag, respectively. It is difficult to convert the PV-10 values to PSV accurately due to the discrepancies between the BS EN 1097-8 and ASTM D3319-11 test procedures as outlined earlier. However, both the calcined bauxite and steel slag demonstrated a PV-10 value that is much greater than the required PSV of 70 for HFST. This can be extended to imply that the steel slag evaluated in this study may be used as an alternative aggregate for HFST with 1~3 mm aggregate.

Presented in Figure 2.5 are the variations of friction value with aggregate size for the calcined bauxite aggregates of the same source. The black column represents the average PV-10 in Table 2.5. The dark grey column represents the average PSV measured by one laboratory in the UK (Georgia Eusner, personal communication, April 14, 2015). It is shown that both the PSV and PV-10 values increase as the aggregate size decreases. However, PV-10 increases more rapidly than PSV. For the 1~3 mm aggregate, the PV-10 with reference to the F-scale is much greater than the PSV. This is more like due to the inherent differences between the BS EN 1097-8 and ASTM D3319-11 test methods. However, there is no evidence to suggest which method is inherently more accurate than the other.

TABLE 2.4
Accelerated Polishing Test Results[a]

	Calcined Bauxite				Steel Slag			
	6.3~9.5 mm		1~3 mm		6.3~9.5 mm		1~3 mm	
Sample No.	PV-i	PV-10	PV-i	PV-10	PV-i	PV-10	PV-i	PV-10
1	50.0	35.0	80.5	59.8	40	26	73.8	50.3
2	46.0	37.0	80.5	58.5	41	28	77.3	50.3
3	48.0	35.0	81.3	64.0	40	26	76.0	56.5
4	48.0	35.0	74.0	54.3	40	31	71.3	49.8
5	49.0	35.0	–	–	42	28	–	–
Average	48.2 (80.3)	35.4 (59.0)	79.1 (ofs[b])	59.1 (98.6)	40.6 (67.6)	27.8 (46.3)	74.6 (ofs[b])	51.7 (86.2)
STD[c]	1.48	0.89	3.40	4.00	0.89	2.05	2.63	3.19

[a]All values were measured on the main scale except for the values in parentheses that were measured on the F-scale.
[b]ofs = out of scale.
[c]STD = standard deviation.

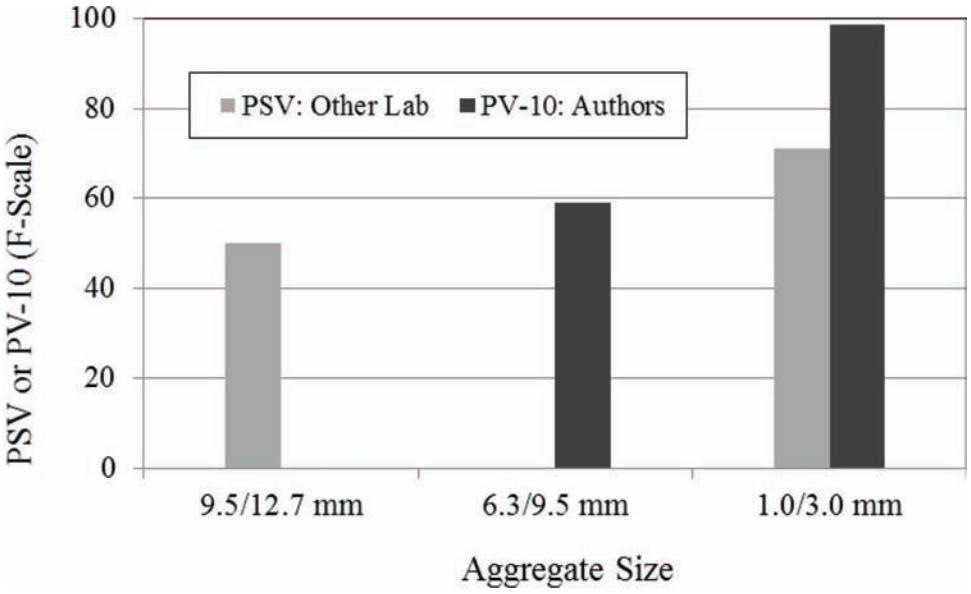

Figure 2.5 Variations of friction value with aggregate size for calcined bauxite.

TABLE 2.5
Current State DOTs' Requirements for HFST Aggregate Mechanical Properties

Property	LAA (%, max.)	Micro-Deval Abrasion (%, max.)	PSV (min.)	Soundness (%, max.)	AIR[h] (%, min.)
AASHTO	20[a]	–	–	–	–
Alabama	20[c]	–	38[d]	–	–
California	10[c]	–	–	30[f]	90
Florida	10[c]	–	–	–	–
Georgia	10[c]	–	–	–	–
Illinois	20[a]	–	–	–	–
Iowa	20[b]	–	70[e]	–	–
Pennsylvania	20[b]	–	38[d]	–	–
South Carolina	20[b]	–	70[e]	–	–
South Dakota	30[b]	–	65[e]	12[g]	–
Texas	10[a]	–	–	30[f]	90
Virginia	20[c]	5	–	–	–

[a]Grading D.
[b]Grading.
[c]No grading specified.
[d]ASTM C3319-11, accelerated polish value.
[e]ASTM E660, three wheel polish value.
[f]Magnesium sulfate.
[g]Sodium sulfate.
[h]AIR—acid insoluble residue.

2.3 Requirements for Mechanical Properties

2.3.1 Current Highway Agencies' Specifications

Summarized in Table 2.5 are the specifications for the mechanical properties of HFST aggregates developed by AASHTO (AASHTO PP 79-14, 2014) and eleven state DOTs (ATSSA, 2014). All these agencies except Georgia DOT require the use of calcined bauxite only. Georgia DOT allows the use of calcined bauxite and highly resistant granite. It is shown that all twelve agencies have requirements for LAA, one agency has the requirement for Micro-Deval abrasion loss, five agencies have requirements for PSV, and three agencies have requirements for aggregate soundness. It is little wonder that the current state DOTs' specifications vary greatly in property scope, quantitative provision, and test method. In addition, there is a lack of consistency with the requirements for different properties, in particular between LAA and PSV.

For the LAA requirements, three agencies, including AASHTO, Illinois DOT and Texas DOT, utilize the aggregate of Grading D, four agencies, including Iowa, Pennsylvania, South Carolina, and South Dakota DOTs, utilize the aggregate of Grading C, and the remaining five agencies have not specified the aggregate grading. The require LAA ranges between 10% and 20% for Grading D and between 20% and 30% for Grading C and is much greater than the LAA test results for both the calcined bauxite and steel slag as shown in Table 2.2. For Micro-Deval abrasion, a maximum loss of 5%, slightly greater than 5.23 and 6.10, i.e., the test Micro-Deval abrasion test results for the calcined bauxite and steel slag, respectively (see Table 2.3), is considered acceptable by Virginia DOT and is slightly greater.

For the PSV requirements, two agencies, including Alabama and Pennsylvania DOTs, utilize the ASTM D3319-11 accelerated polishing testing, and three agencies, including Iowa, South Carolina, and South Dakota, utilize the ASTM E660-90 small-wheel, circular track polishing testing (ASTM E660-90, 2015). The PSV requirement is 38 in accordance with ASTM D3319-11, and 65 or 70 in accordance with ASTM E660-90. Notice that the standard aggregate size for evaluating exposed aggregate specimens in ASTM E660-90 is 9.5~12.7 mm. It is also shown that in addition to the requirements for abrasion and polishing, three agencies, including California, South Dakota, and Texas DOTs, have requirements for aggregate soundness determined in accordance with ASTM C88-13 (2013). The maximum acceptable loss is 30% with reference to magnesium sulfate soundness for both California and Texas DOTs, and 30% with reference to sodium Sulfate Soundness for South Dakota DOT. In addition, both California and Texas DOTs have set forth a requirement for aggregate acid insolubility. The acid insoluble residue (AIR) should not be less than 90% determined in accordance with ASTM D3042-09 (2015).

2.3.2 Recommended Requirements

As indicated earlier, there are inherent differences between the BS EN 1097-8 and ASTM D3319-11 test methods, but no evidence to suggest which method is more accurate for measuring polish-resistance than the other. The AAV test currently used in the UK is rarely used by the state DOTs in the US. However, there is an association between the AAV and Micro-Deval abrasion tests. In addition, the exposed aggregate particles of HFST are protruding above the binder, which results

in greater shear force and impact form traffic tire. It is necessary to set forth a requirement for the resistance to fragmentation that may be measured with reference to the LAA. Therefore, it is advisable to establish requirements for the mechanical properties of aggregate for HFST with reference to LAA, Micro-Deval abrasion, and PV-10. In reality, the LAA, Micro-Deval abrasion, and PV-10 tests are currently being used in INDOT. Presented in Table 2.6 are the requirements (lower bounds at a confidence level of 95%) for the mechanical properties of calcined bauxite and steel slag aggregates for friction surface treatments.

The recommended values were derived by taking into account the test results and their variations. For both the LAA and Micro-Deval abrasion, the variability involved in the test results is very low and the corresponding requirement is the maximum percent loss. At the confidence level of 95% for LAA, for example, the upper bounds of the test results are 12.3% and 14.1% for calcined bauxite and steel slag, respectively. Rounding up the upper bound to the nearest 0.5 yielded the recommended requirements of 12.5% and 14.5% for calcined bauxite and steel slag, respectively. Applying the same approach to Micro-Deval abrasion yielded 5.5% and 6.5% for calcined bauxite and steel slag, respectively. For PV-10, the test results showed much greater variations, and therefore, extreme values were omitted. Considering that the requirement for PV-10 is the minimum polish value, rounding down the average of test results to the nearest 0.5 yielded 59.0 and 50.0 for calcined bauxite and steel slag, respectively. Notice that no provision is provided for either AIR or soundness. The AIR test did not directly measure the hardness of aggregate (Fowler & Rached, 2012). Also, aggregates that passed the Micro-Deval test would likely pass the sulfate soundness test (Cuelho et al., 2008). Calcined bauxite and steel slag are both synthetic, non-carbonate aggregates. The AIR and sulfate soundness become redundant if LAA, Micro-Deval abrasion, and PV-10 have been considered.

2.4 Requirements for Chemical, Physical, and Geometric Properties

2.4.1 Chemical Properties and Effects

The calcined bauxite widely used for HFST in the US is commonly imported from China and is produced by calcining raw bauxite at a temperature between 1450°C and 1700°C. The Chinese calcined bauxite consists of mainly corundum ($\alpha-Al_2O_3$) and mullite ($3Al_2O_3.2SiO_2$) phases and a very small glass phase (Zhong & Li, 1981). Corundum phase is an exceptional hard, tough, and stable phase, which makes calcined bauxite an excellent abrasion-resistant aggregate. Glass phase consists of mainly TiO_2, Fe_2O_3, Cao, and K_2O that affect the hardness, strength, and volumetric stability of the calcined bauxite. Mullite phase is a softer phase. However, it will wear more rapidly than corundum phase, which results in a heterogeneous surface and causes corundum phase to protrude and maintain good microtextures (Dews & Bishop, 1972). The above may imply that the chemical compositions of the calcined bauxite affect not only its lattice, phase, and microstructure, but also its physical and mechanical properties. As a rule of thumb, the strength, stiffness, and hardness of the calcined bauxite increase as the content of Al_2O_3 increases. It is the microstructure made up of closely interlaced corundum and mullite phases that makes calcined bauxite better able to withstand polishing, abrasion, and grinding.

Presented in Table 2.7(a) are the chemical and physical properties for the selected calcined bauxite, including the typical values claimed by the supplier and the test results from the current study. Al_2O_3 and SiO_2, respectively, have the first and second high percentages. However, variations can be seen between the typical values and test results. Based on the test results, Al_2O_3 and SiO_2 account for 86.93% and 6.83% of the total concentration, respectively. There are many factors that will affect the chemical composition of calcined bauxite. The proportions of oxides in calcined bauxite depend not only on raw bauxite, but also on calcination operation conditions, in particular the type of kiln (rotary kiln or shaft kiln), type of fuel, flame temperature, feed amount, and feed speed. Therefore, the oxide proportions may vary from plant to plant, batch to batch, and even vary across a single batch.

Presented in Table 2.7(b) are the X-ray diffraction (XRD) chemical composition test results of two samples taken randomly from the calcined bauxite produced using a shaft kiln in Yangquan, Shanxi, China. Noticeable variations can be found in the proportions of both Al_2O_3 and impurities, in particular SiO_2. It is also demonstrated that in Figure 2.6, these two samples exhibit different visual appearance such as color and texture. Taking into consideration the potential variation in the aggregate plays an important role in developing a realistic implementable specification.

Steel slag is the major byproduct from converting molten iron to steel in a basic oxygen furnace (BOF) or

TABLE 2.6
Recommended Mechanical Property Requirements

Property	Test Method	Aggregate Size	Calcined Bauxite	Steel Slag
LAA Loss, %	ASTM C131	Grading D	12.5 max	14.0 max
Micro-Deval Abrasion Loss, %	ASTM D6928	6.3~9.5 mm	5.5 max	6.5 max
PV-10	ASTM D3319	6.3~9.5 mm	35.0 min	26.0 min
		1~3 mm	55.0 min	49.0 min

TABLE 2.7
Test Results of Calcined Bauxite Chemical and Physical Properties

(a) Calcined Bauxite Selected for Current Study

Source	Chemical Composition, % by Mass						Density	Absorption %
	Al_2O_3	SiO_2	Fe_2O_3	TiO_2	CaO+MgO	K_2O+Na_2O		
Current Study	86.93	6.82	1.63	3.45	0.45	0.21	3.38[a]	0.81
GRIPgrain (n.d.)	88.10	5.10	1.45	3.70	0.47	0.18	3.27[b]	0.30

(b) Calcined Bauxite Samples Taken from a Shaft Kiln

Sample	Al_2O_3	Fe_2O_3	SiO_2	TiO_2	CaO+MgO	K_2O+Na_2O
1	90.32	0.76	2.87	4.84	0.20	0.07
2	81.36	0.411	14.26	3.34	0.19	0.04

[a]Apparent specific gravity for coarse aggregate.
[b]Bulk density, g/cm^3.

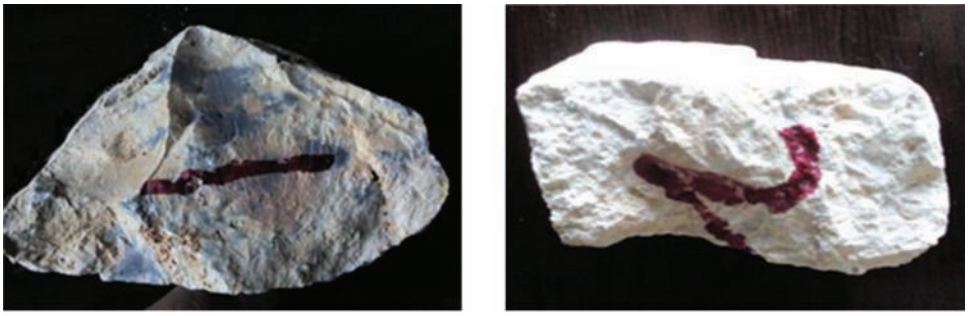

Figure 2.6 Calcined bauxite samples from one production batch.

melting steel scrap to make new steel in an electric arc furnace (EAF). While BOF process mainly uses raw materials such as iron ore, coal and limestone, and EAF process uses steel scrap, both BOF and EAF steel slags consist primarily of oxides such as CaO (lime), FeO, SiO_2, and MgO. The chemical constituents are combined to form the main mineral phases that determine the unique physical and mechanical properties of steel slags, particularly good polish and wear resistance, great hardness, and high compressive strength. It was also commented in email conversations with some steel slag suppliers and state DOTs that Al_2O_3 does contribute to the hardness of steel slag (Patrick Malfitano and Doug Fromm, personal communication, April 13, 2015). Steel slag may contain free Cao and free MgO that can hydrate and expand in contact with moisture and cause detrimental effect, particularly expansion and cracking of the steel slag particles (Chesner, Collins, & Mackay, 1998). However, a friction surface treatment such as HFST is a thin surface treatment and the aggregate particles are partially exposed. Therefore, the effect of expansion, if any, may be minimized.

The test results of chemical property for the BOF steel slag selected for this study are presented in Table 2.8(a). The major oxides such as CaO, Fe_2O_3, SiO_2, and MgO represent more than 90% of the total concentration, and the iron oxide exists mainly in the form of Fe_2O_3, i.e., hematite. In addition, the Al_2O_3 content is greater than 5%. However, the proportions of oxides in steel slags depend on the feed material, type of steel made, and furnace condition, and may vary from plant to plant and even from batch to batch in one plant (Shi, 2004). The researchers at Purdue University examined the chemical composition of two types of steel slag, including BOF and EAF (ladle) produced by steel slag processing plants in Indiana, and the results are presented in Table 2.8(b). Significant differences can be seen between these two types of steel slag in the contents of oxides, particularly FeO and Al_2O_3. Seemingly, EAF (ladle) steel slag has a much higher content of Al_2O_3 but much lower contents of FeO and SiO_2 than BOF steel slag.

2.4.2 Physical Properties and Effects

Density and water absorption are the important physical properties for aggregates used in pavement construction and may indicate the strength and durability of a specific aggregate. Density and water absorption also affects the volume of binder the aggregate may absorb. A high density tends to correlate with a low porosity and therefore a low water absorption for a given aggregate. For synthetic aggregates such as calcined bauxite and steel slag, the density and water absorption depend not

only on the chemical composition, but also on the production process. For calcined bauxite, the specific gravity and water absorption indicate if the raw bauxite is fully calcined. Partially calcined bauxite tends to have lower strength, lower toughness, and lower volumetric stability than fully calcined bauxite. A high density improves mechanical properties such as cold crushing strength and abrasion resistance (Vincent & Sehnke, 2006). As shown in Table 2.8(a) are the typical and measured values of the density and water absorption for the calcined bauxite used in the current study. It is shown that the selected calcined bauxite has a very high density. However, the measured water absorption is much greater than the typical value claimed by the supplier.

For steel slag, the specific gravity and water absorption also relies on the cooling conditions that control both the growth of mineral crystals and the quantity and size of gas bubbles that can escape before being trapped by solidification of the slag mass (Lewis, 1982). It is shown that in Table 2.8(a), the BOF steel slag used in the current study is solid with a specific gravity of 3.59 and a water absorption of 1.11%. However, great variations can arise in the specific gravity and water absorption in both BOF and EAF (ladle) steel slags as shown in Table 2.8 (b). It is demonstrated that BOF steel slag has a density much higher and a water absorption much lower than EAF (ladle) steel slag. This may be attributed to that BOF steel slag usually has a higher iron oxide content than EAF steel slag. A low specific gravity of 2.96 and a high water absorption of 9.1% occurred in the EAF (ladle) steel slag samples. This simply indicates that EAF (ladle) steel slag may have high porosity.

2.4.3 Geometric Properties and Effects

It has been recognized that the frictional performance of pavement surface varies with the aggregate geometric properties. This may be particularly true for a friction surface treatment such as HFST because its surface texture characteristics depend to a great extent on the size, shape, and angularity of the aggregate used in the treatment. In addition, the features of aggregate particle surfaces also affect the frictional performance of the treatment, particularly when it comes to long-term performance. For an aggregate sample of known gradation, aggregate angularity is commonly used to measure the shape of the aggregate particles and the degree of surface irregularities of the aggregate particles. Aggregate angularity decreases as uncrushed, round particles increase.

In reality, it is a fact that aggregates, in particular synthetic aggregates such as calcined bauxite, may contain an excessive amount of rounded particles. As shown in Figure 2.7 are the calcined bauxite sample taken randomly from the aggregate source. The rounded particles

TABLE 2.8
Test Results of Steel Slag Chemical and Physical Properties

(a) BOF Steel Slag Selected for the Current Study

Chemical Composition, % by Mass							
CaO	**Fe_2O_3**	**SiO_2**	**MgO**	**MnO**	**Al_2O_3**	**Specific Gravity[a]**	**Water Absorption %**
38.49	29.53	12.52	10.22	4.24	5.71	3.59	1.11

(b) BOF and EAF Steel Slags from Literature (Yildirim & Prezzi, 2009)

	Chemical Composition, % by Mass							
Steel Slag Type	**CaO**	**FeO**	**SiO_2**	**MgO**	**MnO**	**Al_2O_3**	**Specific Gravity[a]**	**Water Absorption %**
BOF	39.40	30.23	11.97	7.69	2.74	2.16	3.35–3.55	4.2–5.4
EAF (ladle)	47.52	7.61	4.64	7.35	1.0	22.59	2.96–3.18	3.0–9.1

[a]Apparent specific gravity for coarse aggregate.

Figure 2.7 Calcined bauxite particles.

account for approximately 7% of the total sample weight. Because the aggregates recommended for HFST commonly pass No. 4 (4.75 mm) sieve, this current study utilized the fine aggregate angularity (FAA) test to the aggregate angularity. The FAA test indirectly measures the angularity of fine aggregate in terms of the uncompacted void content of the aggregate sample (AASHTO T 304-11, 2011). Table 2.9 presents the FAA test results for the steel slag and calcined bauxite aggregates evaluated in the current study. The FAA values for both steel slag and calcined bauxite are greater than the minimum FAA for heavy traffic HMA mixes (INDOT, 2014).

2.4.4 Recommended Requirements

It is also worth noting that the Chinese refractory calcined bauxite is divided into seven grades in terms of the Al_2O_3 content (see Table 2.10). Grades GL-88 and GL-85 are, respectively, further sub-classified as A and B in terms of the contents of Fe_2O_3 and TiO_2. More likely, the calcined bauxite used in the current study may be GL-88 calcined bauxite based on its Al_2O_3. However, the minimum content of Al_2O_3 is 87% as specified in AASHTO PP 79-14. It is the authors' opinion that the AASHTO specification may be too stringent and not adequately describe the real variability of the calcined bauxite used for HFST. Figure 2.8 shows a stockpile of the calcined bauxite. Different colors simply indicate the variation of chemical composition. It is also interesting to note that in Table 2.10, there is no requirement for SiO_2. The main reasons are the properties of calcined bauxite varies with the Al_2O_3/SiO_2 ratio rather the SiO_2 content itself and the SiO_2 content decreases linearly as the Al_2O_3 content increases (Zhong & Li, 1981).

It is evident the Al_2O_3 content, density, and water absorption are the key chemical and physical properties when evaluating both calcined bauxite and steel slag for friction surface treatments. Bulk density is the weight of aggregate that would fill a container of unit volume that includes the volume of the individual particles and the volume of the voids between the particles. For a specific type of aggregate of a given specific gravity, the bulk density depends how densely the aggregate would be packed, and is particularly used by suppliers when

TABLE 2.9
FAA Test Results

Aggregate	FAA, %
Steel Slag	46
Calcined Bauxite	48

TABLE 2.10
China's Specifications for Calcined Bauxite (NDRC, 2005)

	Chemical Composition, % by Mass						
Grade Code	Al_2O_3	Fe_2O_3	TiO_2	CaO+MgO	K_2O+Na_2O	Bulk Density	Absorption%
GL-90	≥89.5	≤1.5	≤4.0	≤0.35	≤0.35	≥3.35	≤2.5
GL-88: A	≥87.5	≤1.6	≤4.0	≤0.40	≤0.40	≥3.20	≤3.0
GL-88: B	≥87.5	≤2.0	≤4.0	≤0.40	≤0.40	≥3.25	≤3.0
GL-85: A	≥85	≤1.8	≤4.0	≤0.40	≤0.40	≥3.10	≤3.0
GL-85: B	≥85	≤2.0	≤4.5	≤0.40	≤0.40	≥2.90	≤5.0
GL-80	>80	≤2.0	≤4.0	≤0.50	≤0.50	≥2.90	≤5.0
GL-70	70~80	≤2.0	–	≤0.60	≤0.60	≥2.75	≤5.0
GL-60	60~70	≤2.0	–	≤0.60	≤0.60	≥2.65	≤5.0
GL-50	50~60	≤2.5	–	≤0.60	≤0.60	≥2.55	≤5.0

Figure 2.8 A stockpile of calcined bauxite used for HFST.

TABLE 2.11
Recommended Chemical and Physical Requirements

Property	Test Method	Calcined Bauxite	Steel Slag
Al_2O_3, % by Mass, %	ASTM C 311 (2013)	86.5 min	5.0 min
Apparent Specific Gravity	ASTM C 127 (2015)	3.30 min	3.50 min
Water Absorption	ASTM C 127	3.0 max	2.0 max
FAA	AASHTO 304	48	46

aggregate is batched by volume and weight. Specific gravity, however, is commonly used in mix design to calculate the voids in mineral aggregate and the volume of binder likely to absorb. Therefore, specific gravity has potential advantages over bulk density as it covers a greater array of applications. Weighing all the considerations together yields the requirements of chemical, physical, and geometric properties for calcined bauxite and steel slag aggregate for friction surface treatments as shown in Table 2.11.

3. DETERMINATION OF REQUIREMENTS FOR FRICTIONAL PERFORMANCE OF FRICTION SURFACE TREATMENT

3.1 Laboratory Accelerated Polishing and Friction Evaluation

3.1.1 Aggregate Sizes and Gradations

Three main factors were originally considered in selecting the aggregate sizes and gradations. First, aggregate size and gradation affects not only the surface frictional characteristics of surface friction treatment such as a friction surface treatment system, but the application rate of epoxy binder as well. In general, more binder should be used to hold the aggregate chips firmly in position as aggregate size increases. Second, the markets for both calcined bauxite and steel slag are still limited in pavement friction surface treatments and may not be readily available in all sizes. This, therefore, affects the selection of aggregate gradations. As an example, No. 6 sieve is rarely used in producing steel slag aggregate. Incorporation of a No. 6 sieve into the production process of steel slag may not only affect the production process, but also increase the production cost. Third, the polymeric overlays with a proven track record of performance used by state DOTs were examined for aggregate size and gradation as shown in Figure 3.1 (Cargill, 2010; E-Bond, n.d.; Flint Rock Products, n.d.; GRIPgrain RD-88, n.d.; Poly-Carb, Inc., n.d.). RD-88 is intended for the calcined bauxite aggregate of HFST. It is shown that the gradation curve for RD-88 is a convex curve and steeper than the other gradation curves. This implies that RD-88 is finer and has more uniform-sized aggregate than other aggregates.

Presented in Table 3.1 are the aggregate sizes and gradations used to prepare the test slabs for the accelerated polishing test in the laboratory and test strips for field polishing test under actual traffic. The test slabs for steel slag were prepared using No. 8 aggregate. Because the trial slabs for steel slag prepared using the original gradation demonstrated a non-uniform surface, the test slabs used for the accelerated polishing were prepared using the modified gradation. For calcined bauxite, the test slabs were prepared using No. 4 and No. 6

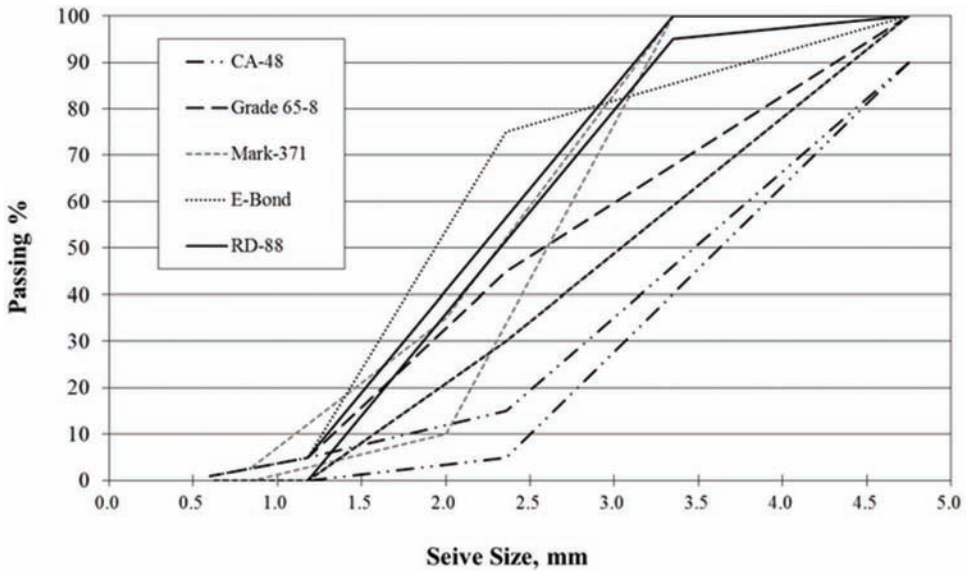

Figure 3.1 Gradations of aggregates available for friction surface treatments (Cargill, 2010; E-Bond, n.d.; Flint Rock Products, n.d.; GRIPgrain RD-88, n.d.; Poly-Carb, Inc., n.d.).

aggregates, respectively. No. 4 calcined bauxite aggregate, composed primarily of 2~5 mm particles, is coarser than No. 6 calcined bauxite aggregate. It was initially anticipated that No. 4 calcined bauxite could provide better friction performance, in particular in the winter.

3.1.2 Test Slabs and Accelerated Polishing

Three types of friction surface treatment systems, including one-course No. 8 steel slag friction treatment system, one-course No. 4 calcined bauxite HFST system, and one-course No. 6 calcined bauxite HFST system (see Figure 3.2), were evaluated using accelerated polishing in the laboratory. Two test slabs were made for each treatment system. Each test slab consisted of a substrate slab and a friction surface treatment system on top of the substrate slab. Two types of substrate slabs were used, new cement concrete slabs and HMA test slabs "left over" from other polishing studies. The recommended application rates for the three treatment systems were 0.312~0.484 gal./m^2 (2.9~4.5 gal./100 ft^2) and 7.32~10.74 kg/m^2 (1.50~2.20 lbs./ft^2) for epoxy binder and aggregate, respectively. The actual application rate for preparing the test slabs was 0.338 gal./m^2 (3.14 gal./100 ft^2) for epoxy binder and 7.5 kg/m^2 (1.55 lb/ft^2) for both steel slag and calcined bauxite aggregates.

The polishing of the test slabs was accomplished using a circular track polishing machine similar to the three wheel polishing device developed by the National Center for Asphalt Technology (NCAT; Vollor & Hanson, 2006). During polishing (INDOT, 2012), a total load of approximately 965 N, i.e., 217 lbs., was applied to the surface of the test slab through the polishing tires, and water was sprayed on the surface of test slab being polished to remove debris produced due to polishing and simulate wet conditions. The rate of rotation of the three rubber tires was 47 revolutions per minute. Because the main objective of the laboratory polishing and friction evaluation was to assess the long-term friction performance of each friction surface treatment, surface friction and texture measurements were taken before polishing and after reaching a terminal polishing condition, instead of every 5,000 polishing cycles (15,000 wheel passes). In the current study, the terminal polishing condition was reached by applying 100,000 polishing cycles (300,000 wheel passes) or fewer when the polishing rubber tire was worn out.

TABLE 3.1
Aggregate Sizes and Gradations Selected for Polishing Testing

(a) No. 8 Steel Slag

Sieve Size		% Passing	
		Original	Modified
No. 4	4.75 mm	100	100
No. 8	2.36 mm	52.5	45
No. 16	1.18 mm	2.5	1.5
No. 30	0.60 mm	1	1

(b) No. 4 and No. 6 Calcined Bauxites

Sieve Size		% Passing	
		No. 6 (1~3 mm)	No. 4 (2~5 mm)
3/8 in.	9.5 mm	–	100
No. 4	4.75 mm	100	97.5
No. 6	3.35 mm	97.5	63
No. 8	2.36 mm	–	20
No. 16	1.18 mm	2.5	2.5

3.1.3 Test Slab Friction and Texture Tests and Analysis

The surface friction and texture were measured in accordance with the ASTM E1911-09 (2009) dynamic friction tester (DFT) and the ASTM E2157-09 (2009) circular track meter (CTM), respectively. Table 3.2 presents the detailed test results for all test slabs. The surface

Figure 3.2 Test slabs for accelerated polishing: No. 4 calcined bauxite, No. 6 calcined bauxite, and No. 8 steel slag (left to right).

texture was measured as the mean profile depth (MPD) before and after polishing. Because the friction was too high and out of scale with the ASTM E1911 DFT, the surface friction was only measured after polishing as DFT friction coefficients for speeds of 20 and 40 km/h, respectively. It is shown that the No. 6 calcined bauxite test slabs reached the terminal polishing condition after 100,000 cycles. The terminal polishing conditions occurred after approximately 80,000 polishing cycles for both the No. 4 calcined bauxite and No. 8 steel slag test slabs, respectively. Figure 3.3 shows the two worn out test tires with through holes due to polishing. This can be extended to indicate that coarse, uniform-sized hard aggregate, in particular calcined bauxite, will produce a harsh surface that could raise concerns about excessive tire wear. Notice that no sign of aggregate loss occurred on the surface of any test slab after polishing.

Before polishing, the No. 8 steel slag system and No. 4 calcined bauxite system demonstrated an average MPD of 2.27 mm and 2.26 mm, respectively. The No. 6 calcined bauxite system demonstrated an average MPD of 1.97 mm, approximately 0.30 mm less than the average MPD values for the No. 8 steel slag system and No. 4 calcined bauxite system. The MPD values for the No. 6 calcined bauxite and No. 8 steel slag systems before polishing agreed closely with those for the calcined bauxite and steel slag reported by Heitzman, Turner, and Greer (2015), while the load applied to the surface of test slab in the referenced study was 405 N (91 lbs.) and much less than that in the current study. The No. 8 steel slag system and No. 4 calcined bauxite HFST system provided similar MPD values before polishing. In addition, larger aggregate tends to produce greater macrotexture MPD than smaller aggregate for such friction surface treatment systems. After polish conditioning, all three friction treatment systems demonstrated a reduction in MPD. The average MPD values decreased to 1.81 mm, 1.86 mm, and 1.53 mm for the No. 8 steel slag, No. 4 calcined bauxite, and No. 6 calcined bauxite systems, respectively. On average, the No. 8 steel slag, No. 4 calcined bauxite, and No. 6 calcined bauxite systems, respectively, experienced a reduction of approximately 20%, 18%, and 22% in MPD.

For surface friction, the two No. 8 steel slag test slabs demonstrated an average DFT friction coefficient of 0.918 at 20 km/h (or 0.923 at 40 km/h). The average DFT friction coefficient was 0.961 at 20 km/h (or 0.966 at 40 km/h) for the two No. 4 calcined bauxite test slabs. The two No. 6 calcined bauxite test slabs produced an average DFT friction coefficient of 0.960 at 20 km/h (or 0.973 at 40 km/h). The friction differences at the terminal polishing condition are not significant

TABLE 3.2
Texture and Friction Measurements before and after Polishing

Friction Treatment System	Slab No.	Substrate	Polishing Revolutions	CTM MPD (mm)		DFT Friction Coefficient (after)	
				Before	After	20 km/h	40 km/h
One-course No. 8 Steel Slag	1	HMA	80,000	2.17	1.66	0.910	0.926
	2	HMA	80,000	2.37	1.95	0.926	0.919
One-course No. 4 Calcined Bauxite	1	PCC	85,348	2.16	1.87	0.952	0.951
	2	PCC	73,600	2.37	1.84	0.969	0.980
One-course No. 6 Calcined Bauxite	1	PCC	100,000	1.94	1.57	0.980	0.995
	2	PCC	100,000	2.01	1.49	0.939	0.951

Figure 3.3 Worn out test tires by No. 8 steel slag and No. 4 calcined bauxite (left to right).

between the three friction surface treatments. It can be concluded that after polishing condition, the No. 8 steel slag, No. 4 calcined bauxite, and No. 6 calcined bauxite treatment systems might, respectively, experience an average reduction of at least 8%, 4%, and 4% in terms of DFT friction at 20 km/h. It was also noted that the friction measurements for the steel slag and calcined bauxite treatments agreed, well with the DFT friction measurements for No. 8 calcined bauxite and steel slag measured in the LAB-2 study as reported by Heitzman et al (2015). It is obvious that smaller aggregate tends to experience greater reduction in MPD. Nevertheless, a friction surface treatment such as HFST with larger surface MPD does not necessarily produce greater surface friction.

3.2 Field Traffic Polishing and Friction Evaluation

3.2.1 Test Strips and Field Placement

The method of test strip was utilized for evaluating the friction surface treatments under the polishing by actual traffic. This method can provide advantages including low cost, large variety of test parameters, same traffic and environment, and easy implementation, and has also been used for field evaluation elsewhere (Denning, 1977, 1978). As illustrated in Figure 3.4 are the six rectangular test strips placed in the driving lane of a composite curve segment on US-52, two for each of the three friction surface treatments, including one-course No. 8 steel slag system, and one-course No. 6 calcined bauxite HFST system, and two-course No. 6 calcined bauxite HFST system. This road segment consisted of four lanes in two directions, carrying an annual average daily traffic (AADT) of 7,952 with 12% of commercial trucks. The posted speed limit is 55 mph. The No. 4 calcined bauxite HFST system evaluated in the laboratory was not included due to the concerns about potential damage to vehicle tires and need for more binder. Nevertheless, a two-course No. 6 calcined bauxite HFST system was included to compare the durability and long-term friction performance with the one-course No. 6 calcined bauxite HFST system.

These test strips were placed around 11:40 am on September 16, 2015. The second application for the two-course No. 6 calcined bauxite HFST system was made approximately three hours after the first application. The existing pavement was HMA pavement with an average MPD of 0.781 mm. All test strips were placed by following the application sequence used to prepare the test slabs for the laboratory polishing and evaluation presented in the preceding sections. During placement, the air temperature varied approximately between 74 and 83 8F and the wind speed varied between 8 and 16 km/h. Each test strip was 1,016 mm (40″) long and 381 mm (15″) wide. The dimensions of the test strip were determined to provide a surface not only large enough for conducting the DFT friction and CTM texture tests, but also large enough for making sure all vehicles in the driving lane would drive over the test strips. For each friction treatment system, one of the two test strips was placed in the right wheel track and the other was placed in the left wheel track.

3.2.2 Test Strip Friction and Texture Test Results and Analysis

Figure 3.5 presents the CTM MPD and DFT friction measurements on the three friction treatment systems before traffic application and those taken on December 11, 2015 and June 21, 2016, i.e., after three and nine months of service, respectively. Because the road segment was scheduled for chip seal in July 2016, the final field testing was carried out after nine months rather

Figure 3.4 One-course No. 8 steel slag, one-course No. 6 calcined bauxite, and two-course No. 6 calcined bauxite test strips (front to back).

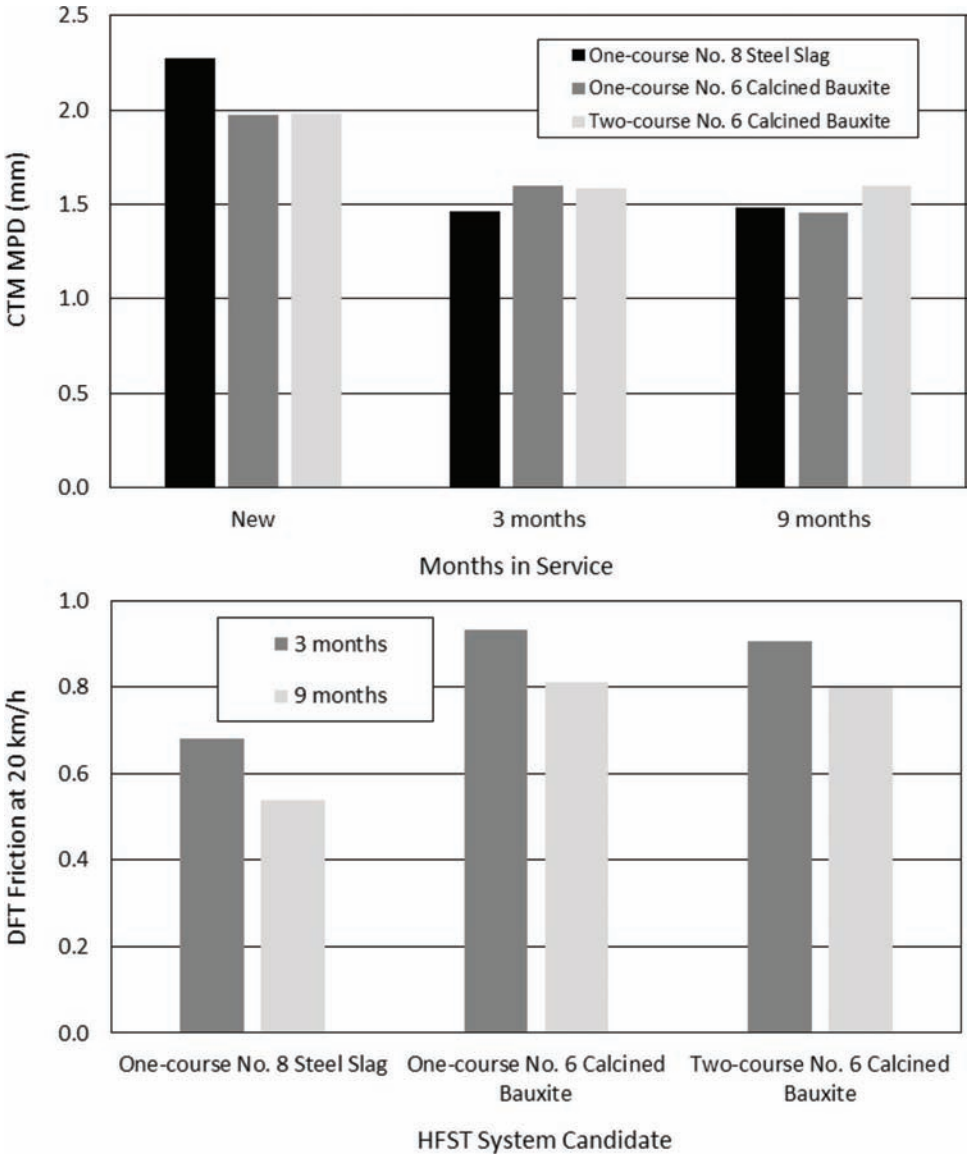

Figure 3.5 CTM MPD and DFT friction measurements on field test strips over time.

than twelve months of service. However, it was estimated that the test strips would be subjected to polishing by at least 800,000 vehicles including approximately 100,000 trucks during the period of nine months. In addition, this period of time covered the entire snow and ice season of 2015 to 2016. Therefore, it became possible to assess the potential effects of environmental variation and snow plowing, in particular, on the bonding between the existing pavement and test trips. For each test strip, two measurements were taken for the CTM MPD and DFT friction, respectively. Notice that the CTM MPD and DFT friction coefficient presented in Figure 3.5 are the average of the corresponding measurements taken on the two test strips for each system.

Two main observations can be made by careful inspection of the CTM MPD and DFT friction measurements in Figure 3.5. First, the MPD measurements for all three of the friction treatment systems demonstrated a noticeable reduction after three months of service. The MPD over the first three months decreased on average by approximately 36%, 19%, and 20% for the one-course No. 8 steel slag, one-course No. 6 calcined bauxite, and two-course No. 6 calcined bauxite systems, respectively. However, the MPD measurements for all three of the friction treatment systems remained very stable over the last six months. While the three friction treatment systems demonstrated different MDP measurements, the differences were not significant after nine months of service. The average MPD measurements were 1.49, 1.46, and 1.60 mm after nine months of service for the one-course No. 8 steel slag, one-course No. 6 calcined bauxite, and two-course No. 6 calcined bauxite systems, respectively. The average reductions in MPD are 35%, 26%, 19% for the one-course No. 8 steel

slag, one-course No. 6 calcined bauxite, and two-course No. 6 calcined bauxite systems, respectively.

Second, all three of these friction treatment systems experienced some reductions in DFT friction after being in service. The average DFT friction coefficients were 0.682, 0.932, and 0.905 at 20 km/h (0.688, 0.950, and 0.893 at 40 km/h) after three months of service, and 0.540, 0.812, and 0.798 at 20 km/h (0.555, 0.801, and 0.779 at 40 km/h) after nine months of service for the No. 8 steel slag, one-course No. 6 calcined bauxite, and two-course No. 6 calcined bauxite systems, respectively. This implies that the one-course No. 8 steel slag system demonstrated the greatest friction reduction that was at least 31% and 45% in terms of DFT friction at 20 km/h after three and nine months of service, respectively. The one- and two-course No. 6 calcined bauxite systems, respectively, experienced a friction reduction more than 6% and 9% after three months of service, and more than 18% and 20% after nine months of service. However, the DFT friction coefficient for the two-course calcined bauxite system is slightly less than that for the one-course calcined bauxite system. The two-course No. 6 calcined bauxite system did not outperform the one-course No. 6 calcined bauxite system in terms of DFT friction after being in service. This can be extended to indicate that a friction surface treatment with larger surface MPD does not necessarily produce better long-term surface friction performance.

It should also be pointed out that the long-term friction performance, particularly the DFT friction under laboratory polishing was noticeably different from that under true traffic polishing. Under laboratory three wheel polishing condition, both steel slag and calcined bauxite demonstrated similar friction performance. Under field true traffic polishing, however, calcined bauxite demonstrated better friction performance than steel slag. Evidently, the friction surface under field traffic polishing decreased more rapidly than those under laboratory three wheel polishing condition for both steel slag and calcined bauxite systems. Moreover, a comparison between the aggregate mechanical properties (see Tables 2.3, 2.3, and 2.4) and DFT friction in Figure 3.5 indicates that the treatment surface friction was related to LAA, Micro-Deval abrasion, and polish value PV-10. Nevertheless, LAA, Micro-Deval abrasion, and PV-10 affected the surface friction to different extents.

3.3 Examination of Test Strip Integrity

3.3.1 Bonding between Test Strip and Substrate Surface

Delamination of a friction surface treatment such as HFST from existing pavement may not only cause voids between the treatment and existing pavement, but also cause cracks in the overlying treatment layer. This may particularly be true when the treatment is placed on an asphalt pavement due possibly to two main reasons. First, asphalt binder may affect the bond between the epoxy resin binder and the existing surface. Second, surface deflection under traffic loading and thermal movement tend to repeat in asphalt pavement and may break the bond between the treatment and existing pavement. As a result, debonding may occur between the treatment and existing asphalt pavement, which will lead to treatment delamination. In order to evaluate the bond between the friction surface treatments and existing pavements, pull-off tests were performed on the test slabs for laboratory three wheel polishing and test trips for field traffic polishing, respectively, to determine the adhesive strength of the epoxy resin binder used in the current study. Presented in Table 3.3 are the summary of the test results.

For the pull-off tests performed on the test slabs for three wheel polishing, it is shown that the adhesive strength was greater on concrete substrate than on HMA substrate. However, the adhesive strength was a bit lower than anticipated. In addition, great variation occurred in the adhesive strength obtained from the test results on the concrete substrates. As illustrated in the left photo in Figure 3.6 is the typical failure mode for the pull-off tests on the test slabs used for the laboratory tests. The failure occurred partially in the epoxy adhesive and partially at the interface between the disk and epoxy adhesive probably due to the reuse of steel disks in the test. Consequently, the cross-section of the broken specimen had an irregular shape. However, the adhesive strength was still calculated using the area of steel disk surface, leading to greater variation and lower adhesive strength. For the pull-off tests performed on the field test strips, the failure occurred in the substrate near the surface (see the right photo in Figure 3.6) for all tests. It is well known that the mechanical properties of HMA mix vary significantly with temperature. The pull-off tests were performed on a sunny day in

TABLE 3.3
Summary of Pull-off Test Results

Polishing Condition	Friction Treatment System	Substrate	Failure Mode	Adhesive Strength (psi/MPa)
Laboratory Three Wheel	No. 8 Steel Slag	HMA	Partial	106/0.73
	No. 6 Calcined Bauxite	Concrete	Partial	276/1.90
	No. 4 Calcined Bauxite	Concrete	Partial	223/1.54
US-52 Field Traffic	No. 8 Steel Slag (One-course)	HMA	In substrate	40/0.276
	No. 6 Calcined Bauxite (One-course)	HMA	In substrate	44/0.303
	No. 6 Calcined Bauxite (Two-course)	HMA	In substrate	66/0.455

September 2016, and the existing pavement surface temperature was up to 103 °F (39 8C) during testing. Therefore, the tensile strength of the substrate (existing asphalt surface layer) might decrease significantly. Accordingly, the results of the pull-off tests measured the tensile strength of the substrate mix rather than the bonding between the test strip and substrate pavement surface.

3.3.2 Distresses in Test Strips

Visual inspection was conducted periodically over the evaluation period of nine months. Presented in Figure 3.7 is a photo taken during the field inspection in September 2016. All test strips remained intact, and no progressive aggregate loss was observed after nine months of service, including traffic, winter weather, and snow plowing. As an experimental effort, thermal imaging was utilized to detect possible anomalies in and underneath the test trips. Presented in Figure 3.8 are the thermograms of the three test strips produced using an infrared camera after pull-off testing. It is very hard to provide an accurate interpretation of the thermogram. However, these three thermograms were fairly uniform in color. This may imply that there were probably no voids or cracks in and beneath the test strips.

3.4 Recommended Requirements for HFST Surface Friction Performance

3.4.1 Current Highway Agencies' Requirements

It has been widely recognized that pavement friction varies with pavement texture, speed, and tire (Henry, 2000; Li, Noureldin, & Zhu, 2004, 2010). Pavement friction depends on both macro- and micro-texture. The former varies with the void and aggregate geometric properties (shape and size) and becomes dominant at high speed or when pavement surface is wet. The latter varies with the feature of aggregate surface and prevails at low speed or when pavement surface is smooth and dry. ASTM E 274 provides two standard test tires such as ribbed tire and smooth tire (ASTM E274M-15, 2015; ASTM E501-08, 2015; ASTM E524-08, 2015). The friction measurement using a smooth tire is sensitive to both macro- and microtexture. The friction measurement using a ribbed tire, however, is insensitive to macrotexture, but is dominated by microtexture. In addition, both macro- and microtexture plays an important role in preventing hydroplaning by discharging bulk water and penetrating water film between tire and pavement surface.

Presented in Table 3.4 are the specification requirements for the surface friction of HFST system developed

(a) Partial failure (test slab, laboratory)

(b) Substrate failure (test strip, field)

Figure 3.6 Steel disks after pull-off tests.

Figure 3.7 Field test strips after nine months of service.

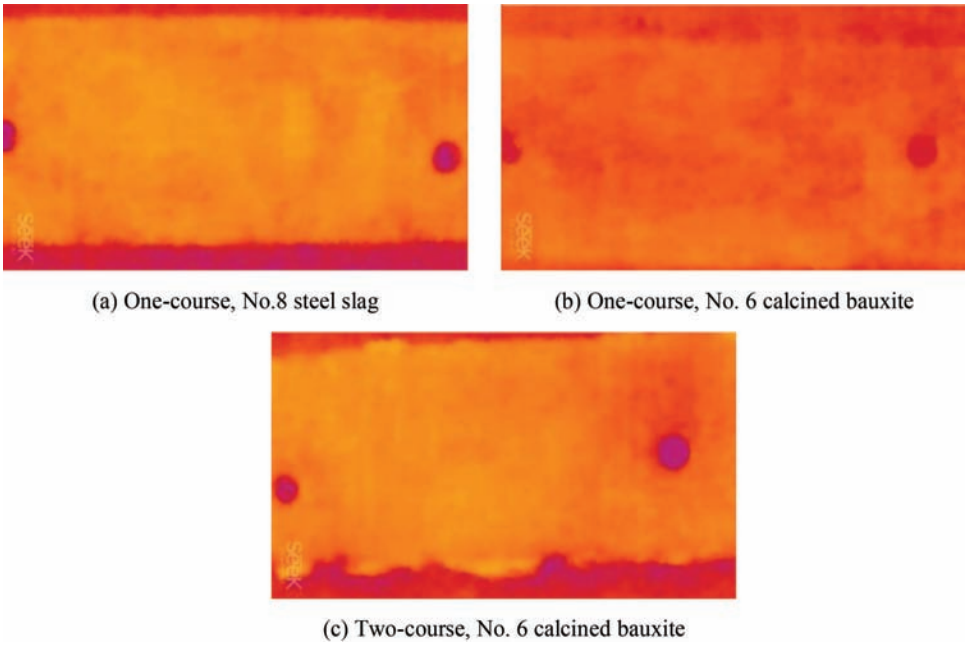

(a) One-course, No.8 steel slag

(b) One-course, No. 6 calcined bauxite

(c) Two-course, No. 6 calcined bauxite

Figure 3.8 Thermograms of steel slag and calcined bauxite test strips.

TABLE 3.4
Current State DOTs' Requirements for HFST Surface Friction

	Requirement		
Agency/State DOT	**Friction Number[a] ASTM E 274**	**DFT Friction ASTM E 1911**	**MPD (mm) ASTM E 2157/ E965**
AASHTO	65	–	–
Alabama	65[a]	–	–
Alaska	–	0.75	–
California	–	0.75	–
Florida	65 (90 days)	–	–
Georgia	65 (90 days)	–	–
Illinois	72 (60 days)	0.90 (20 km/h)	1.0 (60 days)
Iowa	60 (90 days)	–	–
Pennsylvania	65 (90 days)	–	–
South Carolina	70 (90 days)	–	–
South Dakota	72	0.90	1.0
Tennessee	70	–	1.0
Texas	65	–	–
Virginia	55 (90 days)	–	–

[a]All friction numbers except for that by Virginia DOT are measured with a standard ribbed tire. The friction number for Virginia DOT is measured with a standard smooth tire.

by 14 agencies, including AASHTO (AASHTO PP 79-14, 2014) and 13 state DOTs (Alaska DOT, 2004; ALDOT, 2014; Caltrans, 2014; FDOT, 2014; GDOT, 2009; IDOT, 2014; Iowa DOT, 2011; PennDOT, 2014; SCDOT, 2010; SDDOT, 2014; TDOT, 2015; TxDOT, 2014; VDOT, 2012). Four observations can be made through careful inspection of the requirements for HFST. First, three agencies (Illinois, South Dakota, and Tennessee DOTs) provide a minimum requirement in terms of both surface friction and texture depth, and all other agencies provide a minimum requirement in terms of surface friction only. Second, the requirements for surface friction are measured in terms of either DFT friction coefficient or ASTM E 274 friction number, or both. Third, for these agencies with ASTM E 274 friction requirements, only Virginia DOT uses the standard smooth tire, and the other agencies use the standard ribbed tire. Fourth, seven agencies indicate that friction testing should be conducted after 60 or 90 days, and the remaining agencies do not have specific time for acceptance testing. In general, the required DFT friction and MPD are less than the corresponding test results obtained in the current study.

DFT friction testing can be conducted in the laboratory and in the field. The disadvantage associated with the DFT friction coefficient is that it is usually

reported at a test speed of 20 km/h and relies to great extent on the microtexture. This indicates that DFT friction coefficient may not fully characterize the friction performance of a surface treatment such as HFST. It is necessary to provide a requirement for MPD together with the DFT friction requirement. If the friction requirement is established in terms of ASTM E 274 friction number, it is advisable to use the standard smooth tire during testing. A friction number measured using the stand smooth tire is capable of fully assessing the friction performance of HFST. However, ASTM E 274 friction testing can only be used in the field for a pavement segment of at least thirty meters (ninety feet) long. In addition, the MPD measurements in the current study revealed that the surfaces of test strips remained stable after three months of service. This confirms that the friction acceptance testing should be conducted approximately 90 days after being in service.

Presented in Table 3.5 are the recommended aggregate gradations for friction surface treatments. There is a slight difference between the recommended gradation and the gradation specified in AASHTO PP 79-14 for calcined. A requirement for passing No. 30 sieve is added to limit the amount of very fine particles, in particular fillers (passing No. 200 sieve) that may affect the bond between aggregate and epoxy binder. As recommended in Table 3.6 are the requirements (lower bounds at a confidence level of 95%) for frictional performance of friction surface treatment in terms of DFT friction coefficient and macro-texture MPD. Due to lack of reliable, first hand data, no friction requirement is recommended in terms of ASTM E 274 friction number at this stage. However, this will be available in a couple of years when the evaluation of field full-scale test sections is completed.

TABLE 3.5
Recommended Aggregate Gradations for Friction Surface Treatments

(a) No. 6 Calcined Bauxite	
Sieve Size	**Passing %**
No. 4 (4.75 mm)	100
No. 6 (3.35 mm)	95~100
No. 16 (1.18 mm)	0~5
No. 30 (0.6 mm)	0~1
(b) No. 8 Steel Slag	
Sieve Size	**Passing %**
No. 4 (4.75 mm)	100
No. 8 (2.36 mm)	25~65
No. 16 (1.18 mm)	0~5
No. 30 (0.6 mm)	0~1

TABLE 3.6
Recommended Requirements for Frictional Performance

Property	**Test Method**	**No. 6 Calcined Bauxite**	**No. 8 Steel Slag**
DFT Friction Coefficient @20 km/h, 90 days	ASTM E 1911	0.90 min	0.65 min
MPD (mm), 90 days	ASTM E 2157 or E 965-15 (2015)	1.45 max	1.35 min

4. LONG-TERM FRICTION PERFORMANCE OF PAVEMENT PRESERVATION TREATMENTS

4.1 Pavement Preservation Treatments

4.1.1 INDOT Pavement Preservation Program

INDOT (n.d.) manages and maintains more than 11,000 centerline miles of interstate highways, US highways, and state routes. It is recognized that regularly scheduled preservation and maintenance activities preserve and protect pavement and bridges, extending the life of these assets. In the period of 2017 to 2021, INDOT plans to invest more than $1.75 billion on pavement preservation work, including pavement surface preservation treatment, crack sealing, pothole repair, and storm water drainage maintenance. As illustrated in Figure 4.1 is the breakdown of pavement preservation work such as chip seal, ultrathin bonded wearing course (UBWC), microsurfacing, 4.75-mm hot mix asphalt (HMA) thin overlay, and concrete pavement restoration (CPR) by INDOT Greenfield District during 2009–2014. Chip seal made up more than 80% of the total preservation treatment work. CPR work mainly involves different techniques such as joint or crack sealing, dowel bar retrofit, partial- or full-depth repair, and diamond grinding. Diamond grinding has been typically employed to restore surface friction for not only polished concrete pavements, but also polished bridge concrete decks.

4.1.2 Selection of Preservation Treatments for friction Restoration

The selection of preservation treatments for friction restoration was made to align with INDOT's pavement preservation plan. Historical friction data was used to validate the friction performance for different preservation treatments. Consequently, four preservation treatments, including chip seal, UBWC, microsurfacing, and diamond grinding, were considered for friction restoration. In order to develop definitive, long-term friction performances for these treatments, a total of 31 test sections, including 18 chip seal sections, five microsurfacing sections, four UBWC sections, and four diamond grinding sections from a previous study completed in 2011 (Li, Noureldin, Jiang, 2012), were selected by taking into consideration the aggregate size and type, annual average daily traffic (AADT) and truck %, historic friction data availability, and treatment age. The 2011 study mentioned above aimed to provide INDOT pavement engineers with original data on pavement preservation treatments and materials.

Notice that the unit prices shown in Table 4.1 were estimated with respect to the actual construction costs completed by INDOT during the period of 2007 to

2012. Chip seal is the lowest-cost treatment option. Peshkin et al. (2011) evaluated the effects of traffic level, pavement condition, and climate on the pavement preservation treatment performances. They further summarized the expected life ranges as shown in Table 4.1 for different preservation treatments based on the information reported by various sources. Peshkin et al. (2011) also indicated that the life ranges represented a variety of conditions and reported using different performance measures. They further cautioned that these reported ranges may be based as much (or more) on perception instead of on well-designed, quantitative, experimental analyses. It is shown that UBWC is capable of providing a service life of 7–12 years. Chip seal has a service live of 3–7 years. Microsurfacing has a service live of 3–6 years. Diamond grinding may provide a service life up to 15 years.

4.2 Chip Seal Surface Friction

4.2.1 Test Sections

Table 4.2 shows the detailed information such as aggregate type and size, AADT and truck %, and construction time for the 18 chip seal test sections. These sections consist of regular chip seal and fog-chip seal. The fog-chip seal is a combination of a regular chip with a fog seal (0.11 gal/yd^2) applied onto the regular chip seal (Lee & Shields, 2010). All chip seal test sections utilized crushed stone (limestone) aggregates except for the two test sections, including one on SR-341 and the other on US-150, which utilized crushed gravel aggregates. In addition, the chip seal test section on SR-159 consisted mainly of naturally formed chips. The three aggregate gradations commonly used for chip seal by INDOT are presented in Table 4.3. All these three gradations have the same maximum aggregate size, i.e., 12.5 mm. However, No. 11 aggregate contains much more particles of 4.75~12.5 mm than both No. 12 and No. 16 aggregates. Also, No. 16 aggregate contains more aggregate particles of 4.75~9.5 mm than No. 12 aggregate.

4.2.2 Friction and Variation

Figure 4.2 presents the statistics of the friction measurements made on a total of fifteen new chip seal surfaces, i.e., around 30 days after chip seal placement. The solid bar represents the average friction number (Mean) and the empty bar represents the coefficient of variation (COV). The average friction numbers are 61, 49, and 49, for new regular chip with crushed stone, new chip seal with crushed gravel, and fog-chip seal with stone, respectively. Three main observations can also be made through careful inspection of the statistics

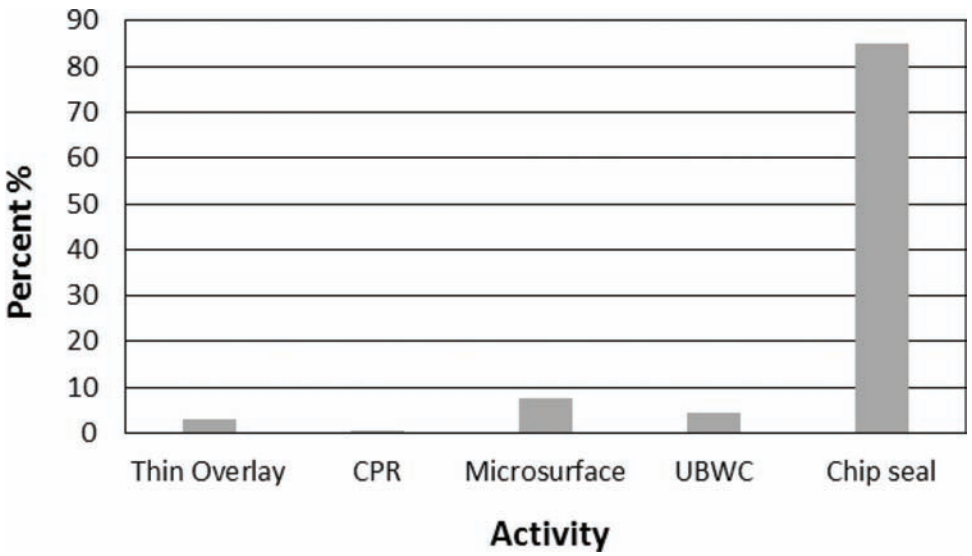

Figure 4.1 Breakdown of pavement surface preservation treatment work.

TABLE 4.1
General Information on Test Sections

Treatment	Expected Life (years) (3)	Unit Price ($/SQY)	AADT	Truck (%)	Age (years)
Chip Seal, 1 course	3~7	1.10	730~6300	5~47	4~7
Microsurfacing, 1 course	3~6	3.62	1700~15600	3~12	7~9
UBWC	7~12	6.44	1000~17400	2~7	7~9
Diamond Grinding	8~15	25.00[a]	5000~33000	6~30	3~10

[a]Bridge deck jobs, including diamond grinding, mobilization, and traffic control.

TABLE 4.2
Information for Chip Seal Test Sections

Treatment	Road	Aggregate		Length (miles)	AADT	Truck (%)	Time Placed
		Size	Type				
CS[a]	SR-32	11	Crushed stone	8.24	732	8.9	08/2007
CS	SR-129	11	Crushed stone	6.5	5892	4.8	07/2007
CS	SR-341	11	Crushed gravel	12.9	955	8.1	07/2009
CS	SR-10	12	Crushed stone	6.3	3372	47.2	07/2007
CS	SR-19	12	Crushed stone	8.9	6129	9.7	07/2007
CS	US-421	12	Crushed stone	9.0	4527	23.5	07/2008
CS	SR-14	12	Crushed stone	14.9	1530	18.3	07/2008
CS	US-150	16	Crushed gravel	12.7	2450	6.4	07/2009
CS	SR-246	16	Crushed stone	4.0	902	8.5	06/2010
CS	SR-159	16	Natural stone	4.0	2467	9.7	06/2010
FCS[b]	US-36	11	Crushed tone	7.7	2085	15.8	10/2008
FCS	US-52(a)	11	Crushed stone	10.3	6307	7.2	10/2008
FCS	US-52(b)	11	Crushed stone	8.70	1531	9.8	07/2009
FCS	SR-11	11	Crushed stone	18.4	1656	4.5	08/2009
FCS	SR-48	11	Crushed stone	7.0	1410	8.5	08/2009
FCS	SR-101	12	Crushed stone	2.1	1047	19.4	08/2008
FCS	SR-67	12	Crushed stone	8.7	2110	39.6	05/2009
FCS	SR-9	12	Crushed stone	6.0	3161	10.8	08/2009

[a]CS = regular chip sea.
[b]FCS = fog-chip seal.

TABLE 4.3
Aggregate Gradations for Chip Seal

Size	Percent Passing (%)						
	1/2″ (12.5 mm)	3/8″ (9.5 mm)	No. 4 (4.75 mm)	No. 8 (2.36 mm)	No. 16 (1.18 mm)	No. 30 (600 μm)	Decant
11	100	75–95	10–30	0–10	–	–	0–2.5
12	100	95–100	50–80	0–35	–	0–4	0–2.5
16	100	94–100	15–45	–	0–4	–	0–2.5

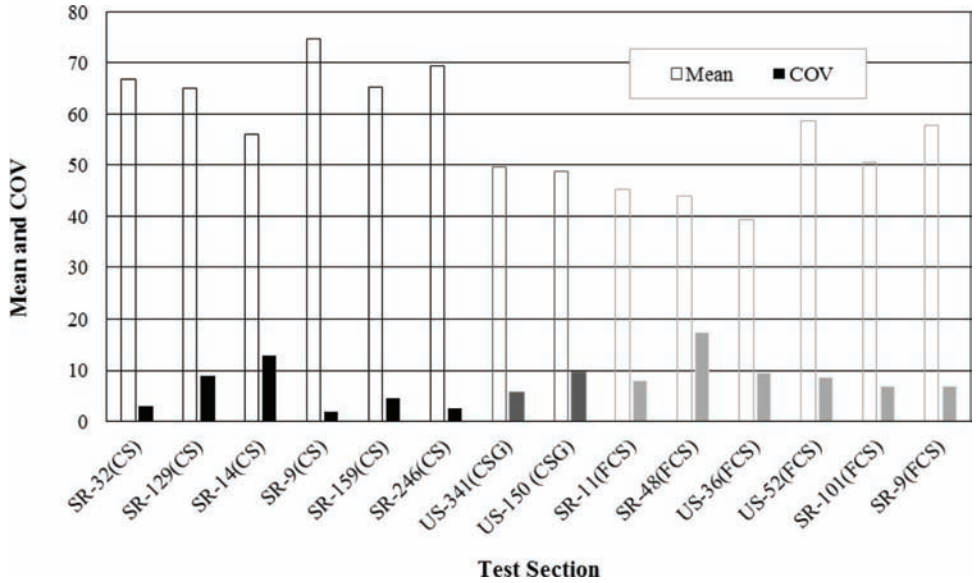

Figure 4.2 Friction measurements on new chip seal surfaces.

(CS=regular chip seal, stone; CSG=regular chip seal, gravel; and FCS=fog-chip seal, stone)

of the friction measurements. First, new regular chip seals produced higher friction numbers and lower variations than new fog-chip seals. Applying a fog seal onto a new chip seal tends to reduce the surface friction by approximately 25%. Second, the chip seals using crushed stone demonstrated friction numbers approximately 25% greater than the chip seals using crushed gravel. Third, there is no clear trend that indicates the possible effect of aggregate sizes used in the test sections on the friction performance of a new chip seal surface.

Presented in Figure 4.3 are the friction numbers measured in the regular chip seal and fog-chip seal test sections over time. The friction number for regular chip seal decreased rapidly in the first 12 months, and then slowly over time. The friction number for fog-chip seal, however, increased in the first six months, and then decreased in the next six months. Afterwards, the friction number decreased slowly over time. The above confirms a finding reported elsewhere (Lee, Shields, Noureldin, & Jiang, 2012), i.e., it takes about 12 months for chip seal to form a stable mosaic surface. While the friction measurements fluctuated over time and from section to section, the friction variations in both the regular chip seal and fog-chip seal test sections followed a similar trend. In the three test sections, including two regular chip seals on SR-10 and US-421 and a fog-chip seal on US-36, the friction decreased rapidly in the first 12 months to a value of 20~25 that may indicate chip seal failure due to excessive chip loss, or bleeding, or both (Lee, Shields, et al., 2012).

It is also shown that all regular chip seals except for the two failed test sections demonstrated a friction number of around 30 and greater after 60 months in service. This simply indicates that a successful chip seal is capable of providing satisfactory friction performance for a period of five years or more. While only 50 months of friction measurements are available for the fog-chip seal, the trend of friction variation over time may be extended to imply that a successful fog-chip seal can provide a service life comparable to that of a regular chip seal with respect to friction performance. The above

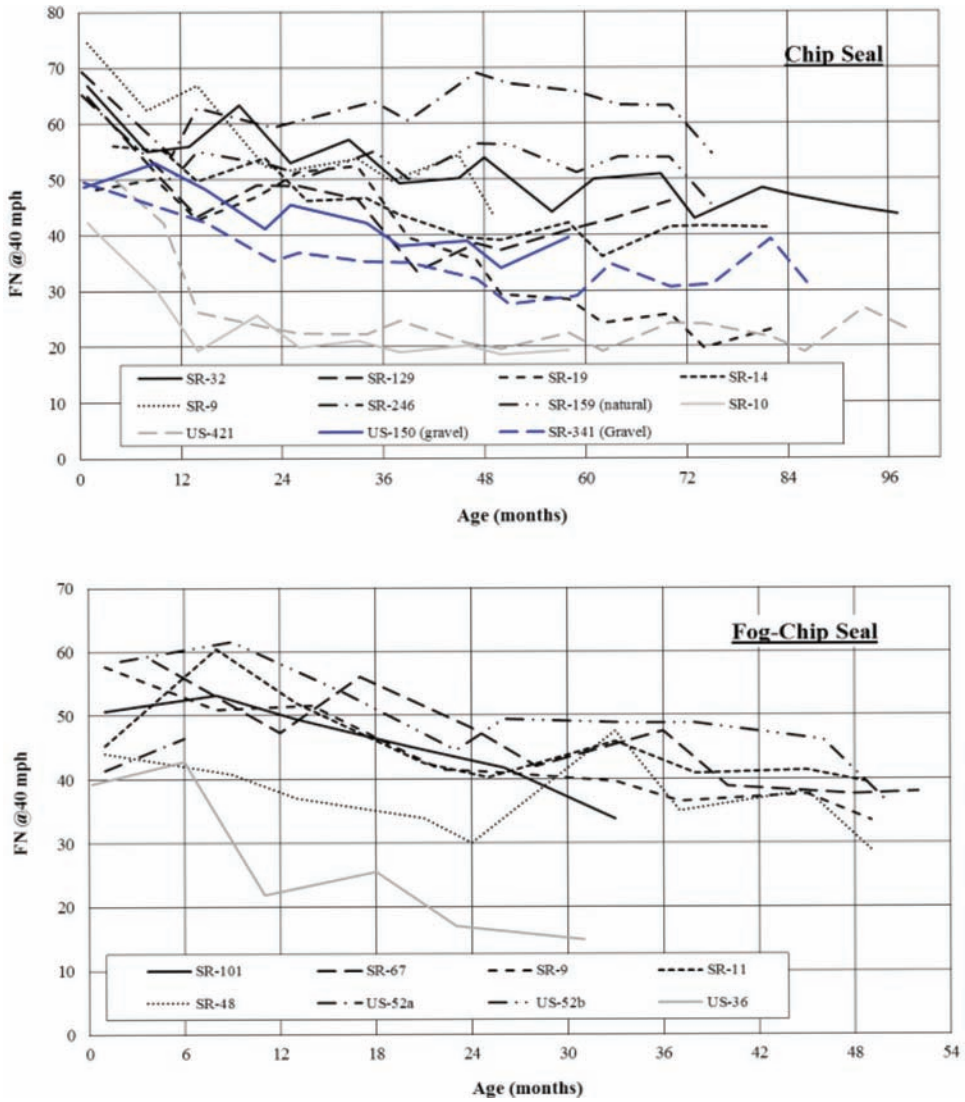

Figure 4.3 Chip seal surface friction measured over time.

may be utilized to conclude that a successful chip seal should provide an expected life no less than five years with respect to friction performance. Provided in Eq. 4.1 is a general form of regression model developed for estimating friction performance of regular chip seal with crushed stone, regular chip seal with crushed gravel, and fog-chip seal with crushed stone. Notice that all friction regression models were developed with respect to the mean values of friction measurements, i.e., 50% reliability.

$$FN = k_1 e^{-k_2 t} \quad (4.1)$$

in which, k_1 and k_2 are the regression constants depending on factors such as type of chip seal, type of aggregate, surface uniformity, and traffic. For regular chip seal with crushed stone, k_1=58.5 and k_2=-0.0047. For regular chip seal with crushed gravel, k_1=47.0 and k_2=-0.0055. For fog-chip seal with crushed stone, k_1=51.8 and k_2=-0.0068. Notice that the correlation coefficient=-0.4732, -0.7534, and -0.6086 for these three regression models. The negative correlation coefficients simply indicate a negative correlation between chip seal surface friction and service age.

4.3 Microsurfacing Surface Friction

4.3.1 Test Sections

Presented in Table 4.4 are the detailed information for the five microsurfacing test sections, including aggregate class and type, AADT and truck %, and construction time. All these five test sections utilized aggregates of Class A that requires a Los Angeles abrasion (LAA) value of 40% max., a brine freeze and thaw soundness of 30% max., a sodium sulfate soundness of 12% max., and a minimum of 70% crushed particles (INDOT, 2014). The aggregate used in the test section on SR-227 is a crushed limestone. The test sections on SR-22 and SR-28 utilized a blend of limestone and steel slag (1:1) due to high traffic. The blended aggregate demonstrated smaller LAA and larger sand equivalency than pure limestone aggregate. The test sections on SR-70 and SR-56 also used same limestone aggregate. However, the limestone source was different from that used in SR-227. Figure 4.4 shows the aggregate gradations for the aggregates used in the test sections. All gradations were very similar. The maximum aggregate size was 9.5 mm. Particles larger than 4.75 mm accounted for no more than 5% of the total aggregate.

4.3.2 Friction and Variation

Plotted in Figure 4.5 are the surface friction measurements made in these five microsurfacing test sections over a time period of up to 107 months. In general, microsurfacing friction increased in the first 12 months, and afterwards, decreased very slowly. For the two test sections including SR-227 and SR-70 with traffic volume less than 2000 AADT, the friction numbers fluctuated between 50 and 60 over a time period of eight years. While the two test sections on SR-22 and SR-28, respectively, used the same blended aggregate, the friction number on SR-28 was approximately 8 digits less than that on SR-22. This may be attributed to the effect of truck traffic. The test sections on SR-28 and SR-22, respectively, experienced an AADT of 7578 and 15596, and a truck traffic of 840, and 500 per day. The test section on SR-56 used pure limestone aggregate, but experienced an AADT and a truck traffic volume between those on SR-28 and SR-22. However, the friction number in the test section on SR-56 was approximately 5 digits larger than those on SR-28 and SR-22 that used a blended aggregate of limestone and steel slag. The above may imply the combined effects of AADT, truck traffic, and aggregate.

Overall, microsurfacing demonstrated very stable surface friction over time. In addition, the comparison between the microsurfacing surface friction and the chip seal surface friction (see Figure 4.3) seems to indicate that microsurfacing is capable of provide more

TABLE 4.4
Information for Microsurfacing Test Sections

Item	SR-227	SR-22	SR-28	SR-70	SR-56
AADT	1964	15596	7578	1744	10320
Truck %	3.9	3.2%	11.1	11.8	6.6
Construction	10/2009	10/2007	07/2008	07/2008	10/2008
Aggregate Class	A	A	A	A	A
Aggregate Type	LS1[a]	BLS[b]	BLS	LS2[c]	LS2
LAA, %	28.6	21.0	21.0	N.A.	N.A.
Sodium Sulfate Soundness, %	1.8	N.A.	N.A.	N.A.	N.A.
Brine Freeze-Thaw Soundness	1.6	3.9	3.9	3.0	3.0
Sand Equivalency, %	79	81	81	73	73
Fractured Particles, %	100	100	100	100	100

[a]LS1 = limestone of source #2363.
[b]BLS1 = blended LS1 and steel slag of source 2791.
[c]LS2 = limestone of source #2540.

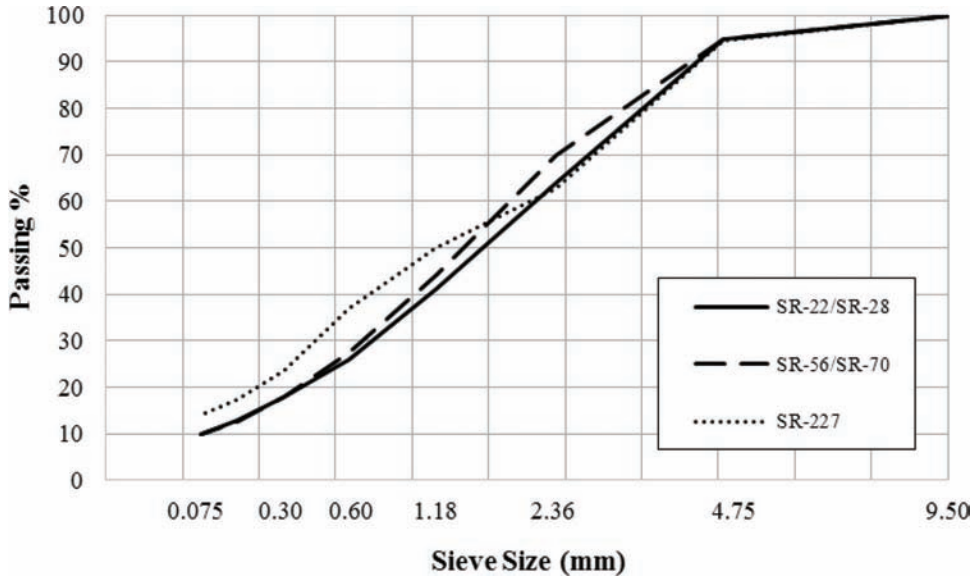

Figure 4.4 Aggregate gradations for microsurfacing test sections.

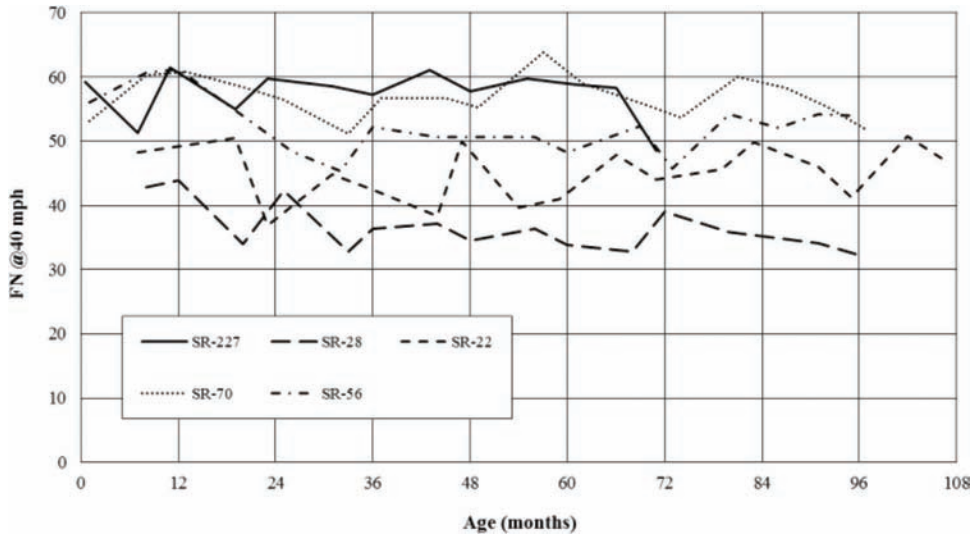

Figure 4.5 Microsurfacing surface friction measured over time.

durable, larger surface friction than chip seal for a wide range of traffic volume over a time period of eight years or more. Figure 4.6 shows the regression models developed for predicting the surface friction of microsurfacing with a traffic volume no less than 7000 AADT and no greater than 2000 AADT, respectively. Notice that for the microsurfacing experiencing a traffic volume between 2000 and 7000 AADT, the surfacing friction may be approximated using linear interpolation based on the two models shown in Figure 4.6. It is shown that both models have a negative, poor correlation between surface friction and service age. Therefore, the effect of service age on surface friction is not significant for microsurfacing within a certain traffic volume category. The above may also be extended to confirm again that microsurfacing is capable of providing durable surface friction over a time period longer than the expected life shown in Table 4.1.

4.4 UBWC Surface Friction

4.4.1 Test Sections

Presented in Table 4.5 is the information for the four UBWC test sections, particularly the aggregate properties that may affect the surface friction of UBWC. The traffic volume varied between 1047 AADT on SR-11 and 17401 AADT on US-40, and the truck traffic volume varied between 44 trucks per day on SR-11 and 700 trucks per day on SR-3. Three main types of aggregate, including steel slag, dolomite, and limestone, were used in the test sections, respectively. The two test

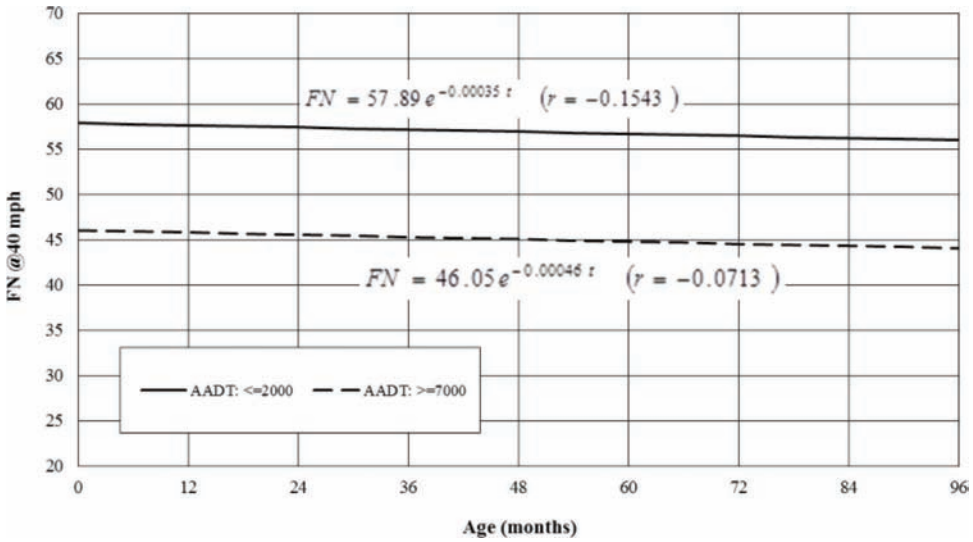

Figure 4.6 Regression models for microsurfacing surface friction.

TABLE 4.5
Information for UBWC Test Sections

Item	US-40	SR-3	SR-114	SR-11
AADT	17401	9721	8755	1047
Truck %	1.7	7.2	5.7	4.2
Construction Time	04/2007	05/2009	05/2008	11/2009
Aggregate Type	Steel Slag, 72%[a]	Dolomite, 77%[a]	Limestone, 80%[a]	Limestone, 73%[a]
LAA, %	23.0	25.4	28.0	25.1
Micro-Deval Abrasion, %	6.0	9.6	12.0	13.2
FAA	44.0	48.7	N.A.	45.4
Sand Equivalency, %	94	86	93	70
Crushed Single Face, %	98	100	100	100
Crushed Two Faces, %	91	100	100	100

[a]% = percentage in the blended aggregate.

sections, respectively on SR-114 and SR11 used the same limestone aggregate. It is shown that the steel slag demonstrated the best mechanical properties, in particular, the Micro-Deval abrasion value was much lower than those for both dolomite and limestone aggregates. The FAA ranged between 44.0 on US-40 and 48.7 on SR-3, and the sand equivalency ranged between 70% on SR-11 and 94 on US-40. Both the dolomite and limestone aggregates consisted of 100% particles with two crushed faces. For the steel slag aggregate, however, the particles with two crushed faces accounted for 91% of the total aggregate. Plotted in Figure 4.7 are the aggregate gradations for the UBWC mixes used in the test sections. All gradations had a maximum aggregate size of 12.5 mm and contained around 55% of aggregate particles between 4.75 mm and 12.5 mm.

4.4.2 Friction and Variation

Plotted in Figure 4.8 are the surface friction measurements made in these four UBWC test sections over a time period of up to 113 months. In general, surface friction increased during the first six months of placement. Between six and 30 months, the values decreased slowly and stabilized near the initial testing values. It is shown that the surface friction in the test section on SR-114 was noticeably lower than that in other test sections. This may be attributed to the limestone aggregate used in the test section on SR-114. It was reported that elsewhere (Li, Zhu, & Noureldin, 2007), limestone in Indiana demonstrated greater variation in friction properties and experienced greater decreasing rate in polish resistance. However, the friction number on SR-114 remained between 30 and 40 over time. It is obvious that the friction variation trend over time for a UBWC surface is different from those for chip seal and microsurfacing surfaces. No noticeable decrease was observed in the surface friction measurements on SR-11 after 30 months in service. All UBWC test sections demonstrated a friction number above 30. The above confirms that UBWC is capable of maintaining durable, sound surface friction even under high traffic conditions.

There is no identifiable reason for the special variation trend associated with the surface friction of UBWC. UBWC commonly consists of a heavy application of

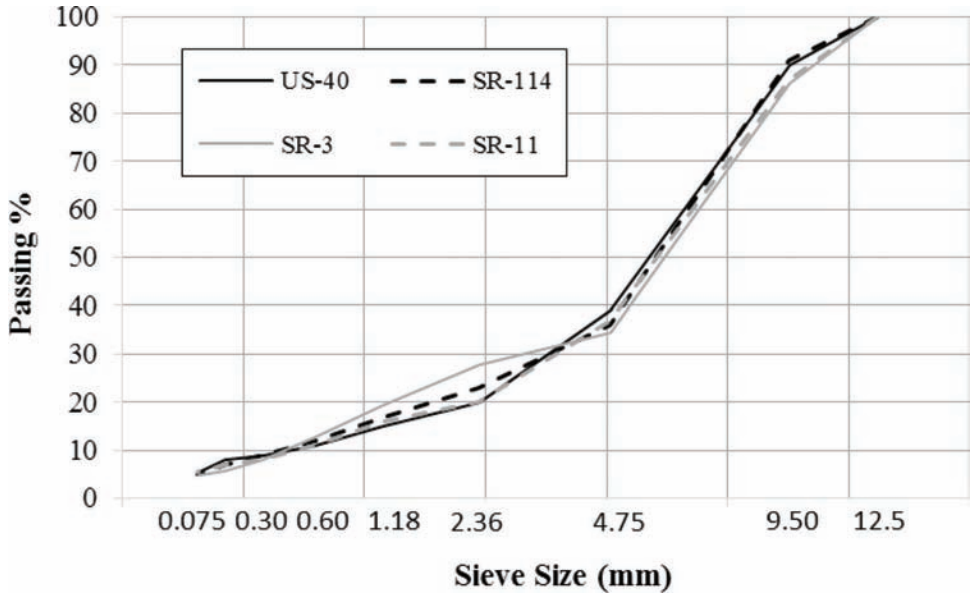

Figure 4.7 Aggregate gradations for UBWC test sections.

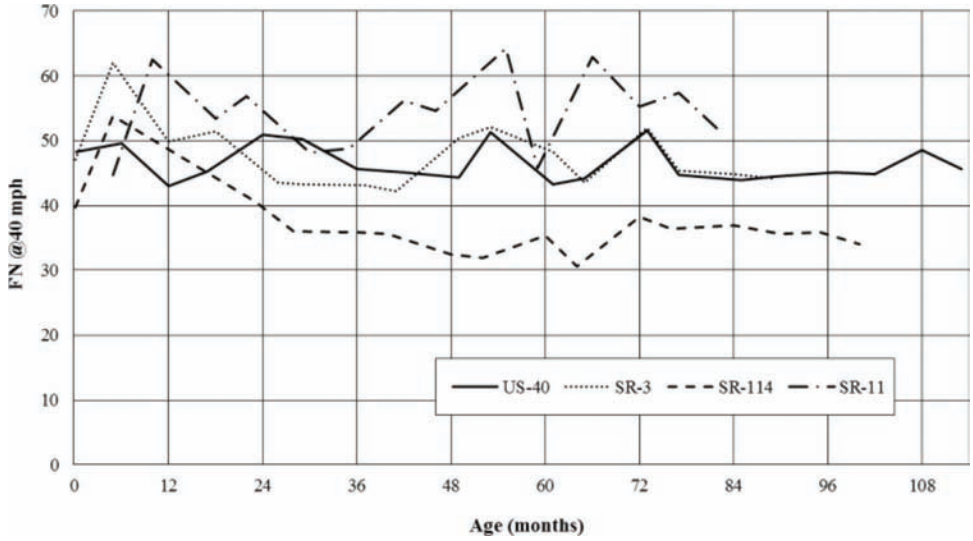

Figure 4.8 UBWC surface friction measured over time.

polymer-modified asphalt emulsion followed by an ultrathin gap-graded HMA with polymer-modified asphalt binder. It was reported that elsewhere (Li, Sun, Jiang, Noureldin, & Shields, 2012), polymer-modified asphalt binder may be beneficial to HMA surface friction, particularly in the long-term. In addition, use of polishing resistant aggregate will be beneficial to the long-term friction performance of UBWC (Li, Yang, et al., 2013). Illustrated in Figure 4.9 are the regression models for predicting the variation of UBWC surface friction over time. Because there was only one UBWC test section with an AADT of around 1000 and because the surface friction in the test section fluctuated over time, the 95% confidence interval was developed and recommended to estimate the long-term friction performance of UBWC carrying low traffic. For UBWC with high traffic volume, the surface friction decreases slowly over time.

4.5 Diamond Grinding Surface Friction

4.5.1 Test Sections

Presented in Table 4.6 is the information for the four diamond grinding test sections, including one existing HMA pavement on SR-162, two existing concrete pavements on US-50 and I-469 and one new concrete pavement on US-24. In addition, friction testing was conducted on a total of sixteen bridge decks on I-90 before and after diamond grinding. It is shown that all test sections experienced very high traffic, in particular the concrete test sections. The traffic volume ranged

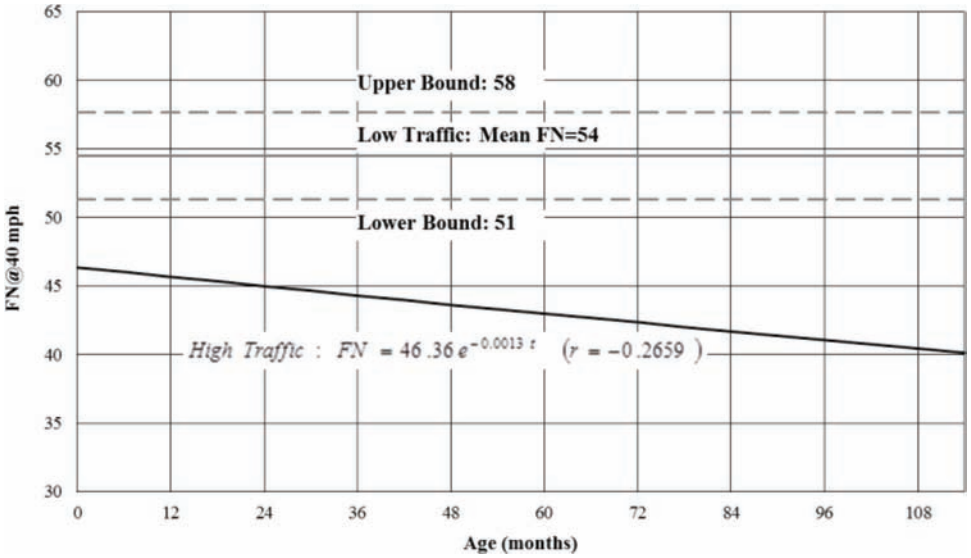

Figure 4.9 Regression models for UBWC surface friction.

TABLE 4.6
Information for Diamond Grinding Test Sections

Road	Surface Type	Length (miles)	AADT	Truck (%)	Construction Time
SR-162	Existing HMA	3.0	5095	9.6	10/2007
US-50	Existing Concrete	1.2	33143	5.7	06/2008
I-469	Existing Concrete	8.5	24597	31.6	10/2008
US-24	New Concrete	3.0	12150	46.0	08/2012
I-90	Existing Concrete Deck	16 Bridges	28800	35.0	07/2012

between 5096 AADT on SR-162 and 33143 AADT on US-50. The truck traffic volume ranged between 489 trucks per day on SR-162 and 7772 trucks per day on I-469. As stated earlier, diamond grinding is commonly used as a CPR technique for correcting irregularities including faulting and roughness on concrete pavements. However, diamond grinding also appears to be very promising for restoring the surface friction of an HMA pavement. It not only improves surface smoothness, but also enhances surface friction through restoring surface texture.

4.5.2 Friction and Variation

Figure 4.10 shows the friction numbers measured over time in the four diamond grinding test sections. The grey dot indicates the average friction number for 16 bridge decks on I-90 after diamond grinding. The trend of friction variation for diamond grinding on HMA pavement was different from that on concrete pavement. For the diamond grinding in the HMA test section, surface friction fluctuated over time. There is no trend to indicate a reduction in surface friction over time. HMA materials tend to age with time, resulting in surface raveling. HMA surface distresses may also occur due to traffic and weather applications. Surface raveling and distresses may cause surface irregularities, and therefore produce larger surface textures. For the diamond grinding in the concrete test sections, the surface friction decreased over time. The decreasing rate was more rapid in the first 36 months than afterwards.

It can also be observed in Figure 4.10 that the surface friction for diamond grinding on new concrete pavement was greater than that on existing concrete pavement, particularly in the first 24 months. This may be attributed to the effect of surface characteristics in the land areas. There are many factors that may affect the texture characteristics and friction variation of diamond grinding surface. The detailed information can be found elsewhere (Li, Harris, & Wells, 2016). Although a great degree of variability clearly existed in the friction measurements regardless of pavement type as shown in Figure 4.10, there is no doubt that diamond grinding can provide durable, sound surface friction for both concrete and asphalt pavements. Figure 4.11 presents the models developed for predicting the friction of diamond grinding on concrete and HMA pavements. For diamond grinding on existing concrete pavement, the model has a correlation coefficient of -0.7586. For diamond grinding on HMA pavement, the surface friction varies between 37 and 42 within a confidence level of 95%.

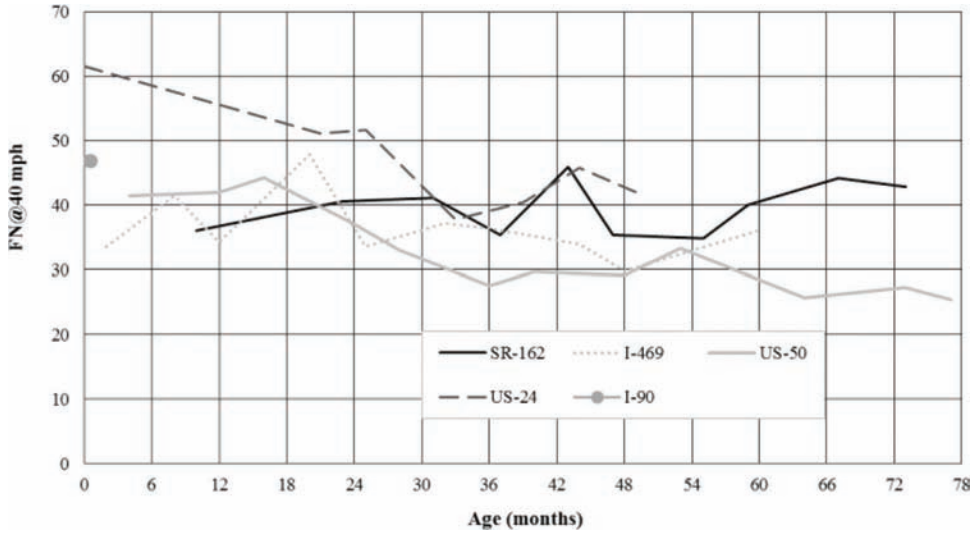

Figure 4.10 Diamond grinding surface friction measured over time.

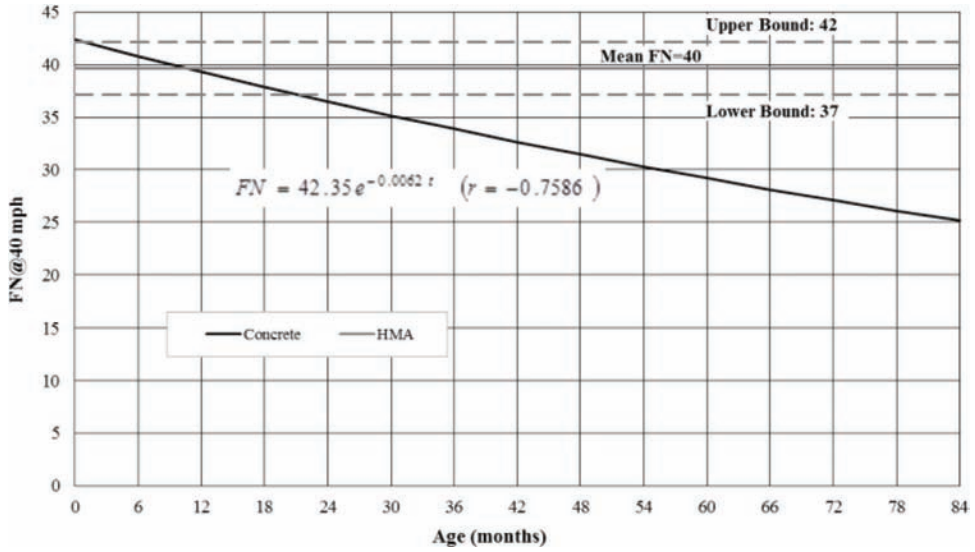

Figure 4.11 Regression models for diamond grindings.

5. QUANTIFICATION OF SAFETY EFFECTIVENESS OF PAVEMENT SURFACE FRICTION PERFORMANCE

5.1 Analysis of Statewide Vehicle Crashes

5.1.1 Crash Data Processing

Vehicle crash data in the State of Indiana was used in the current study to determine the vehicle crash statistic and estimate the safety effectiveness of pavement surface friction performance. The vehicle crash records over a period of five years, i.e., between 2010 and 2014, were obtained from Automated Reporting Information Exchange System (ARIES, n.d.), the vehicle crash data report database of Indiana State Police. Each crash record consists of a total of 59 fields containing information in the following seven areas:

1. *ID and Time:* Information about officer, agency, and investigation.
2. *Crash Involvement:* Information about numbers of vehicles, injuries, and fatalities, numbers of non-motorists, deer, and commercial vehicles.
3. *Crash Date and Location:* Information about when and where the crash occurred, including collision date and time, county, city, town, road classification, and global positioning system (GPS) coordinates.
4. *Primary Roadway:* Information about the road where the crash occurred, including roadway name, direction, interchange and ramp.
5. *Intersection:* Information about the intersecting roadway where the crash occurred, including roadway name, direction, and mile marker.
6. *Primary Cause and Location:* Information about primary factor, locality (rural or urban), school zone, construction zone, safety and control devices, light condition, weather condition, pavement surface condition (dry, wet,

snow/slush, or ice), road character (straight: level, grade, or hillcrest; curve: level, grade, or level), pavement type (asphalt or concrete), manner of collision (head on, run-off-road, rear end, right angle, sideswipe, backing, turning, and non-collision crashes such as jackknifed semi-trucks and vehicle fires), and estimated property damage.

7. *Vehicle and Driver:* Information about all vehicles and drivers involved in the crash and the impact areas on the vehicles.

In order to better evaluate the potential association between vehicle crash and pavement friction performance, the original crash data was reduced in terms of the possible influential factors such as road name (class), crash involvement (severity), surface condition, road character, primary factor, crash locality (rural and urban), and manner of collision. Initial data processing was performed as follows:

1. All roads were divided into three categories, including interstate, US, and state highways.
2. Crash involvement was primarily concerned with the crash severity, particularly the number of injuries and the number of fatalities.
3. Road characters were regrouped into two categories, i.e., Curve and Straight. The former includes curve/level, curve/grade, and curve/hillcrest; the latter includes straight/level, straight/grade, and straight/hillcrest.
4. Surface conditions were regrouped into two categories: Wet and Dry. Wet indicates that pavement surface is wet, icy, slushy, or snow-covered. Dry indicates that pavement surface is dry and clean.

5.1.2 Selected Crash Statistics and Patterns

Table 5.1 presents the annual average number of crashes, injuries, fatalities, and the corresponding percentages that occurred on curves between 2010 and 2014. On average, 61333 crashes occurred each year, and approximately 13% of all crashes occurred on curves. However, the fatalities on curves accounted for approximately 22% of total fatalities. Figure 5.1 shows the percentage breakdowns of crashes on curves and straight segments, respectively, by number of vehicles involved, i.e., single and multiple vehicle crashes. On curves, there were many more single vehicle vehicles than multiple vehicle crashes. On state highways, in particular, there were approximately twice as many single vehicle crashes as multiple vehicle crashes. Figure 5.2 shows the percentage breakdowns of crashes by pavement surface condition. It is shown that when pavement is wet, the percentage of crashes is greater on curves than on straight segments. Approximately 32% of crashes on curves occurred when pavements were wet, and 25% of crashes occurred on straight segments occurred when pavements were wet. It is also noteworthy that the percentage of crashes on wet pavements is greater on interstate highways than on either US or state highways regardless of road character. On average, 29% of interstate crashes occurred when pavements were wet, while 24% of crashes on US and state highways occurred when pavements were wet.

Figure 5.3 illustrates the percentage breakdowns of crashes by crash locality on curves and straight segments. Overall, approximately one-half of the total crashes occurred in rural areas and the other half occurred in urban areas. However, the percentages of curve crashes on US and state highways are much greater in rural areas than those in urban areas. In addition, the percentages of crashes on US and state highways are greater on curves than those on straight segments. Presented in Figure 5.4 are the breakdowns of all crashes by manner of collision on curves and straight segments. It shown that on curves, run-off-road (ROR) crashes accounted for the highest percentage of all crashes, followed by rear-end crashes, head-on crashes, sideswipe crashes, and so on. On straight segments, rear-end crashes accounted for the highest percentage of all crashes, followed by right angle crashes, sideswipe crashes, head-on crashes, ROR crashes, and so on. Notice that right angle crashes usually occur at signal- and stop-controlled intersections on non-interstate highways.

5.1.3 Countermeasure Implications

A cautious interpretation of the crash statistics and patterns clearly suggests the followings:

1. Vehicle crashes were more severe on curves than on straight segments, particularly on US and state highways.
2. Vehicle speed played an important role not only in single vehicle crashes, but also vehicle crashes on wet pavements, and rural crashes on non-interstate, particularly state highways.
3. Vehicles tended to have a higher likelihood of crashing on curves than on straight segments when pavements became wet.
4. Motorists tended to drive less cautiously on interstate highways than on US and state highways when pavements were wet. In addition, motorists tended to drive less cautiously in rural areas than in urban areas.

TABLE 5.1
Annual Average Crashes, Injuries, and Fatalities

	Crashes		Injuries		Fatalities	
Road Category	**Total Number**	**% on Curve**	**Total Number**	**% on Curve**	**Total Number**	**% on Curve**
Interstate	15320	16.8	3085	16.6	83	12.1
State	27500	13.3	8342	14.4	209	27.3
US	18513	8.5	5873	8.9	120	20.0
Sum	61333	12.7	17300	12.9	412	22.1

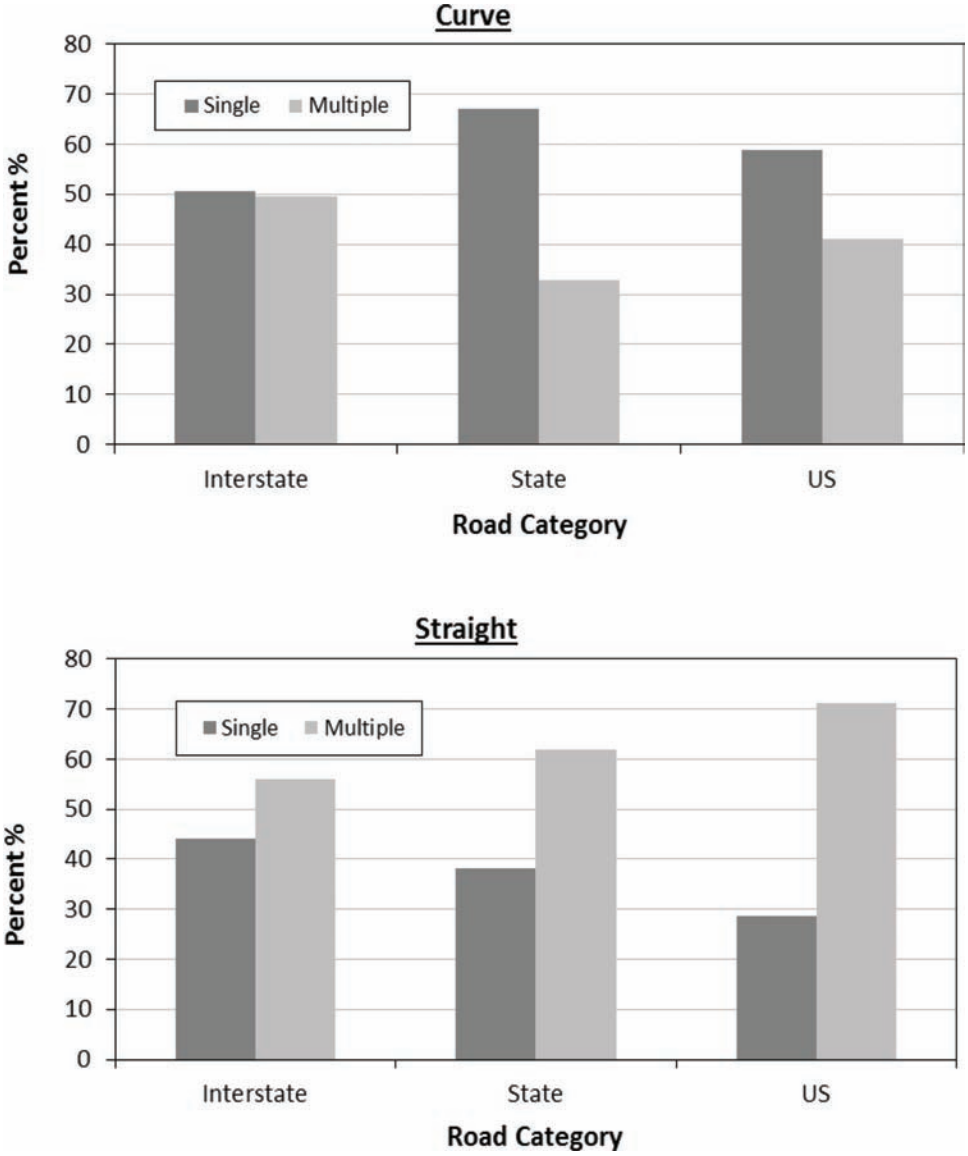

Figure 5.1 Percentage breakdowns of crashes by No. of vehicles involved.

5. ROR and rear-end crashes were the two most common types of crashes, followed by head-on, sideswipe, and right angle crashes in descending order. Vehicles tended to have higher likelihoods of these types of crashes on straight segments than on curves.

All the above confirms that speed, road character, road class, pavement surface condition, weather, and traffic control are the most important transportation-related factors influencing single-vehicle crashes (Guarino & Champaneri, 2010). Many countermeasures, including roundabouts, corridor access management, backplates with retroreflective borders, rumble strips, enhanced delineation, pavement friction, safety edge, medians and pedestrian crossing islands, pedestrian hybrid beacon, and road diet, have shown great effectiveness in reducing vehicle crashes (FHWA, 2012). Of these countermeasures, enhanced pavement friction results in not only reduced stopping distance, wheel skidding, and hydroplaning, but also safer braking, cornering, and accelerating operations. Therefore, pavement friction plays an important role in reducing ROR, rear-end, head-on, right angle, and sideswipe crashes.

5.2 Crash and Friction Data Processing

5.2.1 Crash and Fiction Data Matching

In order to quantify the probabilistic association between vehicle crash and friction performance, the ARIES crash data between 2010 and 2014 were matched to the annual inventory friction data collected by the INDOT Research and Development Division between 2010 and 2014. The data-matching procedures consisted of two major efforts. First, the size of the crash data was reduced. There were a total of more than 60,000 crashes occurring each year. The annual

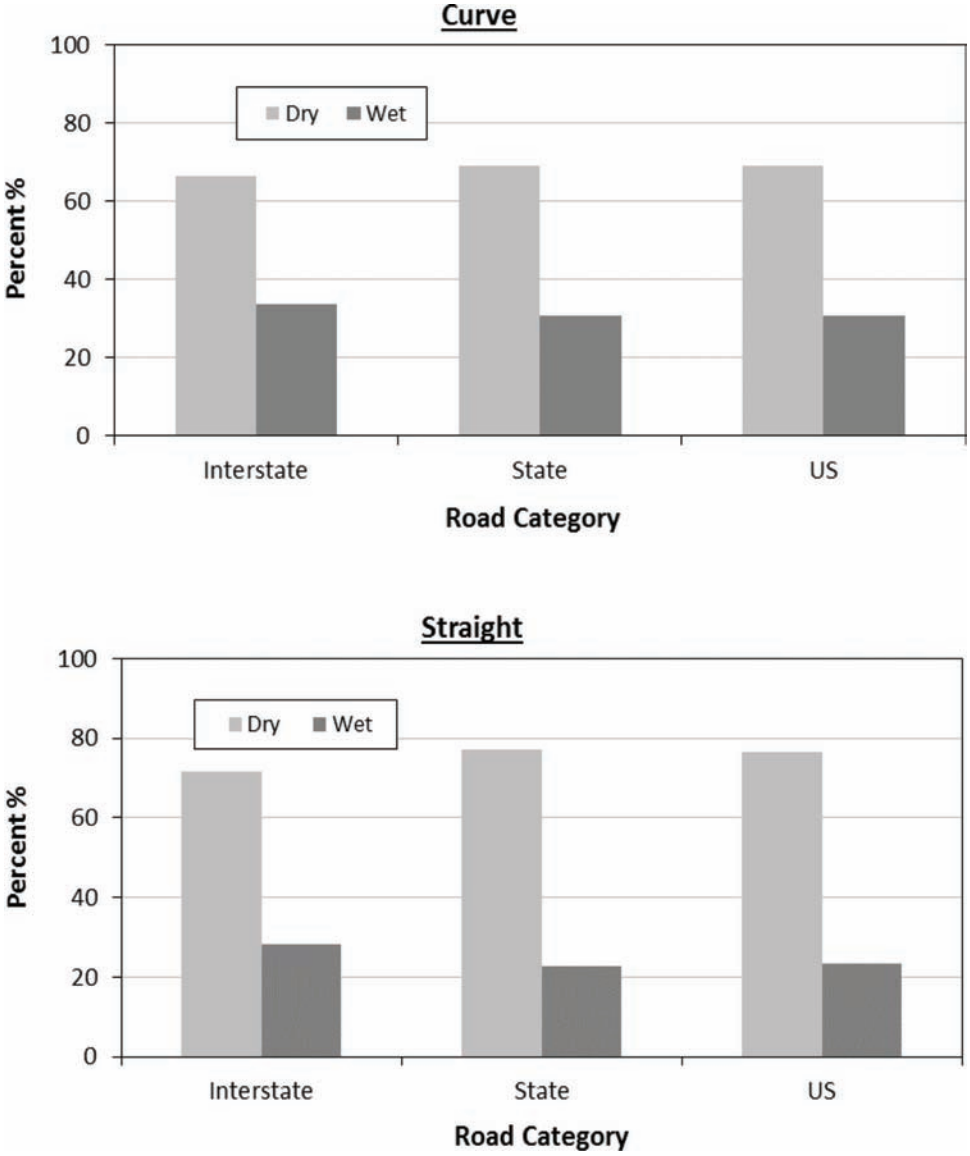

Figure 5.2 Percentage breakdown of crashes by pavement surface condition.

inventory friction testing was performed at one-mile intervals, and altogether, approximately 6500 friction numbers were measured on interstate, US, and state highways. The vehicle crash dataset was reduced according to the names of roadways with friction data through data sorting and data reduction using SAS 9.4 software (SAS Institute, 2015). Figure 5.5 is an illustration of the data sorting and reduction process for US highways in 2011. Crash data on US 12, US 150, US 20, US 231, and US 30, and so on were removed, and crash data on US 136, US 24, US 27, US 41, US 52, and US 6 were kept according to the friction data. Consequently, a reduced crash dataset was generated for further analysis.

Second, the crash data in the reduced crash dataset were matched to the friction data in the inventory friction dataset according to the corresponding GPS coordinates. It should be pointed out that there is currently no pure scientific method for performing data matching. Because both the crash and friction datasets included GPS coordinates, it is natural to use the physical positions of crash and friction data as a requirement for data matching in the current study. During data matching, a crash record was first selected from the reduced crash dataset, and then, the friction test record within one-half mile of the location of the selected crash was identified from the inventory friction dataset. The distance between the crash and friction test spots was calculated according to Pythagoras' theorem as follows (Read & Watson, 1975):

$$D_d = \sqrt{(\varphi_c - \varphi_f)^2 + (\lambda_c - \lambda_f)^2)} \qquad (5.1)$$

where, D_d is the distance in decimal degrees, φ_c and λ_c are, respectively, the latitude and longitude of the crash

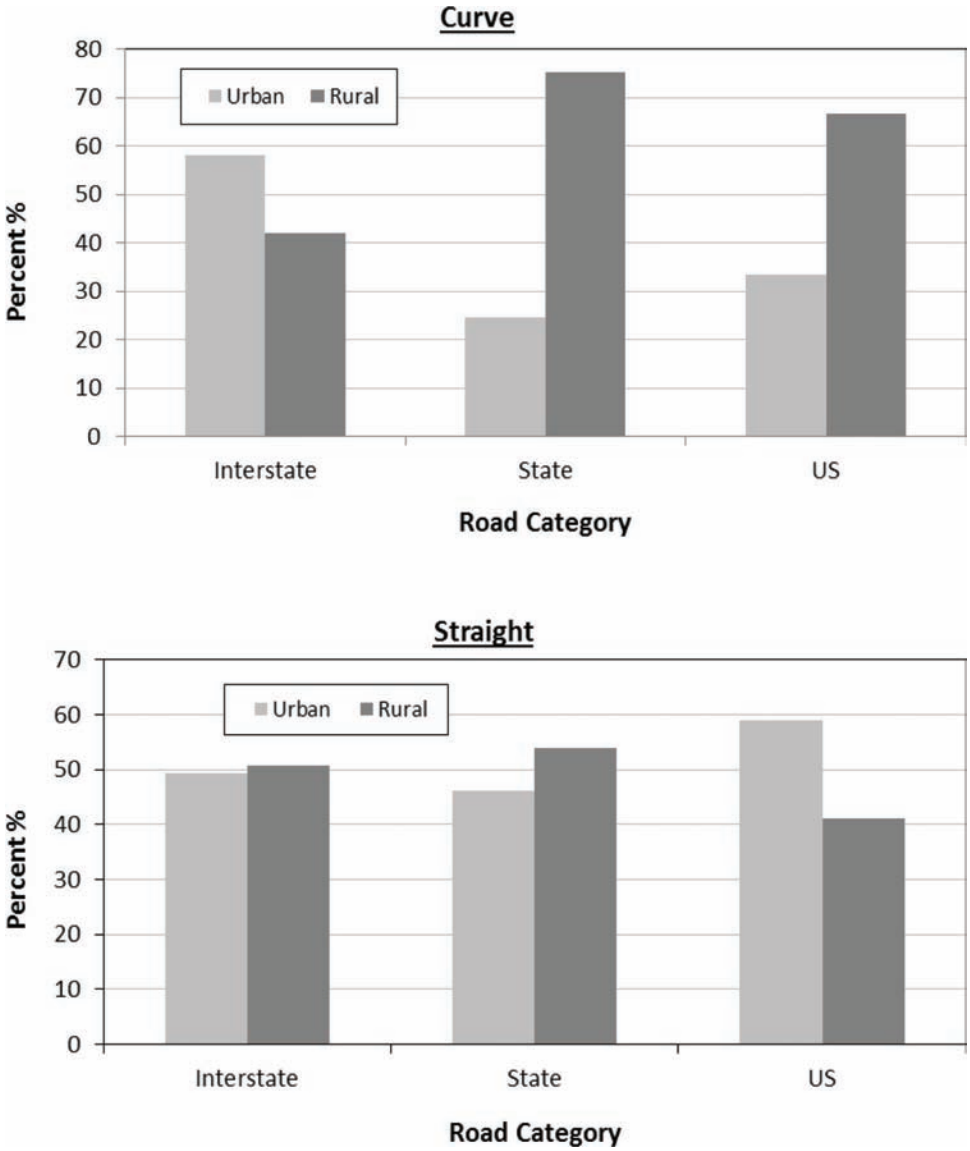

Figure 5.3 Percentage breakdowns of crashes by crash locality.

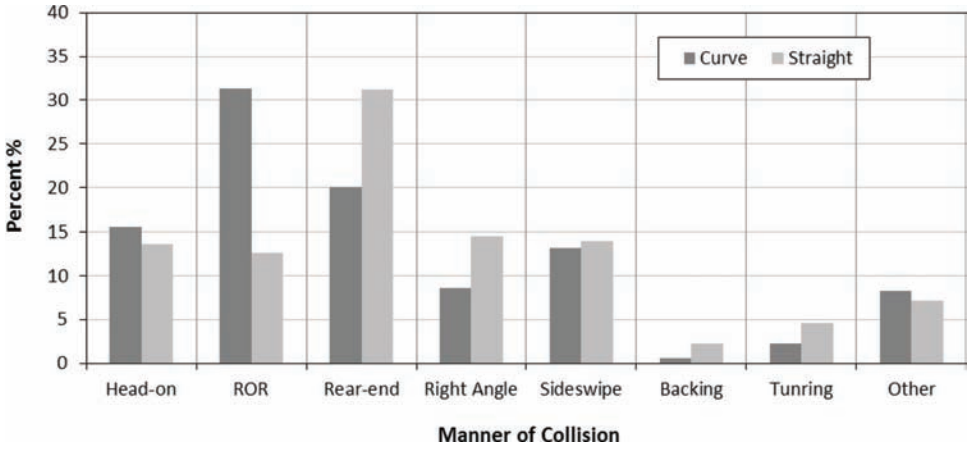

Figure 5.4 Percentage breakdowns of crashes by manner of collision.

spot, and φ_f and λ_c are, respectively, the latitude of and longitude of the pavement friction test spot.

The distance was converted from degrees to miles by assuming that the Earth is a sphere (Morse & Feshback, 1953):

$$D_m = D_d \times cosine(\varphi_c) \times a \quad (5.2)$$

where, D_m is the distance in miles, D_d and φ_c are, respectively, as defined in Eq. 5.1, and a is the average distance of one degree of latitude, which is equal to 68.172 miles.

If friction testing was conducted in both directions such as on interstate highways or conducted at intervals less than one mile when bridges, intersections, or curves were involved, multiple friction test spots could fall with one-half mile of the crash as shown in Figure 5.6, where the grey dots indicate the crash spots and the black dots represent the friction test spots. Therefore, the selected crash was matched to the friction test spot with the smallest D_m. The above data matching process was repeated using the MATLAB Student R2014a (MathWorks, 2014). The matched crash and friction data was then used to produce a combined dataset. However, abnormal crash data, either far off the road or with wrong road name (see the crash highlighted with a red arrow in Figure 5.6) might be included due to human errors during crash reporting. ArcGIS software was utilized to visualize the combined dataset and remove the abnormal data manually. After the entire data matching process, a final combined dataset was produced for each highway category.

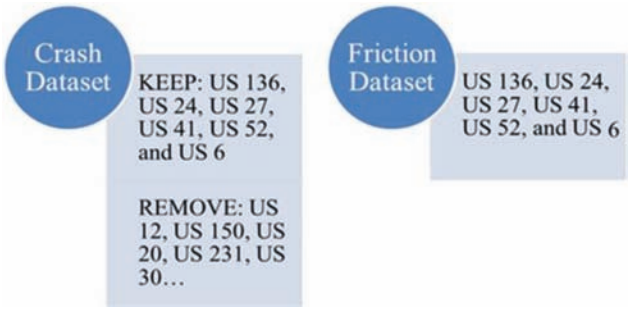

Figure 5.5 Crash data reduction for US Highways.

5.2.2 Crash and Friction Data Pair Grouping

As illustrated in Table 5.2, the generated final dataset consists of 50,251 data pairs on interstates, 25,727 data pairs on US highways, and 19,847 data pairs on state highways. In order to identify the underlying trend of crash variation with pavement friction, the friction number (FN), a continuous variable, was transformed to a categorical variable, and the crash-friction data pairs in each of the three final datasets were grouped according to friction categories. The purpose for grouping crash-friction data pairs in each of the final datasets is to minimize the potential effects of extreme events. For instance, there were some circumstances, at certain friction values, where not enough crash data was available for meaningful interpretation. In addition, there were also some circumstances, at certain friction values, where extremely high crash occurrence existed and might result in misleading interpretation. Consequently, the grouped frequency distribution might yield a better approximation of the actual crash tendencies.

The grouped distribution of crash numbers is illustrated in Figure 5.7. The grouped crash numbers exhibit a slightly right skewed, bell-shaped distribution on the x-axis, i.e., the friction category. Given a certain friction category, interstate highways experienced the

Figure 5.6 Crash and friction test spots visualized with ArcGIS.

largest number of crashes, and US Highways experienced the smallest number of crashes. The highest number of crashes occurred with friction numbers ranging from 35 to 40 on interstate highways, and from 30 to 35 on both US highways and state roads. The bell-shaped distribution of crash numbers does not contradict that the number of crashes should become smaller as friction number increases. The reason is that there were many more road segments with intermediate friction numbers. The average crash number, rather than the total crash numbers, should be used as a measure of actual crash tendency for each friction category. The average crash numbers were herein computed by dividing the crash number by the number of road segments in each friction category. Notice that, in each friction category, the number of road segments is the same as the number of crash locations that were identified using the SAS software.

TABLE 5.2
Numbers of Crash-Friction Data Pairs by Friction Category

FN Range	FN Category Index	Final Dataset		
		Interstate	State	US
0–5	1	5	0	0
5–10	2	74	56	20
10–15	3	584	269	139
15–20	4	1877	1092	1024
20–25	5	4335	2666	2199
25–30	6	5287	3659	2892
30–35	7	6416	4210	3314
35–40	8	7690	3923	2988
40–45	9	6669	3310	2423
45–50	10	4855	2299	2041
50–55	11	3924	1911	1276
55–60	12	3342	1017	805
60–65	13	2925	577	461
65–70	14	1598	447	163
70–75	15	426	143	91
75–80	16	112	77	10
80–85	17	44	56	1
85–90	18	47	4	0
90–95	19	19	6	0
95–100	20	22	5	0
All	–	50251	25727	19847

5.3 Development of Prediction Models

5.3.1 Crash Rate Normalization

Crash rate has long been used as a basic measure for assessing the relative safety of a roadway segment or intersection by involving crash risk exposure data. Two factors have been considered while pairing crash-friction data as presented in Table 5.2. First, the network inventory friction testing was conducted at one-mile intervals and each of the crash-friction data paired accordingly represents a roadway segment of one mile in length. Second, the crash-friction data pairs were clustered by highway class. Crash risk exposure such as traffic volume and vehicle-miles traveled (VMT) was implied to some extent. To further take into consideration the effect of pavement friction, the crash rate may be normalized by dividing the number of crashes by the number of crash locations and the number of years as follows:

$$\overline{CR} = \frac{N}{M \times n} \tag{5.3}$$

where, N and M are, respectively, the number of crashes (see Table 5.2) and crash locations (see Table 5.3), n is the number of years in the analysis period, and $\overline{CR}$ is the normalized crash rate with respect to friction category or performance.

The numbers of crash locations in Table 5.3 were identified using the SAS software. Plotted in Figure 5.8 are the normalized crash rates with respect to the friction category by road category. Two observations

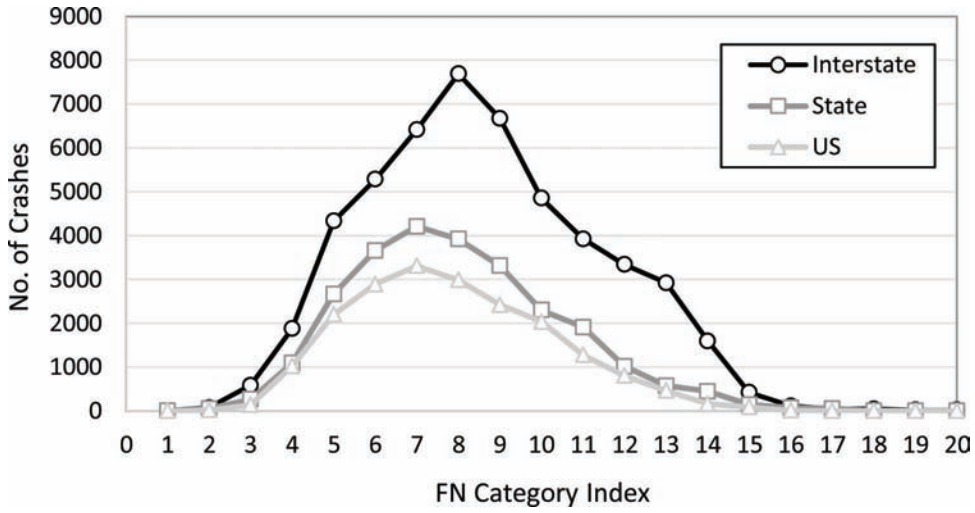

Figure 5.7 Distributions of crash numbers by road category.

can be made through careful inspection of the variations of the normalized crash rates. First, the variations of the normalized crash rates on these three highway classes exhibit a similar trend, i.e., the crash rate decreases as friction category (performance) increases. Second, abnormalities associated with friction category 1, 2, 3, or 20 as marked by black solid dots arose regardless of road category. One of the possible reasons is that friction categories 1, 2, and 20 represent the situations in which extreme friction performance could only rarely occur. Therefore, the corresponding samples were likely too small to produce conclusive results.

5.3.2 Prediction Models

Taking into consideration the shapes of plotted data in Figure 5.8, exponential models were employed to fit the normalized crash rates in a general form below:

$$y_i = \beta_0 \exp(\beta_1 x_i) + \in_i \tag{5.4}$$

where, y_i is the number of crashes per mile per year for the ith friction category, x_i is the friction category, β_0 is the model parameter, β_1 is the friction category parameter, and $\in_i$ is the error term that is assumed independent and identically distributed normally.

TABLE 5.3
Summaries of Crash Location Numbers and Normalized Crash Rates

FN Range	FN Category Index	No. of Crash Locations			Normalized Crash Rate, $\overline{CR}$		
		Interstate	State	US	Interstate	State	US
0–5	1	1	–	–	1.00	–	–
5–10	2	4	20	8	3.70	0.56	0.31
10–15	3	62	76	25	1.88	0.71	0.22
15–20	4	238	188	84	1.58	1.16	2.44
20–25	5	553	447	226	1.57	1.19	1.95
25–30	6	782	686	355	1.35	1.07	1.63
30–35	7	1069	892	487	1.20	0.94	1.36
35–40	8	1336	974	525	1.15	0.81	1.14
40–45	9	1249	932	544	1.07	0.71	0.89
45–50	10	982	743	502	0.99	0.62	0.81
50–55	11	823	664	375	0.95	0.58	0.68
55–60	12	702	395	273	0.95	0.51	0.59
60–65	13	563	252	168	1.04	0.46	0.55
65–70	14	366	155	64	0.87	0.58	0.51
70–75	15	91	79	31	0.94	0.36	0.59
75–80	16	18	35	4	1.24	0.44	0.50
80–85	17	10	26	1	0.88	0.43	0.20
85–90	18	13	4	–	0.72	0.20	–
90–95	19	4	3	–	0.95	0.40	–
95–100	20	1	2	–	4.40	0.50	–

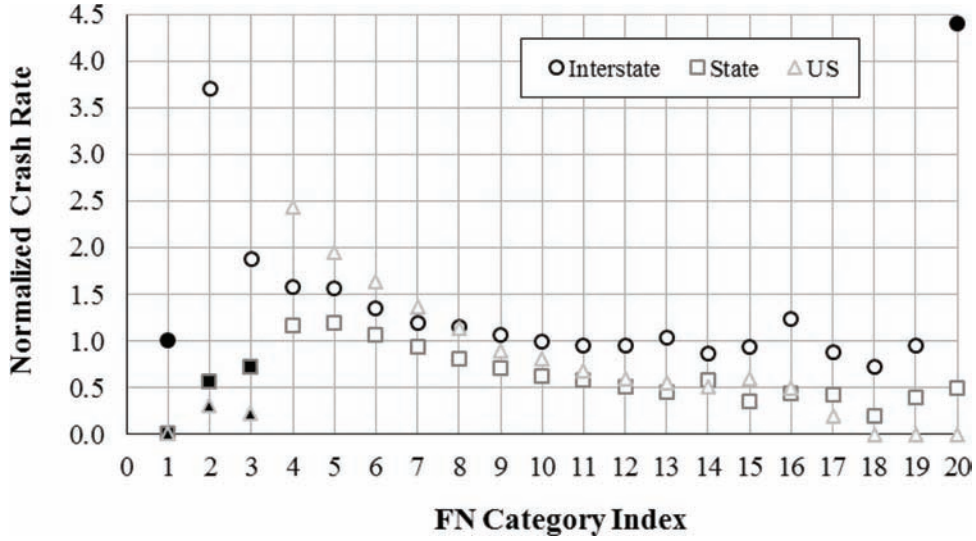

Figure 5.8 Variations of normalized crash rates with friction category.

Applying linear transformation to Eq. 5.4 yielded a new equation below:

$$Ln(y_i) = Ln(\beta_0) + \beta_1 x_i \quad (5.5)$$

where, all variables are as defined in Eq. 5.4.

Summarized in Table 5.4 are the results of regression analysis, including regression constants, coefficients, and estimated models by road category. Based on the model estimations, model regression curves are plotted in Figure 5.9. It is shown that US highway, denoted by triangles has the deepest decreasing trend followed by state road and interstate denoted by square and circle, respectively. Although interstate curve is flatter than state road, crash rates of interstate are higher than those of state road in each friction category. Additionally, Figure 5.9 indicates pavement friction improvement may incur the largest crash reductions at US highway compared with those at Interstate or state road.

5.4 Model Diagnostics for Linear Regression

5.4.1 Interstate Model

The validation of linear regression is to verify if the relationship between crash rate and friction category is linear and if the error term follows a normal distribution with constant variance. This was accomplished using graphical analyses such as scatter, residual, and Q-Q plots (see Table 5.5). In the scatter plot (see Figure 5.10), the horizontal axis represents friction category and the vertical axis, i.e., logcrash, represents the natural logarithm of the crash rate. A clear linear pattern exists when friction category is less 11. For friction categories greater than 11, the logcrash fluctuates but generally follows a decreasing trend except for friction category 16, an outlier in the model.

In the residual plot (see Figure 5.10), the residual for friction category 16 is far greater than those for other friction categories. In addition, the scatter plot demonstrates a V-shape, which implies that the variances of the error terms for the intermediate friction categories are smaller than those for friction categories less than 5 and greater than 15. Table 5.6 shows the results of variance analysis for the interstate model, including degree of freedom (DF), sum of squares, mean square, F-value and p-Value. Since p-Value is smaller than 0.0001, null hypothesis can be rejected. This concludes that the model is overall significant. The strength of the relationship between logcrash and friction category index was evaluated by the Pearson's correlation coefficient or R-square, which is 0.08057 for the interstate model. This implies that around 81 percent of the logcrash variation can be explained by the linear model.

Table 5.7 illustrates the estimation of model parameters. The t-test yielded a p-Value less than a significance level of 0.05 that indicates a significant relationship between the logcrash and friction category. In addition,

TABLE 5.4
Summaries of Model Estimations

Road Category	Linear Regression			
	$Ln(\beta_0)$	β_1	R Square	Model
Interstate	0.5779	-0.0456	0.8057	$y_i = 1.782e^{-0.046x_i}$
State Road	0.4378	-0.0813	0.7669	$y_i = 1.550e^{-0.081x_i}$
US Highway	1.3781	-0.1507	0.9133	$y_i = 3.967e^{-0.151x_i}$

TABLE 5.5
Graphical Analyses of Regression Validation

Type of Plot	Test Purpose
Scatter Plot	Linearity
Residual Plot	Linearity; Constant Variance
Q-Q Plot	Normality

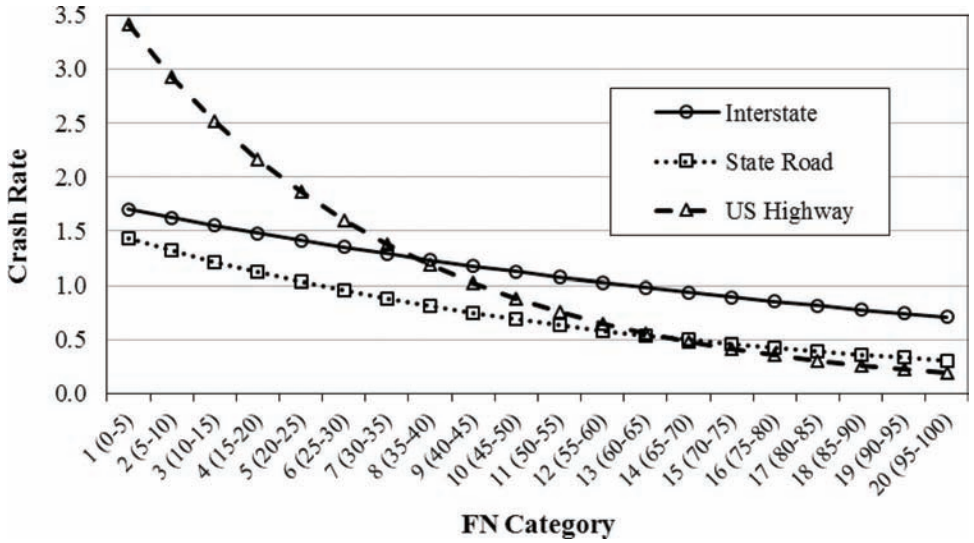

Figure 5.9 Comparisons of models.

the parameter estimate indicates that a decrease of 0.0456 in the logcrash will occur if the friction category increases by one unit. For the Q-Q plot shown in Figure 5.10, the horizontal axis represents the quantiles from the standard normal distribution, and the vertical axis represents the residuals for logcrash. All values, except for some seemingly extreme values in the central area, generally fall along a straight line. This indicates that the error term of the model follows the normal distribution. Based on all validation results presented above, it can be concluded that it is valid to utilize the linear model to readily explain the interstate logcrash by the friction category.

5.4.2 State Road Model

The analysis of variance for the state road model is summarized in Table 5.8. The general linear F-test yielded a p-Value less than 0.0001, which indicates that the linear model of logcrash explained by friction category is overall significant with a significance level of 0.05. The Pearson's correlation coefficient, i.e., R-square, for

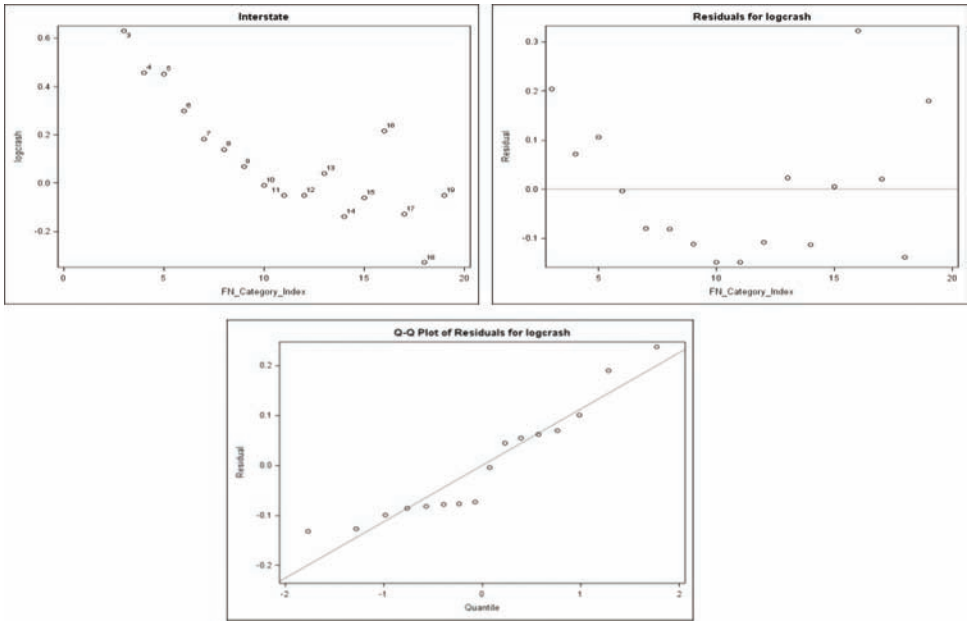

Figure 5.10 Scatter, residual, and Q-Q plots for interstate model.

TABLE 5.6
Analysis of Variance for Interstate Model

Source	DF	Sum of Squares	Mean Square	F-Value	p-Value
Model	1	0.7933	0.7933	58.04	<0.0001
Error	14	0.1914	0.0137	–	–
Corrected Total	15	0.9847	–	–	–

TABLE 5.7
Parameter Estimation of Interstate Model

Variable	DF	Parameter Estimate	Standard Error	t-Value	P-Value
Intercept	1	0.5779	0.0703	8.22	<0.0001
FN Category	1	-0.0456	0.0060	-7.62	<0.0001

TABLE 5.8
Analysis of Variance for State Road Model

Source	DF	Sum of Squares	Mean Square	F-Value	p-Value
Model	1	2.6985	2.6985	49.36	<0.0001
Error	15	0.8201	0.0547	–	–
Corrected Total	16	3.5186	–	–	–

the state road model was calculated as 0.7669. This simply indicates that the friction category can explain 77% of the variance associated with the response variable, logcrash. The results of parameter estimation are presented in Table 5.9. Since the t-test resulted in a p-Value less than 0.0001, it is significant to include the friction category index in the state road model. In addition, the logcrash will decrease by 0.081 if the friction category index increases by one unit.

Graphical analyses were also conducted to test the basic assumptions of linear regression as shown in Figure 5.11. The scatter plot indicates that a linearly decreasing pattern exists except for some friction categories such as 19 and 20. As the residual plot shows, almost all residuals are within the range of 0.2 from zero except for friction categories 18 and 20, which can be considered as outliers and excluded in the state road model. Consequently, the assumption of constant variance for the error term can be considered valid. Notice that the data points in the residual plot demonstrate a V-shaped pattern, which implies that changing the linear model into non-linear one may further improve model estimation. The Q-Q plot demonstrates that the data points follow a clear straight line pattern. It is valid to assume that the error terms of state road model is normally distributed. Therefore, it can be concluded that the linear state road model fits the data well.

5.4.3 US Highway Model

The results of variance analysis for the US highway model are summarized in Table 5.10. The p-Value is less than 0.0001 in F-test, which indicates the model is overall significant. The R-square value was calculated as high as 0.9133, which indicates that 91% of variance in logcrash can be explained by the friction category. Table 5.11 shows the results of parameter estimation for the US highway model. It is shown that in the t-test results, the predictor variable, friction category, is

TABLE 5.9
Parameter Estimation of State Road Model

Variable	DF	Parameter Estimate	Standard Error	t-Value	p-Value
Intercept	1	0.4378	0.1500	2.92	0.0106
FN Category Index	1	-0.0813	0.0116	-7.03	<0.0001

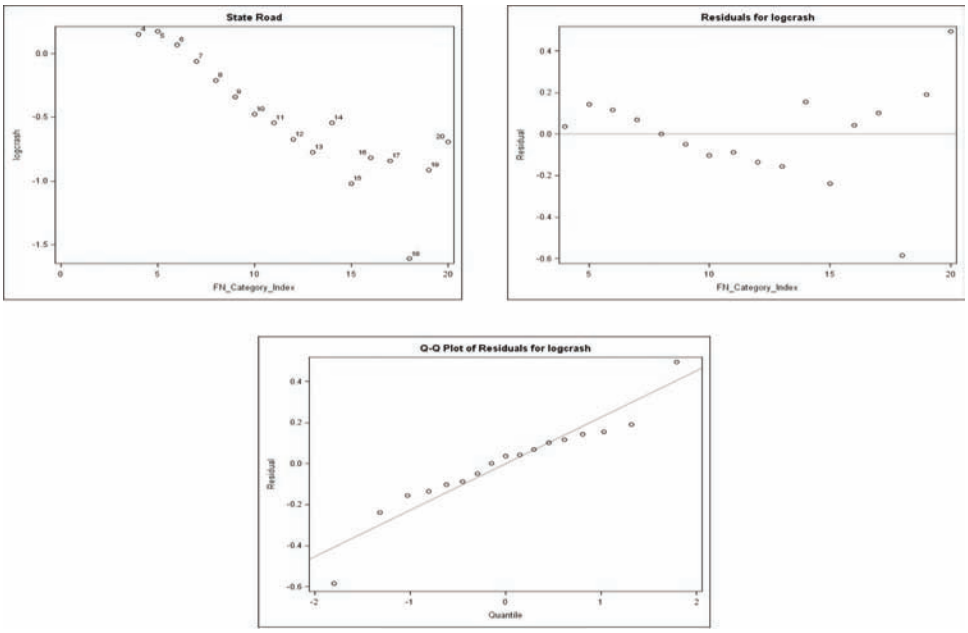

Figure 5.11 Scatter, residual, and Q-Q plots for state road model.

TABLE 5.10
Analysis of Variance for US Highway Model

Source	DF	Sum of Squares	Mean Square	F-Value	p-Value
Model	1	5.16441	5.16441	126.34	<0.0001
Error	12	0.49051	0.04088	–	–
Corrected Total	13	5.65491	–	–	–

significant in the US highway model. With every one-unit increase of friction category, the logcrash decreases by 0.151.

As shown in the scatter plot (see Figure 5.12), all data points show a clear linear pattern, and therefore, the assumption of linearity is valid. The residual plot indicates that except for the last three friction categories, all other residuals are within the range of 0.2 from zero. This can be extended to conclude that the assumption of constant variance is valid without considering those extreme cases. It is also demonstrated that in the Q-Q plot (see Figure 5.12), the residuals for logcrash generally follow the diagonal line with no point extremely deviated. Consequently, it is valid to assume that the error terms of the model is normally distributed. Thus, the linear model for US highway logcrash fits the data well.

5.5 Comparison between Published and Predicted Results

5.5.1 Reported Safety Effectiveness of HFST

Summarized in Table 5.12 are the published effectiveness for applying HFST using calcined bauxite for restoring pavement surface friction on roadway horizontal curves, intersections, and interchange ramps by various agencies across the country (ATSSA, 2013). The annual reduction rate was calculated with reference

TABLE 5.11
Parameter Estimation of US Highway Model

Variable	DF	Parameter Estimate	Standard Error	t-Value	p-Value
Intercept	1	1.3781	0.1508	9.14	<0.0001
FN Category Index	1	-0.1507	0.0134	-11.24	<0.0001

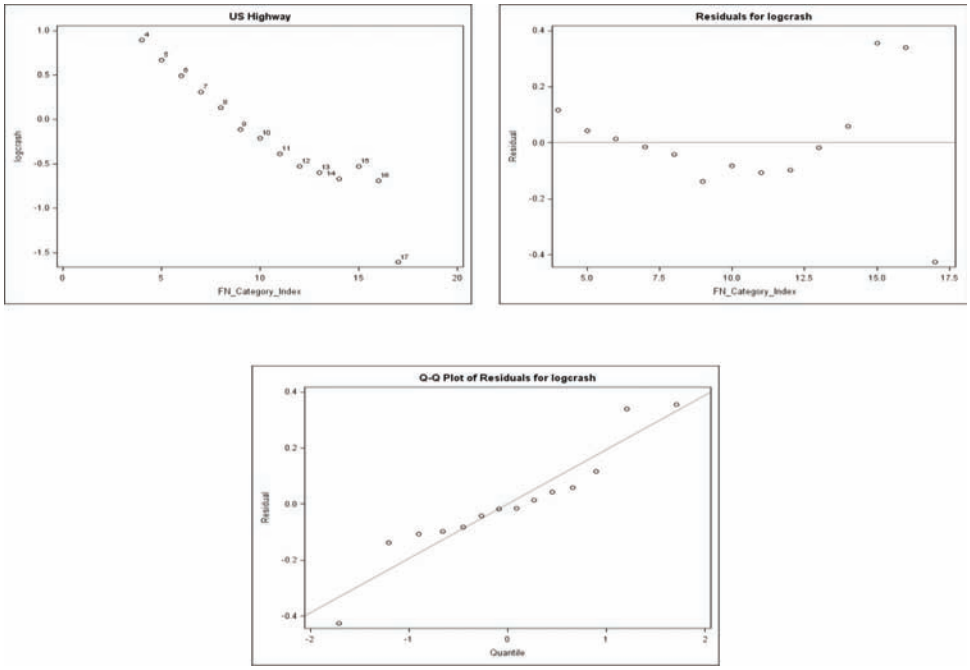

Figure 5.12 Scatter, residual, and Q-Q plots for US highway model.

TABLE 5.12
Effectiveness of HFST Applications by Highway Agencies

Agency	Application	Time Period	AnnualReduction Rate
Northampton, Co., PA	SR-611, curve, 2007	5.2 years	100%
Madison Co., KY	KY-21, curve, 2010	1.9 years	21.1%
Madison Co., KY	KY-21, curve, 2011	1.5 years	Wet/Dry: 68.4%/37.5%
Oldham Co., KY	KY-22, curve, 2009	3.18 years	Wet/Dry: 91.1%/5.7%
Bellevue, WA	Intersection, 2004	3 years	81.5%
Knox Co., KY	Intersection, 2011	1.3 years	Wet/Dry: 23.1%/57.3%
Milwaukee, WI	Interstate ramp, 2011	2 years	96%

to the crash numbers before and after the installation of HFST. For the application on roadway horizontal curves, HFST yielded an annual crash reduction of 100% in Pennsylvania, around 91.1% and 5.7%, respectively, under dry and wet conditions in Kentucky. For intersection applications, HFST resulted in an annual crash reduction of 81.5% in Bellevue, Washington, and 23.1% and 57.3%, respectively, under wet and dry conditions in Knox County, Kentucky. For interchange ramp applications, vehicle crash decreased by up to 96% per year after the installation of HFST. It was also reported that HFST effectiveness varies by location, but overall, can result in crash reductions of anywhere from 45% to 100% with the crash reductions being even greater during wet road conditions (Atkinson, Clark, & Ercisli, 2016).

Merritt, Lyon, and Persaud (2015) examined the before and after crash data collected at a total of 57 HFST sites and more than 200 comparison sites in around eight states nationwide. They applied the Empirical Bayes (EB) method to 27 HFST ramp sites and 43 HFST curve sites, respectively, and obtained a corrected CMF of 0.484 and 0.628 on ramps and curves, respectively, for all crashes. They further applied the Comparison Group (C-G) method to 12 HFST ramp sites and 35 HFST curves, respectively, and obtained a corrected CMF of 0.653 and 0.759 on ramps and curves, respectively, for all crashes. It was also concluded that HFST has a substantial beneficial impact on safety, especially for wet-road crashes. However, one major drawback to the CMFs above is that pavement surface friction generally decreases over time due to vehicle tire polishing. Consequently, a CMF associated with friction surfacing such as HFST is not constant, but varies over the expected service life.

5.5.2 Published Crash-Friction Prediction Models

Rizenbergs, Burchett, and Napier (1973) examined the relationship between the pavement friction and crash data for rural interstates and parkways in Kentucky, and determined the overall crash rate, wet-surface crash rate, and the ratio of wet-surface crash rate to overall crash under different friciotn and AADT levels. Moore and Humphreys (1973) examined the crash-friction correlation based on a total of 75 high crash frequency locations in Tennessee, and concluded that the ratio of wet-surface crashes to overall crashes decreased significantly when the friction number was above 41. After examining the friction and crash data in Denmark, Hemdorff, Leden, Sakshaug, Salusjärvi, and Schandersson (1989) concluded that the accident rate (the number of crashes per 10^7 vehicle-km) decreased with the increasing friction number. To date, efforts have been made by researchers worldwide to determine the correlations between vehicle crash and pavement friction and develop prediction models. Due to the lack of detailed information, however, only the models presented in Table 5.13 were utilized to yield meaningful comparison.

One of the major advantages associated with the crash-friction prediction models as shown in Table 5.13 is their ability to allow for a dynamic evaluation of the CMF associated with friction surfacing for life-cycle cost analysis (LCCA). It should be pointed out that currently, most state DOTs in the US are conducting pavement friction testing using the locked wheel trailer with either a ribbed tire or smooth tire. In European countries, side force measuring devices are commonly utilized for pavement friction testing with a smooth tire. The locked wheel method measures the skidding resistance along the travel direction and the side force method measures the skidding resistance perpendicular to the travel direction. The former plays an important role in determining the stop distance, and the latter in determining the radius of horizontal curve in roadway geometric design.

5.5.3 Model Comparisons

It was reported that the friciton number measured using the standard rib tire is approximately 12 points greater than the friction number by the standard smooth tire (Li, Zhu, & Noureldin, 2005). Therefore, the crash rates computed using the Kentucky models were adjusted to those with respect to the standard smooth tire. In addition, the test results conducted in

TABLE 5.13
Models Selected for Comparison

Source	Model	Application
Burchett and Rizenbergs[a] (1982) (ribbed tire)	$CR=0.14+10^{0.478-0.0383\times FN}$(AADT: 750–2499) $CR=0.27+10^{1.097-0.0518\times FN}$ (AADT: 2500–4999) $CR=0.66+^{101.294-0.0491\times FN}$ (AADT: 5000–14000)	Wet surface, and two-lane road
Kuttesch[b] (2004) (smooth tire)	$CR=5.8-0.077\times FN$ $CR=2.54-0.01492\text{-}FN-0.000026\times AADT$ $CR=2.1-0.025\text{-}FN$	All All Interstate only
Davies et al.[c] (2005) (SCRIM)	$CR=\frac{10^{10}}{365}e^{L}$ (L is function of AADT, friction, and so on)	All

[a]CR = No. of crashes per mile per year.
[b]CR = No. of wet-surface crashes per 10^7 VMT.
[c]CR = Number of crashes per 10^8 vehicle-km.

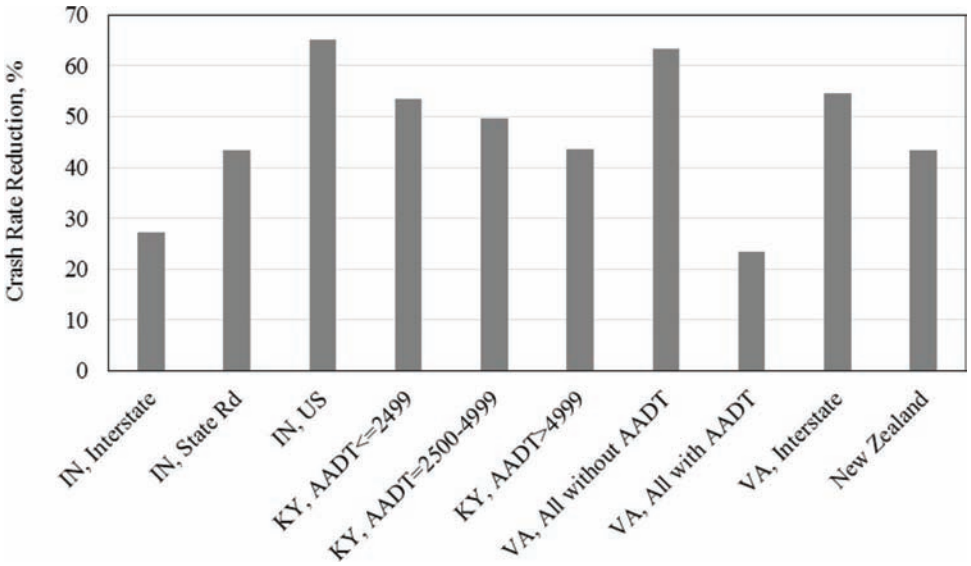

Figure 5.13 Crash rate reductions predicted using different models.

the INDOT friciton test tracks indictaed that the friction coefficient measured using the ASTM E-274 locked wheel trailer was approximately 0.05 greater than that measured using a side force test device such as SCRIM (BS 7941-1, 2006). The crash rates computed using the New Zealand model were adjusted accordingly. Notice that that the models presented in Table 5.13 were developed using different crash and friction data sources and the crash rates predicted using different models were defined differently. Therefore, the model comparison was performed by examining the crash rate reduction between two reference friction numbers, i.e., 20 and 55. The former indicates a slippery surface (100) and the latter indicates the minimum friction number for HFST (VDOT, 2012). In reality, the crash rate reduction above is equal to the CMF by increasing the surface friction number from 20 to 55.

Presented in Figure 5.13 are the crash rate reductions computed using the crash rates predicted using different models. For the models developed in the current study, the greatest crash rate reduction occurs on US highway, followed by state road and interstate, respectively. For the current models, the crash rate reduction decreases as AADT increases. For the Virginia models, the greatest crash rate reduction occurs when AADT is not included in the model for all roadway categories. When AADT is included in developing the model, the crash rate reduction becomes the smallest. The New Zealand model yields a crash rate reduction of 43%. It is shown that the predicted results vary from model to model. For interstate highways, the Kuttesch (2004) model yields much greater reduction than the model developed in the current study. Overall, the predicted crash rate reduction falls within a 95% confidence interval between 38 and 55. It should be noted that the three models proposed in the current study were developed with respect to well-documented historic friction and crash data. In addition, dividing all roadways into interstate, state, and US highways makes it possible to implicitly consider the effect of AADT to some extent.

6. CONCLUSIONS

6.1 Aggregate Mechanical, Physical, Chemical, and Geometric Properties

6.1.1 Mechanical Properties

The PSV of BS EN 1097-8 test differs from the PV-10 of ASTM D3319-11 in many aspects such as load, polishing time duration, abrasion material and procedure, and reading scale. There is no unique correlation between PSV and PV-10 and no evidence to suggest which one is more accurate for measuring polishing resistance. The Micro-Deval abrasion test uses saturated aggregate sample and better reflects the effects of the environment and therefore the durability of aggregate properties. The exposed aggregate particles of HFST are protruding above the binder and undergo greater shear force and impact from vehicle tire. The resistance of aggregate to the shear force and impact of tire may be measured with reference to the LAA loss to some extent.

The LAA loss of calcined bauxite increased as aggregate size decreased. However, the LAA loss of the steel slag was insensitive to aggregate size. The LAA loss of steel slag was greater than that of calcine bauxite. However, the difference between the LAA losses of these two aggregates became much smaller as aggregate size decreased. Steel slag demonstrated a greater Micro-Deval abrasion loss than calcined bauxite. The 1~3-mm aggregates yielded greater PV-10 than the 6.3~9.5-mm aggregates for both calcined bauxite and steel slag. The PV-10 values from 1~3-mm aggregates also demonstrated greater variations than those from 6.3~9.5-mm aggregates because smaller aggregates tended to produce specimens with greater surface variability.

Specification requirements for the mechanical properties of aggregates with reference to LAA, Micro-Deval abrasion, and PV-10 can be easily implemented by the State DOTs in accordance with the current ASTM standard test methods.

6.1.2 Chemical Properties

The Chinese refractory calcined bauxite is divided into seven grades in terms of the Al_2O_3 content. AASHTO PP 79-14 requires an Al_2O_3 content not less than 87% for calcined bauxite, i.e., Chinese calcined bauxite of Grade GL-88 or above. However, the proportions of oxides in calcined bauxite depend on many factors such as raw bauxite, type of kiln, type of fuel, flame temperature, feed amount, and feed speed, and may vary from plant to plant, batch to batch, and even vary within a single batch. Taking into consideration the potential variation in the aggregate plays an important role in developing a realistic implementable specification.

Both BOF and EAF steel slags consist primarily of oxides combined to form the main mineral phases that determine the unique physical and mechanical properties of steel slags. The experience with using steel slag in friction surfacing in other states indicated that Al_2O_3 no less than 5% does contribute to the hardness of steel slag. However, the proportions of oxides in steel slags vary with the feed material, type of steel made, and furnace condition.

6.1.3 Physical and Geometric Properties

For calcined bauxite, the specific gravity and water absorption indicate if the raw bauxite is fully calcined. Partially calcined bauxite tends to have lower strength, toughness and volumetric stability than fully calcined bauxite. For steel slag, the specific gravity and water absorption also relies on the cooling conditions. BOF steel slag may have a density much higher and a water absorption much lower than EAF (ladle) steel slag.

For a particular gradation, aggregate angularity is commonly used to measure the shape of the aggregate particles and the degree of surface irregularities of the aggregate particles. Synthetic aggregate such as calcined bauxite tended to contain an excessive amount of rounded particles. It is necessary to minimize the content of rounded particles with reference to a minimum FAA.

6.2 Evaluation of Friction Performance under Laboratory Accelerated and Field True Traffic Polishing

6.2.1 Evaluation under Laboratory Accelerated Polishing

It was demonstrated in the laboratory polishing evaluation, that the friction surfacing systems with No. 8 steel slag (1–5 mm) and No. 4 calcined bauxite (1–5 mm) provided similar MPD values before polish conditioning. Larger aggregate tended to produce larger macrotexture MPD than smaller aggregate. After polish conditioning, all three systems, including No. 8 steel slag, No. 4 calcined bauxite, and No. 6 calcined bauxite, respectively, demonstrated a reduction of approximately 20%, 18%, and 22% in MPD. After polish conditioning, the No. 8 steel slag, No. 4 calcined bauxite, and No. 6 calcined bauxite systems, respectively, experienced an average reduction of 8%, 4%, and 4% in terms of DFT friction at 20 km/h. Smaller aggregates tended to experience greater reduction in MPD. Nevertheless, friction surfacing such as HFST with larger surface MPD does not necessarily produce greater surface friction. In addition, No. 4 calcined bauxite raised concerns about tire damage.

The aggregate gradations for calcined bauxite and steel slag should be determined by taking into consideration friction performance, amount of epoxy binder, aggregate production process, proven track record, surface uniformity (appearance), and potential damage to vehicle tire. Coarse, uniform-sized hard aggregate, in particular calcined bauxite, demonstrated a harsh surface that caused concerns about tire damage.

6.2.2 Evaluation under Field True Traffic Polishing

Three friction surfacing systems, including one-course No. 8 steel slag, one-course No. 6 calcined bauxite, and two-course No. 6 calcined bauxite, were installed in real-world pavements for polishing by actual traffic loadings. The MPD values were 2.27 mm, 1.98 mm, and 1.98 mm before polishing, 1.46 mm, 1.60 mm, and 1.58 mm after three months of service, and 1.49 mm, 1.46 mm, and 1.60 mm after nine months of service, for these three systems, respectively. The average DFT friction coefficients at 20 km/h were 0.682, 0.932, and 0.905 after three months of service, and 0.540, 0.812, and 0.798 after nine months of service for these three systems, respectively. The one-course No. 8 steel slag system experienced the greatest friction reduction, approximately 31% and 45% after three and nine months of service, respectively. The one- and two-course No. 6 calcined bauxite systems, respectively, experienced a friction reduction more than 6% and 9% after three months of service, and more than 18% and 20% after nine months of service. The two-course No. 6 calcined bauxite did not outperform the one-course No. 6 calcined bauxite after being in service. HFST with a larger surface MPD value does not necessarily produce better, more durable surface friction.

The long-term friction performance under laboratory polishing was different from that under true traffic polishing. Under the laboratory accelerated polishing, MPD decreased much more rapidly than DFT friction for both steel slag and calcined bauxite. Under the true traffic polishing, MPD decreased slower than DFT friction for both steel slag and calcined bauxite. In addition, the DFT friction after nine months of traffic polishing decreased much more rapidly than that after laboratory accelerated polishing for both steel slag and calcined bauxite. The MPD for steel slag decreased more rapidly after nine months of field traffic polishing than after laboratory three wheel polishing condition.

The MPD under traffic polishing decreased in a rate similar to that under laboratory accelerated polishing for calcined bauxite.

6.3 Long-Term Friction Performance of Pavement Preservation Treatments

6.3.1 Chip Seal

New chip seals produced higher friction numbers and lower variations than new fog-chip seals. Applying a fog seal onto a new chip seal tended to reduce the surface friction by 25%. Chip seals using crushed stone demonstrated friction numbers 25% greater than the chip seals using crushed gravel. There was no clear trend to indicate the differences in friction performance between No. 11, No. 12, and No. 16 aggregates. The friction variations in both regular and fog-chip seals followed a similar trend. It took 12 months for the chip seals to form a stable mosaic surface. A successful chip seal is capable of providing satisfactory friction performance for a period of five years or more.

6.3.2 Microsurfacing

The surface friction relied on the combined effect of AADT, truck traffic, and aggregate. Microsurfacing friction increased in the first 12 months, and afterwards, decreased very slowly, and remained very stable over time. Overall, microsurfacing is capable of providing better surface friction than chip seal for a wide range of traffic volume, and providing durable surface friction over a time period longer than six years.

6.3.3 UBWC

UBWC surface friction tended to increase in the first six to ten months, and then decreased between six and thirty months in service. Afterwards, the surface friction fluctuated around a certain value that is greater than 30. UBWC with limestone aggregate demonstrated greater variation in friction properties. In addition, the trend of friction variation over time for UBWC was different from those for chip seal and microsurfacing surfaces. UBWC is capable of maintaining durable, sound surface friction even under high traffic conditions.

6.3.4 Diamond Grinding

The trend of friction variation over time for diamond grinding on HMA pavement was different from that on concrete pavement. On HMA pavement, diamond grinding surface friction fluctuated over time and no trend existed to indicate a significant reduction in surface friction. On concrete pavement, diamond grinding surface friction decreased over time. The decreasing rate was more rapid in the first 36 months than afterwards. The diamond grinding on new concrete pavement produced greater friction than on existing concrete pavement, particularly in the first 24 months. Diamond grinding can provide durable, sound surface friction for both concrete and asphalt pavements.

6.4 Crash Statistics and Friction Surfacing Safety Effectiveness

6.4.1 Selected Crash Statistics and Patterns

Approximately 13% of all crashes occurred on curves, resulting in about 22% of total fatalities in Indiana. For vehicle crashes on curves, 32% occurred when pavements were wet. For crashes on straight segments, 25% occurred when pavements were wet. It is also noteworthy that the percentage of crashes on wet pavements was greater on interstate highways than on either US or state highways regardless of road character. On average, 29% of interstate crashes occurred when pavements were wet, and 24% of crashes on US and state highways, occurred when pavements were wet.

Overall, one-half of the total crashes occurred in rural areas and the other half occurred in urban areas. However, the percentages of curve crashes on US and state highways were much greater in rural areas than those in urban areas. In addition, the percentages of crashes on US and state highways were greater on curves than those on straight segments.

On curves, ROR crashes accounted for the highest percentage of all crashes, followed by rear-end crashes, head-on crashes, sideswipe crashes, and so on. On straight segments, rear-end crashes accounted for the highest percentage of all crashes, followed by right angle crashes, sideswipe crashes, head-on crashes, ROR crashes, and so on.

6.4.2 Quantifying Effectiveness of Friction Surfacing

One major drawback associated with the CMFs currently available for friction surfacing is caused due to pavement surface friction generally decreasing under vehicle tire polishing over time. Consequently, a CMF associated with a friction treatment such as HFST is not constant, but varies over the expected service life. Nevertheless, one of the major advantages associated with a crash-friction prediction model is its ability to allow for a dynamic evaluation of the CMF due to friction surfacing for life-cycle cost analysis (LCCA). The current study developed three crash-friction prediction models for interstate, state, and US highways.

Model diagnostics were performed with respect to linear regression validation and graphical analyses such as scatter, residual, and Q-Q plots. The results indicated that it is valid to utilize the linear model to readily explain the vehicle crash data using friction category index, regardless of roadway category. Comparison of the models developed in the current study was performed with the models published in other studies. Although mixed results were obtained, it is the authors' opinion that the three models developed in the current study rely on well-documented historic friction and crash data, and are capable of producing more convincing prediction results.

REFERENCES

AASHTO PP 79-14. (2014). *Standard practice for high friction surface treatment for asphalt and concrete pavements*. Washington, DC: American Association of State Highway and Transportation Officials.

AASHTO T 304-11(2015). (2011). *Standard method of test for uncompacted void content of fine aggregate*. Washington, DC: American Association of State and Highway Transportation Officials.

Alaska DOT. (2004). *Section 405: High friction surface treatment* (Special Provision). Juneau, AK: Alaska Department of Transportation. Retrieved from https://s3.amazonaws.com/media.atssa.com/HFS/Specifications_AlaskaDOT.pdf

ALDOT. (2014). *Section 431: High friction surface treatments for asphalt pavements* (Special Provision No. 12-0817). Montgomery, AL: Alabama Department of Transportation. Retrieved from https://s3.amazonaws.com/media.atssa.com/HFS/Specifications_AlabamaDOT.pdf

Alexander, M., & Mindess, S. (2005). *Aggregates in concrete*. New York, NY: Taylor & Francis.

ARIES. (n.d.). Indiana State Police. Retrieved from https://www.ariesportal.com/Public/Home.aspx

ASTM C127-15. (2015). *Standard test method for relative density (specific gravity) and absorption of coarse aggregate*. West Conshohocken, PA: ASTM International.

ASTM C131/C131M-14. (2006). *Standard test method for resistance to degradation of small-size coarse aggregate by abrasion and impact in the Los Angeles machine*. West Conshohocken, PA: ASTM International.

ASTM C311/C311M-13. (2013). *Standard test methods for sampling and testing fly ash or natural pozzolans for use in portland-cement concrete*. West Conshohocken, PA: ASTM International.

ASTM C88-13. (2013). *Standard test method for soundness of aggregates by use of sodium sulfate or magnesium sulfate*. West Conshohocken, PA: ASTM International.

ASTM D3042-09(2015). (2015). *Standard test method for insoluble residue in carbonate aggregates*. West Conshohocken, PA: ASTM International.

ASTM D3319-11. (2011). *Standard practice for accelerated polishing of aggregates using the British wheel*. West Conshohocken, PA: ASTM International.

ASTM D6928-10. (2010). *Standard test method for resistance of coarse aggregate to degradation by abrasion in the Micro-Deval apparatus*. West Conshohocken, PA: ASTM International.

ASTM E1911-09. (2009). *Standard test method for measuring paved surface frictional properties using the dynamic friction tester*. West Conshohocken, PA: ASTM International.

ASTM E2157-09. (2009). *Standard test method for measuring pavement macrotexture properties using the circular track meter*. West Conshohocken, PA: ASTM International.

ASTM E274M-15. (2015). *Standard test method for skid resistance of paved surfaces using a full-scale tire*. West Conshohocken, PA: ASTM International.

ASTM E303-93(2013). (2013). *Standard test method for measuring surface frictional properties using the British pendulum tester*. West Conshohocken, PA: ASTM International.

ASTM E501-08(2015). (2015). *Standard specification for standard rib tire for pavement skid-resistance tests*. West Conshohocken, PA: ASTM International.

ASTM E524-08(2015). (2015). *Standard specification for standard smooth tire for pavement skid-resistance tests*. West Conshohocken, PA: ASTM International.

ASTM E660-90(2015). (2015). *Standard practice for accelerated polishing of aggregates or pavement surfaces using a small-wheel, circular track polishing machine*. West Conshohocken, PA: ASTM International.

ASTM E965-15. (2015). *Standard test method for measuring pavement macrotexture depth using a volumetric technique*. West Conshohocken, PA: ASTM International.

Atkinson, J., Clark, J., & Ercisli, S. (2016). *High friction surface treatment curve selection and installation guide* (Leidos Publication No. FHWA-SA-16-034). Washington, DC: Federal Highway Administration, U.S. Department of Transportation.

ATSSA. (2013). *Safety opportunities in high friction surfacing*. Fredericksburg, VA: American Traffic Safety Services Association.

ATSSA. (2014). *High friction surfacing: Specifications*. Fredericksburg, VA: American Traffic Safety Services Association. Retrieved from http://www.atssa.com/Resources/HighFrictionSurfacing/StateSpecifications.aspx

BS 7941-1:2006. (2006). *Measurements for measuring the skid resistance of pavement surfaces—Part 1: Sideways-force coefficient routine investigation machine*. London, England: British Standards Institution.

BS EN 1097-8:2009. (2009). *Tests for mechanical and physical properties of aggregates-determination of the polished stone value*. London, England: British Standards Institution.

BS EN 13036-4:2011. (2011). *Road and airfield surface characteristics—Test methods— Method for measurement of slip/skid resistance of a surface: The pendulum test*. London, England: British Standards Institution.

Burchett, J., & Rizenbergs, R. (1982). Frictional performance of pavements and estimates of accident probability. In C. Hayden (Ed.), *Pavement surface characteristics and materials* (STP28464S, pp. 73–97). West Conshohocken, PA: ASTM International. https://doi.org/10.1520/STP28464S

Caltrans. (2014). *Add as Section 37-6: High friction surface treatment*. Sacramento, CA; California Department of Transportation. Retrieved from https://s3.amazonaws.com/media.atssa.com/HFS/Caltrans_Section37-6_1-15-14.pdf

Cargill. (2010). *SafeLane surface overlay* (CA-48 Technical Specification). North Olmsted, OH: Cargill Deicing Technology.

Chesner, W. H., Collins, R. J., & Mackay, M. H. (1998). *User guidelines for waste and byproduct materials in pavement construction* (Publication No. FHWA-RD-97-148). Washington, DC: Federal Highway Administration, U.S. Department of Transportation.

Cuelho, E., Mokwa, R., Obert, K., & Miller, A. (2008). Comparative analysis of Micro-Deval, L.A. abrasion, and sulfate soundness tests. In *TRB 87th annual meeting compendium of papers* [CD-ROM]. Washington, DC: Transportation Research Board.

Davies, R. B., Cenek, P. D., & Henderson, R. J. (2005). The effect of skid resistance and texture on crash risk. In *First international conference on surface friction: Roads and runways*. Christchurch, New Zealand: New Zealand Transport Agency.

Denning, J. H. (1977). *High-performance surface dressing: 1. Road experiments with new thermoplastic binders* (TRRL Report SR 314). Crownthorn, England: Transport and Road Research Laboratory.

Denning, J. H. (1978). *High-performance surface dressing: 2. Road experiments with new thermoplastic binders* (TRRL Report SR 416). Crownthorn, England: Transport and Road Research Laboratory.

Dews, S. J., & Bishop, R. J. (1972). Factors affecting the skid-resistance of calcined bauxite. *Journal of Chemical Technology and Biotechnology*, *22*(10), 1117–1124. https://doi.org/10.1002/jctb.5020221009

E-Bond. (n.d.). *Epoxy multi-layer rapid set skid-resistant polymer concrete for bridge and parking decks*. Ft. Lauderdale, FL: E-Bond Epoxies Inc.

FDOT. (2014). *Section 333: High friction surface treatment* (REV 8-13-14). Tallahassee, FL: Florida Department of Transportation. Retrieved from https://s3.amazonaws.com/media.atssa.com/HFS/Specifications_FLDOT.pdf

FHWA. (n.d.a). Every day counts: High friction surface treatments. Retrieved from http://www.fhwa.dot.gov/everydaycounts/edctwo/2012/friction.cfm

FHWA. (n.d.b). High friction surface treatments (HFST). https://safety.fhwa.dot.gov/roadway_dept/pavement_friction/high_friction/

FHWA. (n.d.c). Proven safety countermeasures. Retrieved from https://safety.fhwa.dot.gov/provencountermeasures/

FHWA. (2012, January 12). *Guidance memorandum on promoting the implementation of proven safety countermeasures*. Washington, DC: Federal Highway Administration, U.S. Department of Transportation.

Flint Rock Products. (n.d.). *Gradation specifications: Bridge deck aggregate* (Flint 65/8). Picher, OK: Flint Rock Products.

Fowler, D. W., & Rached, M. M. (2012). Polish resistance of fine aggregates in portland cement concrete pavements. *Transportation Research Record*, *2267*, 29–36. https://doi.org/10.3141/2267-03

GDOT. (2009). *Section 424: High friction surface treatment* (Special Provision). Atlanta, GA: Georgia Department of Transportation.

GRIPgrain RD-88. (n.d.). *Chinese calcined bauxite for high friction surface treatment*. Wurtland, KY: Great Lake Minerals, LLC.

Guarino, J., & Champaneri, A. (2010). *Factors involved in fatal vehicle crashes* (Rita TR-008). Washington, DC: Research and Innovative Technology Administration, U.S. Department of Transportation.

Heitzman, M., Turner, P., & Greer, M. (2015). *High friction surface treatment alternative aggregates study* (NCAT Report No. 15-04). Auburn, AL: National Center for Asphalt Technology.

Hemdorff, S., Leden, L., Sakshaug, K., Salusjärvi, M., & Schandersson, R. (1989). *Trafiksäkerhet och vägytans egenskaper (TOVE): Slutrapport* (Tiedotteita 1075). Espoo, Finland: VTT Technical Research Centre of Finland.

Henry, J. J. (2000). *Evaluation of pavement friction characteristics* (NCHRP Synthesis 291). Washington, DC: Transportation Research Board.

Hosking, J. R., & Tubey, L.W. (1972). *Aggregates for resin-bound skid-resistant road surfacings* (TRLL Report No. LR 466). Crowthorn, England: Transport and Road Research Laboratory.

Hunt, E. A. (2001). *Micro-deval coarse aggregate test evaluation* (Publication No. OR-RD-01-13). Salem, OR: Oregon Department of Transportation.

IDOT. (2014). *Special provision for high friction surface treatment (BMPR/BSE)*. Springfield, IL: Illinois Department of Transportation. Retrieved from https://s3.amazonaws.com/media.atssa.com/HFS/Illinois_ProvisionContract70A52.pdf

INDOT. (n.d.). Preservation initiative: Pavement preservation. Retrieved February 2, 2017, from http://www.in.gov/indot/3371.htm

INDOT. (2012). *Acceptance procedures for HMA surface mixture coarse aggregates for ESAL ≥ 10,000,000* (ITM No. 221-12P). Indianapolis, IN: Office of Materials Management, Indiana Department of Transportation.

INDOT. (2014). *Standard specifications*. Indianapolis, IN: Indiana Department of Transportation.

Iowa DOT. (2011). *Special provision for high friction surface treatment* (SP-090134). Ames, IA: Iowa Department of Transportation.

Kandhal, P. S., & Parker, Jr., F. (1998). *Aggregate tests related to asphalt concrete performance in pavements* (NCHRP Report 405). Washington, DC: Transportation Research Board.

Kuttesch, J. S. (2004). *Quantifying the relationship between skid resistance and wet weather accidents for Virginia data* (Master's thesis). Blacksburg, VA: Virginia Tech.

Lee, J., & Shields, T. (2010). *Treatment guidelines for pavement preservation* (Joint Transportation Research Program Publication No. FHWA/IN/JTRP-2010/01). West Lafayette, IN: Purdue University. https://doi.org/10.5703/1288284314270

Lewis, D. W. (1982). *Properties and uses of iron and steel slags*. Paper presented at Symposium on Slag National Institute for Transport and Road Research, South Africa, February.

Li, S., Harris, D., & Wells, T. (2016). Surface texture and friction characteristics of diamond-ground concrete and asphalt pavements. *Journal of Traffic and Transportation Engineering*, *3*(5), 475–482. https://doi.org/10.1016/j.jtte.2016.08.001

Li, S., Noureldin, S., & Zhu, K. (2004). *Upgrading the INDOT pavement friction testing program* (Joint Transportation Research Program Publication No. FHWA/IN/JTRP-2003/23). West Lafayette, IN: Purdue University. https://doi.org/10.5703/1288284313338

Li, S., Noureldin, S., & Zhu, K. (2010). *Safety enhancement of the INDOT network pavement friction testing program: Macrotexture and microtexture testing using laser sensors* (Joint Transportation Research Program Publication No. FHWA/IN/JTRP-2010/25). West Lafayette, IN: Purdue University. https://doi.org/10.5703/1288284314248

Li, S., Noureldin, S., Jiang, Y., & Sun, Y. (2012). *Evaluation of pavement surface friction treatments* (Joint Transportation Research Program Publication No. FHWA/IN/JTRP-2012/04). West Lafayette, IN: Purdue University. https://doi.org/10.5703/1288284314663

Li, S., Shields, T., Noureldin, S., & Jiang, Y. (2012). Field evaluation of surface friction performance of chip seals in Indiana. *Transportation Research Record*, *2295*, 1–18. https://doi.org/10.3141/2295-02

Li, S., Sun, Y., Jiang, Y., Noureldin, S., & Shields, T. (2012). Field evaluation of ultrathin 4.75-mm hot-mix asphalt dense-graded overlay: Aggregate properties and pavement surface friction. In *TRB 91st annual meeting compendium of papers*. Washington, DC: Transportation Research Board.

Li, S., Yang, Y. H., Guan, B. W., Zhao, G. Y., Harris, D., Jiang, Y., & Noureldin, S. (2013). Surface characteristics of ultrathin bonded wearing course preservation treatments. In *TRB 92nd annual meeting compendium of papers*. Washington, DC: Transportation Research Board.

Li, S., Zhu, K., & Noureldin, S. (2005). Considerations in developing a network pavement inventory friction test program for a state highway agency. *Journal of Testing and Evaluation*, *33*(5), 1–8. https://doi.org/10.1520/JTE11885

Li, S., Zhu, K., & Noureldin, S. (2007). Evaluation of friction performance of coarse aggregates and hot-mix asphalt pavements. *Journal of Testing and Evaluation*, *35*(6), 571–577. https://doi.org/10.1520/JTE100903

MathWorks. (2014). MATLAB and Statistics Toolbox Release R2014a [Software]. Natick, MA: MathWorks.

McGee, H. W., & Hanscom, F. R. (2006). *Low-cost treatments for horizontal curve safety* (Publication No. FHWA-SA-07-002). Washington, DC: Federal Highway Administration, U.S. Department of Transportation.

Merritt, D. K., Lyon, C. A., & Persaud, B. N. (2015). *Evaluation of pavement safety performance* (Publication No. FHWA-HRT-14-065). McLean, VA: Federal Highway Administration, Turner-Fairbank Highway Research Center.

Moore, A. B., & Humphreys, J. B. (1973). High speed skid resistance and the effects of surface texture on the accident rate. In *Skid resistance of highway pavements* (STP 530, pp. 91–100). Philadelphia, PA: American Society for Testing and Materials.

Morse, P. M., & Feshbach, H. (1953). *Methods of theoretical physics*. New York, NY: McGraw-Hill.

NDRC. (2005). *Ferrous metallurgy industry standard YB/T 5179-2005: Bauxite Clinker*. Beijing, China: National Development and Reform Commission. [In Chinese]

NHTSA. (2011). *Traffic safety facts 2011* (DOT HS 811 754). Washington, DC: National Highway Traffic Safety Administration, U.S. Department of Transportation.

PennDOT. (2014). *Special provision: 00-c9001 ITEM 9000-0002 high friction surface treatment (HFST)*. Harrisburg, PA: Pennsylvania Department of Transportation. Retrieved from https://s3.amazonaws.com/media.atssa.com/HFS/Specifications_PADOT.pdf

Peshkin, D., Smith, K. L., Wolters, A., Krstulovich, J., Moulthrop, J., & Alvarado, C. (2011). *Preservation approaches for high-traffic-volume roadways* (SHRP 2 Report S2-R26-RR-1). Washington, DC: Transportation Research Board, National Academies Press. https://doi.org/10.17226/14487

Poly-Carb, Inc. (n.d.). Mark-174 exterior non-skid overlay [Technical data sheet hs/HN 04-141]. Cleveland, OH: Poly-Carb, Inc.

Rangaraju, P. R., & Edlinski, J. (2008). Comparative evaluation of micro-deval abrasion test with other toughness/abrasion resistance and soundness tests. *Journal of Materials in Civil Engineering*, *20*(5), 343–351. https://doi.org/10.1061/(ASCE)0899-1561(2008)20:5(343)

Read, H. H., & Watson, J. (1975). *Introduction to geology*. New York, NY: Halsted.

Rizenbergs, R. L., Burchett, J. L., & Napier, C. T. (1973). *Accidents on rural interstate and parkway roads and their relation to pavement friction* (KYTC Report No. 377). Lexington, KY: Kentucky Bureau of Highways. https://doi.org/10.13023/KTC.RR.1973.377

Rogers, C. A., & Senior, S. A. (1994). Recent development in physical testing of aggregates to ensure durable concrete. In M. W. Grutzeck (Ed.), Proceedings of engineering foundation conference: *Advances in cement and concrete* (pp. 338–361). New York, NY: American Society of Civil Engineers.

SAS Institute. (2015). *SAS/STAT® 14.1 user's guide*. Cary, NC: SAS Institute.

SCDOT. (2010). *Supplemental specification: High friction surface treatment*. Columbia, SC: South Carolina Department of Transportation.

SDDOT. (2014). *Addendum No. 1: High friction surface treatment special provisions*. Pierre, SD: Office of Project Development, South Dakota Department of Transportation.

Senior, S. A., & Rogers, C. A. (1991). Laboratory tests for predicting coarse aggregate performance in Ontario. *Transportation Research Record*, *1301*, 97–106.

Shi, C. (2004). Steel slag—its production, processing, characteristics, and cementitious properties. *Journal of Materials in Civil Engineering*, *16*(3), 230–236. https://doi.org/10.1061/(ASCE)0899-1561(2004)16:3(230)

Stock, A. F., Ibberson, C., & Taylor, I. F. (1996). Skidding characteristics of pavement surfaces incorporating steel slag aggregates. *Transportation Research Record*, *1545*, 35–40. https://doi.org/10.3141/1545-05

TDOT. (2015). *SP406HFST: Special provision regarding high friction surface treatment (HFST)*. Nashville, TN: Tennessee Department of Transportation.

Torbic, D. J., Harwood, D. W., Gilmore, D. K., Pfefer, R., Neuman, T. R., Slack, K. L., & Hardy, K. K. (2004). *A guide for reducing collisions on horizontal curves* (NCHRP Report 500, Vol. 7). Washington, DC: Transportation Research Board.

TxDOT. (2014). *Special specification 3289: High friction surface treatment*. Austin, TX: Texas Department of Transportation.

VDOT. (2012). *Special provision for high friction epoxy aggregate roadway surface treatment*. Richmond, VA: Virginia Department of Transportation. Retrieved from https://s3.amazonaws.com/media.atssa.com/default-file/VIRGINA20120625093442198.pdf

Vincent, G. H., & Sehnke, E. D. (2006). Bauxite. In J. E. Kogel, N. C. Trivedi, J. M. Barker, & S. T. Krukowski (Eds.), *Industrial minerals & rocks*: *Commodities, markets, and uses* (7th ed., pp. 227–262). Littleton, CO: Society for Mining, Metallurgy, and Exploration, Inc.

Vollor, T. W., & Hanson, D. I. (2006). *Development of laboratory procedure for measuring friction of HMA mixtures—Phase I* (NCAT Report No. 06-06). Auburn, AL: National Center for Asphalt Technology.

Woodward, W. D., Woodside, A. R., & Jellie, J. H. (2005). Higher PSV and other aggregate properties. In *First international conference on surface friction: Roads and runways*. Christchurch, New Zealand: New Zealand Transport Agency.

Wu, Y., Parker, F., & Kandhal, K. (1998). Aggregate toughness/abrasion resistance and durability/soundness tests to asphalt concrete performance in pavements. *Transportation Research Record*, 1638, 85–93. https://doi.org/10.3141/1638-10

Yildirim, I. Z., & Prezzi, M. (2009). *Use of steel slag in subgrade applications* (Joint Transportation Research Program Publication No. FHWA/IN/JTRP-2009/32). West Lafayette, IN: Purdue University. https://doi.org/10.5703/1288284314275

Zhong, X. C., & Li, G.P. (1981). Sintering characteristics of Chinese bauxites. *Ceramics International*, *7*(2), 65–68. https://doi.org/10.1016/0272-8842(81)90016-X

About the Joint Transportation Research Program (JTRP)

On March 11, 1937, the Indiana Legislature passed an act which authorized the Indiana State Highway Commission to cooperate with and assist Purdue University in developing the best methods of improving and maintaining the highways of the state and the respective counties thereof. That collaborative effort was called the Joint Highway Research Project (JHRP). In 1997 the collaborative venture was renamed as the Joint Transportation Research Program (JTRP) to reflect the state and national efforts to integrate the management and operation of various transportation modes.

The first studies of JHRP were concerned with Test Road No. 1—evaluation of the weathering characteristics of stabilized materials. After World War II, the JHRP program grew substantially and was regularly producing technical reports. Over 1,600 technical reports are now available, published as part of the JHRP and subsequently JTRP collaborative venture between Purdue University and what is now the Indiana Department of Transportation.

Free online access to all reports is provided through a unique collaboration between JTRP and Purdue Libraries. These are available at: http://docs.lib.purdue.edu/jtrp

Further information about JTRP and its current research program is available at: http://www.purdue.edu/jtrp

About This Report

An open access version of this publication is available online. This can be most easily located using the Digital Object Identifier (doi) listed below. Pre-2011 publications that include color illustrations are available online in color but are printed only in grayscale.

The recommended citation for this publication is:

Li, S., Xiong, R., Yu, D., Zhao, G., Cong, P., & Jiang, Y. *Friction surface treatment selection: Aggregate properties, surface characteristics, alternative treatments, and safety effects* (Joint Transportation Research Program Publication No. FHWA/IN/JTRP-2017/09). West Lafayette, IN: Purdue University. https://doi.org/10.5703/1288284316509